FINAL REPORT
PERFORMANCE OF STATISTICAL ENERGY ANALYSIS

June 1973

DRA

By: R. F. DAVIS and D. E. HINES

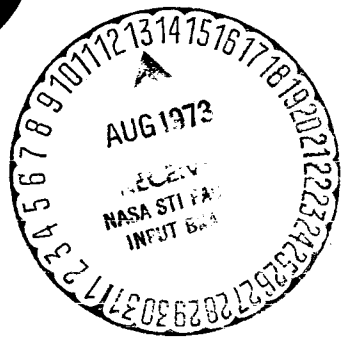

Prepared under Contract No. NAS8-28435
by McDonnell Douglas Astronautics Company
Huntington Beach, California
for
NATIONAL AERONAUTICS AND SPACE ADMINISTRATION

FINAL REPORT
PERFORMANCE OF STATISTICAL ENERGY ANALYSIS

June 1973

By: R. F. DAVIS and D. E. HINES

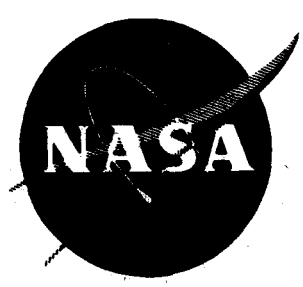

Prepared under Contract No. NAS8-28435
by McDonnell Douglas Astronautics Company
Huntington Beach, California
for
NATIONAL AERONAUTICS AND SPACE ADMINISTRATION

PREFACE

This document is submitted by the McDonnell Douglas Astronautics Company to the National Aeronautics and Space Administration and was prepared under Contract NAS8-28435, "Performance of Statistical Energy Analysis." The study was directed by D. E. Hines, with R. F. Davis acting as principal investigator. R. W. Schock of the Analytical Mechanics Division of Marshall Space Flight Center administered and directed the contract, with technical assistance provided by Dr. R. Glaser.

CONTENTS

FIGURES

TABLES

SUMMARY

High-frequency random vibration environments have become increasingly significant in the design of aerospace structures. Analytical prediction of these environments is beyond the current scope of classical modal techniques. Statistical energy analysis (SEA) methods have been developed that circumvent the difficulties of high-frequency modal analysis.

These SEA methods are evaluated by comparing analytical predictions to test results. Simple test methods are developed for establishing SEA parameter values. Techniques are presented, based on the comparison of the predictions with test values, for estimating SEA accuracy as a function of frequency for a general structure.

Analytical studies are performed on simple systems to gain insight into the application of SEA, required parameter accuracies, and high-frequency random vibration in general. In addition, the SEA equations are developed in a form that is easily adaptable to a majority of the existing matrix abstraction computer programs.

SYMBOLS

A	area
a	acceleration
$[B]$	dummy matrix formed in creating $[C]$
C/C_c	fraction of critical damping
$[C]$	coupling matrix
$c_{j,k}$	elements of $[C]$
C_L or C'_L	longitudinal wave velocities
c_o	speed of sound in air

CF	cylindrical correction factor for modal densities
D	dissipation of damping; bending stiffness
d_j	elements of damping matrix $[D]$
E	total energy of an element
e	total energy of a single mode of an element
f	frequency
G, g	gravitational acceleration
h	thickness
$[K]$	intermediate matrix for developing $[C]$
l	length
$[M]$	mass matrix
m	mass
N	number of modes
$n(\omega)$	modal density
n_p	modal density of a plate
n_c	modal density of a curved plate
P	pressure
S	power input
V	volume; velocity
v	velocity
Δ	incremental value
η_a	damping loss factor $\left(= \frac{D}{2\pi E} = 2\ C/C_c\right)$
$\eta_{a,b}$	coupling loss factor $\left(= \frac{\phi_{a,b} N_b}{\omega}\right)$
μ	average value
ν	Poisson's ratio
π	3.14159
ρ	surface mass density
ρ_o	density of air
ρ_l	material density
τ	radiation efficiency, standard deviation
$\phi_{a,b}$	average mode-to-mode coupling between Elements a and b
ϕ_c	circumferential coupling

ϕ_{eq}	equivalent coupling
ϕ_i	base set of values for ϕ_o, established by test
ϕ_o	field-joint coupling (base for selection of relative coupling values)
$\psi_{i,i}$	$\omega \eta_i N_i$
$\psi_{i,j}$	$\phi_{i,j} N_i N_j$
ω	angular frequency, normally center frequency of a frequency band

SUBSCRIPTS

a, b, i, j	dummy subscripts
ac	indicates quantity is for acoustic media

NOTATION

Element	a set of modes modeled as one unit of a system, all modes in a frequency band having identical energy (on the average)
System	the total structure and associated energy sources under consideration (may be only a portion of an actual structure)
$<\overline{\quad}>$	indicates averaging over both time and space
e_i^j	energy of the i^{th} element in a system having a total of j elements
ψ_e	equivalent coupling of a combined system (see p. 34)
$\psi^a_{1,3_e}$	equivalent coupling between Elements 1 and 3 of System a

NOTE ON UNITS

Dimensions presented in this report were measured in inches with conversion to meters performed in accordance with NASA SP-7012,

The International System of Units, Physical Constants and Conversion Factors, revised 1969. No conversion of station numbers for the UpSTAGE acoustic test specimen is accomplished in order to avoid any confusion with previously published information. The mathematical constants in Table 6 of the text were utilized directly for computational results presented in this report and have dimenions of inches to the appropriate power. Panel test specimens are referred to by their thickness in customary units of inches.

INTRODUCTION

The increasing performance of aerospace vehicles has resulted in external acoustic fields and aerodynamic boundary layers that cause increasingly significant high-frequency random vibration environments. In general, these environments have been predicted using empirical scaling techniques; however, the advent of reusable space vehicles featuring new configurations with unique forcing fields requires extending these techniques beyond the configurations from which they were developed. These factors, together with a desire for optimal vehicle designs, have made the analytical prediction of high-frequency random vibration response in structures an important aspect of the design and development of such vehicles.

The classical modal analysis techniques for predicting dynamic response work well in the frequency range of the lower structural resonances. However, when these techniques are extended into the higher frequency range, the complexity and size of the model and the required solution time increase rapidly. Consequently, classical solutions in the high frequency range are well beyond the current state of the art for computer hardware.

Statistical energy analysis (SEA) techniques that can successfully circumvent the problems of classical determination of high frequency response were developed a decade ago. Although fundamentals were established, minimal effort was made to apply such methods to the complex structural systems that are typical of flight hardware. Reference 1 contains an excellent bibliography of the development of SEA.

The first SEA application to a complex vehicular structure was performed for the UpSTAGE program (see Reference 2). The SEA effort on UpSTAGE was directed to the scaling of data from an acoustic test specimen into design

and component vibration test criteria for a flight design. Because of the specific interest in using SEA as a scaling technique, the approach was not evaluated in depth as a predictive technique. However, a considerable amount of vibration response test data was obtained with controlled acoustic inputs, which could provide a basis for a more comprehensive evaluation of SEA in application to a complex system.

This report documents the results of such a study using experimental data from UpSTAGE tests to evaluate the use of SEA with general structural systems. The study includes a mathematical examination of simple systems to identify phenomena that apply to more complex systems, an evaluation of simple approximations to complex systems, a test program to examine the effects of SEA parameters and to evaluate methods of measuring these parameters, and the formulation of an equation format that is amenable to computerized solution. Some additional information has been added to make this report a self-contained document on SEA. The results of this study and content of the report are briefly summarized below.

The report shows the development of the basic SEA equations used in this study. These expressions are then expanded to cover complex structures and put into a form readily compatible with available matrix abstraction programs. An analytical study of elementary systems is performed yielding some useful information concerning SEA and high frequency response in general. The major portion of the report is devoted to the evaluation of SEA in application to a complex structure. This application incorporates a test program that successfully provided damping and coupling parameter values through the use of very simple test methods. A technique for introducing acoustic energy into the SEA model is derived which gives good results with reverberant acoustic fields but requires further development before valid application to nonreverberant fields is indicated. This statistical structural analysis, in conjunction with the simple test methods, resulted in high-frequency vibration response predictions with an accuracy of ±3 dB in comparison with test measurements. Frequency scaling methods are presented that may be used to evaluate the frequency range in which this accuracy can be expected for general structures. The complex structure considered in

this report is an elliptical cone excited with a range of acoustic configurations. In many respects, this represents a more complex analysis problem than that for typical vehicles. Considering the complexity of the structure examined in this study, together with the various types of acoustic input configurations, one can expect the results to be valid for a wide range of structural problems.

DEVELOPMENT OF STATISTICAL ENERGY ANALYSIS (SEA) EQUATIONS AND SOLUTION FORMAT

Statistical energy methods have been developed to consider the distribution and transfer of energy among the modes of a vibrating system. These methods assume that the modes of a system being analyzed contain all the vibratory energy of that system. Therefore, for SEA to have valid application, all significant energy of a system must be "resonant" as opposed to "nonresonant." A parameter for evaluating this condition is examined in Reference 3.

The SEA methods separate the frequency range of interest into frequency bands, which are analyzed independently. The methods assume that the energy in the modes of one frequency band is not transmitted (through coupling) to modes in other frequency bands either within an element or among the elements of a system.

These energy analysis techniques are denoted "statistical" because they involve averaging structural response over portions of the structure. This averaging is performed over time, space, and in frequency bands. The time averaging results in the use of root-mean-squared representation for quantities such as acceleration, which vary with time. The space averaging assumes that the energy of a system element is evenly distributed throughout the element. The frequency band averaging consists of the assumption that the energy of an element in one frequency band is evenly distributed among the element modes occurring at frequencies within the band.

An important factor in validating the space and frequency averaging is the number of modes included in each frequency band. With many modes excited in one frequency band of an element, the vibratory energy may be expected to

be well distributed throughout the element and among the various modes, and averaging will furnish a valid approximation to actual values. When frequency bands that are a constant percentage of the center frequency, such as third-octave bands, are utilized for analysis, the bands will contain progressively greater numbers of modes as the center frequency increases. Therefore, a closer approximation to the true response is obtained as frequency increases. The use of very wide frequency bands should permit SEA to have valid application at lower frequencies. However, problems with frequency resolution require a compromise. One-third-octave bandwidths were chosen for the analysis of a complex system that appears later in this

The assumptions, then, upon which statistical energy analysis is based are:

A. The modes of the elements of a system contain all the vibratory energy of the system.

B. Only modes occurring within the same frequency band are coupled.

C. The energy in one frequency band of a system element is equally distributed among the modes of that element occurring in the frequency band.

D. For two coupled elements, all of the modes occurring in one of the elements in one frequency band are equally coupled to each mode occurring in the same frequency band in the other element.

Derivation of Basic Equations*

The basic SEA equations for a simple, two-element system are developed below in order to indicate the application of the SEA methods and to introduce the nomenclature that will be used throughout this report. Following this basic development, the basic SEA formulation will be expanded to a form suitable for the representation of a system of any size.

*The development of basic equations follows that of Reference 2.

The following schematic represents the two-element system.

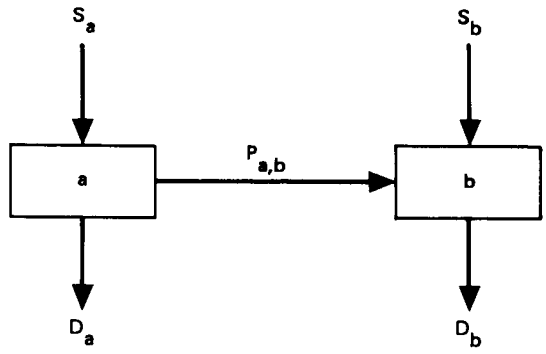

In this schematic of the two elements, a and b, the following nomenclature is used:

S_a — power introduced into Element a from an external source.

D_a — power dissipated within Element a.

$P_{a,b}$ — net power transmitted from Element a to Element b ($= -P_{b,a}$).

N_a — number of modes in Element a.

These values and the following derivation are for only a single frequency band.

A power flow equation for all energy passing into Element a may be expressed as

$$D_a + P_{a,b} = S_a$$

Each of these terms will be examined by considering a single mode of Element a. The energy in that mode is e_a.

The energy dissipated by damping during one radian of vibration by the single mode is defined in terms of the element loss factor as $\eta_a e_a$. Multiplying by the angular center frequency of the subject frequency band, the energy

dissipated per unit time (power loss) is therefore $\omega \eta_a e_a$, which corresponds to the contribution of a single mode to D_a.

The net power transmitted by the single mode is the difference between the power being transmitted by the mode and the power received by it. The Element a mode is transmitting equally (on the average) to each Element b mode in this frequency band. The power transmitted to each one of these b modes is $\phi_{a,b} e_a$, which is the defining relation for the SEA coupling factor. Since there are N_b modes to which the a mode is transmitting, the total power given up by the Element a mode to Element b is $N_b \phi_{a,b} e_a$.

The power being received by the single Element a mode from Element b must be considered. Each b mode is transmitting $\phi_{a,b} e_b$ power to the a mode. Since there are N_b modes transmitting to the a mode, the total power received is $N_b \phi_{a,b} e_b$. Because this term represents an increase in the energy of the a mode, it must be a negative term.

Summing the two contributions to the net power transmission yields:

$$N_b \phi_{a,b} e_a - N_b \phi_{a,b} e_b$$

The external input to the single a mode may be expressed by dividing the total input power to Element a equally among all the modes of the a element: S_a/N_a.

Substituting these expressions into the power flow relation for the single a mode yields:

$$\omega \eta_a e_a + N_b \phi_{a,b} e_a - N_b \phi_{a,b} e_b = \frac{S_a}{N_a}$$

Because this expression is for an average mode, the power flow equation for the entire Element a may be obtained by multiplying the expression by the total number of modes in Element a, N_a, yielding

$$\omega \eta_a N_a e_a + N_b \phi_{a,b} N_a e_a - N_a \phi_{a,b} N_b e_b = S_a$$

or, since $E_a = N_a e_a$,

$$\omega \eta_a E_a + N_b \phi_{a,b} E_a - N_a \phi_{a,b} E_b = S_a$$

This is the form that will be adopted for the remainder of this report as the basic SEA power flow equation for an element of a coupled system. It is important to note that this expression is in terms of the total energies of the system elements rather than their kinetic energies, as sometimes found in the literature. It should be noted that a 2 was erroneously placed before the first term of the equation in the derivation of Reference 2.

The corresponding equation for Element b completes the total system of equations for the two-element system:

$$\omega \eta_b E_b + N_a \phi_{a,b} E_b - N_b \phi_{a,b} E_a = S_b$$

If the equations for the two elements are added, the result is

$$\omega \eta_a E_a + \omega \eta_b E_b = S_a + S_b$$

This is the total power equation for the system, stating that the total energy input to the system is dissipated within the system. It may sometimes be convenient in obtaining SEA solutions for a system to replace one of the element equations with the total power equation for the system.

The basic SEA equation may be expressed in an alternate form, which is sometimes more convenient. This is accomplished by defining a coupling loss factor as

$$\eta_{a,b} = \frac{\phi_{a,b} N_b}{\omega}$$

Using this expression to substitute for the ϕN terms yields

$$\omega \eta_a E_a + \omega \eta_{a,b} E_a - \omega \eta_{b,a} E_b = S_a$$

or

$$E_a \left(\eta_a + \eta_{a,b} \right) - E_b \eta_{b,a} = \frac{S_a}{\omega}$$

It can be seen that these coupling loss factors represent an equivalent damping, which is due to the coupling between elements. This equivalent damping causes both positive and negative power flow terms to occur. It is important to note that, unlike $\phi_{a,b}$, this alternate coupling parameter is not symmetric $\left(\eta_{a,b} \neq \eta_{b,a} \right)$.

Matrix Format for General Systems

The basic SEA equations will now be expanded in a matrix form suitable for general systems. The matrix form is easily solved using available computerized matrix abstraction programs. The formulation of this solution, as presented below, again parallels that presented in Reference 1.

Consider the system shown in Figure 1. The j element is only coupled to the elements having common boundaries (i, j-1, j+1, and k).

The power lost by the j^{th} element is the result of damping $\left(\omega \eta_j E_j \right)$ plus that lost to adjacent panels. If the coupling across each border is described by

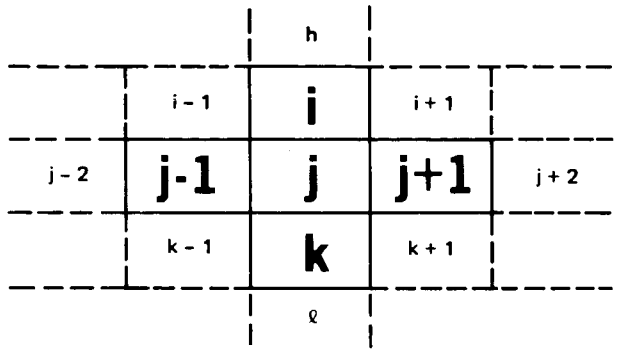

Figure 1. Block Diagram of a Portion of a General Structural System

$\phi_{j,m}$, then the energy lost across each border is $E_j \phi_{j,m} N_m$. The net energy loss to the adjacent panels is $E_j[\phi_{j,i} N_i + \phi_{j,j-1} N_{j-1} + \phi_{j,j+1} N_{j+1} + \phi_{j,k} N_k]$. The power gained by the j^{th} element will be that received from some external source (S_j) plus that received from adjacent panels $N_j [\phi_{j,i} E_i + \phi_{j,j-1} E_{j-1} + \phi_{j,j+1} E_{j+1} + \phi_{j,k} E_k]$.

Equating the power flow expressions for the j^{th} elements leads to

$$-\phi_{j,i} N_j E_i - \phi_{j,j-1} N_j E_{j-1} + \Big(\omega \eta_j + \phi_{j,i} N_i + \phi_{j,j-1} N_{j-1}$$

$$+ \phi_{j,j+1} N_{j+1} + \phi_{j,k} N_k \Big) E_j - \phi_{j,j+1} N_j E_{j+1} - \phi_{j,k} N_j E_k = S_j$$

If the power balance equations for all the sections are put into a matrix form, then the above equation would represent the j^{th} row of that matrix, as shown in Figure 2. In the power balance equation for the n^{th} element the coefficient

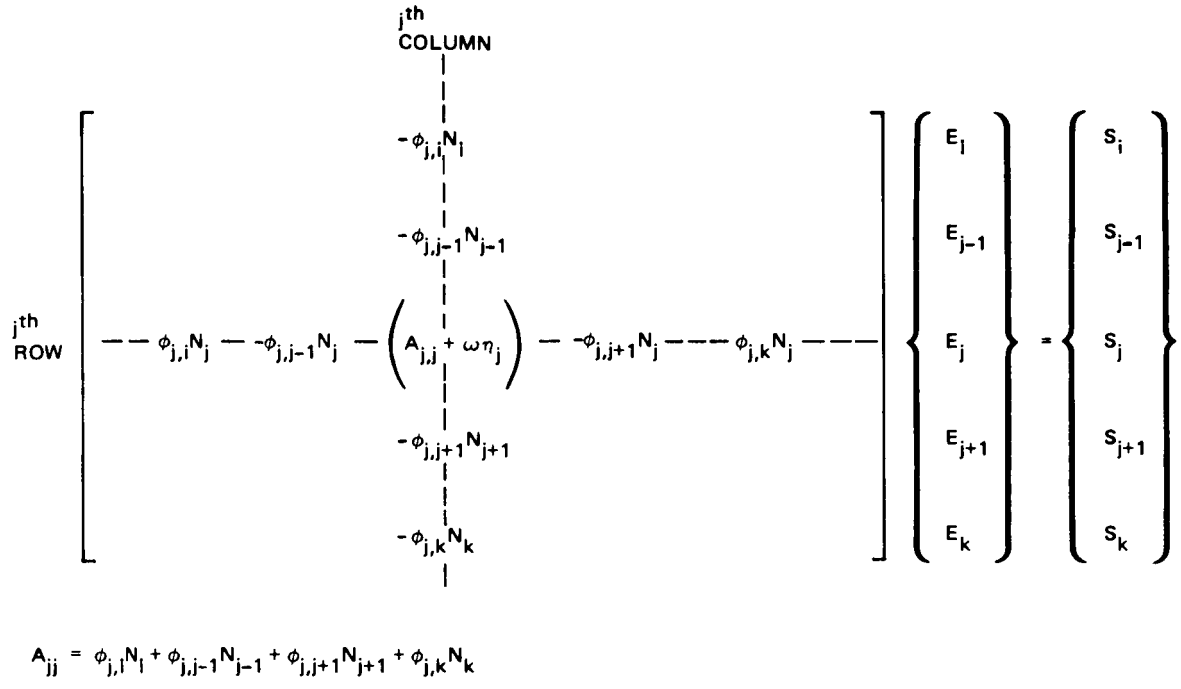

Figure 2. Matrix Form of SEA Equation for a General Structural System

for E_j will be $\phi_{j,n} N_n$. These terms result in the values in the j^{th} column, as indicated in Figure 2. It is interesting (and helpful in programming) to note that the positive value of the sum of the off-diagonal terms in the j^{th} column plus the damping term is equal to the diagonal term.

The matrix form of the model can be written as

$$\left([D] + [C]\right)\{E\} = \{S\}$$

where D describes the damping and is a diagonal matrix whose elements are of the form

$$d_j = \omega\eta_j$$

$[C]$ is the coupling matrix where

$$c_{j,k} = -\phi_{j,k} N_j \text{ for } j \neq k$$

$$c_{j,j} = -\sum_{m} c_{jm} \text{ for } j \neq m$$

$c_{j,k}$ are zero for uncoupled elements.

The E and S matrices are the energy and input power, respectively.

$[C]$ can be formed in the following way. Let $[N]$ be the diagonal matrix describing the number of modes in each element in the frequency band of interest, and $[\Phi]$ be the coupling matrix with elements

$\phi_{i,j}$ = average mode-to-mode coupling between i and j

This gives

$$[C] = -[\Phi][N] + [B]$$

$[B]$ can be formed by diagonalizing

$$[1\ 1 \text{---} 1\ 1][\Phi][N]$$

where the order of the row of ones is that of $[\Phi]$.

The total energy (twice the time kinetic energy) for each of the elements is

$$E_i = \int_i \overline{V^2}\, dm$$

for a conservative (linear) system.

One of the fundamental assumptions is that for uniform structures

$$E_i = m_i \langle \overline{V_i^2} \rangle$$

where m_i = mass of the i^{th} element.

It is assumed that the bandwidths chosen for analysis are sufficiently narrow so that

$$E_i = m_i \langle \overline{V_i^2} \rangle = m_i \frac{\langle \overline{V_i^2} \rangle}{\omega^2}$$

is a valid expression for the vibrating system.

In matrix notation

$$\{E\} = \frac{1}{\omega^2} [M] \{\langle \overline{a^2} \rangle\}$$

Performing the indicated substitutions and solving for $\{\langle \overline{a^2} \rangle\}$ yields

$$\{\langle \overline{a^2} \rangle\} = \omega^2 [M]^{-1} \left([D] + [C] \right)^{-1} \{S\},$$

where $[E]$ is formed from $[\Phi]$ and $[N]$ matrices. This basic SEA response format is suitable for application to general systems. The use of this format is straightforward, and the expression is easily adapted to solution with any matrix abstraction program.

In general, the number of modes is the only one of the terms appearing in the basic format that may be considered well defined for general structures at the present time. Table 1 (reprinted from Reference 7) presents

Table 1

MODAL DENSITIES OF SOME UNIFORM SYSTEMS*

System	Motion	Modal Density, $n(\omega)$	Auxiliary Expressions
String	Lateral	$L/\pi c_S$	$c_s = \sqrt{T/\rho A}$
Shaft, Beam	Torsion	$L/\pi c_T$	$c_T = \sqrt{Gk/\rho J}$
Shaft, Beam	Longitudinal	$L/\pi c_\ell$	$c_\ell = \sqrt{E/\rho}$
Beam	Flexure	$\frac{L}{2\pi}\left(\omega \kappa_b c_\ell\right)^{-1/2}$	$\kappa_b c_\ell = \sqrt{EI/\rho A}$
Membrane	Lateral	$A_s \omega/2\pi c_m^2$	$c_m = \sqrt{S/\rho h}$
Plate	Flexure	$A_s/4\pi\kappa_p c_\ell$	$\kappa_p c_\ell = \sqrt{D/\rho h}$ $= \sqrt{Eh^2/12\rho(1-\nu^2)}$
Room, (Acoustic Volume)	Sound (Compression)	$V_o \omega^2/2\pi^2 c_a^3$	
Cylindrical Shells (Ref. 15)	Flexure	$\begin{cases} \sim n_p & \text{for } \omega/\omega_r > 1 \\ \sim n_p \left(\frac{\omega}{\omega_r}\right)^{2/3} & \text{for } \omega/\omega_r < 1 \end{cases}$	$\omega_r = c_\ell/a$ $n_p = A_s/4\pi\kappa_p c_\ell$
Doubly Curved Shells	Flexure	Expressions are complex, given in Reference 11	

*See next page for definitions of symbols.

Symbol Definitions for Table 1

A	cross-section area
A_s	surface area
c_a	acoustic wave velocity
c_ℓ	longitudinal wave velocity
c_m	membrane wave velocity
c_s	string wave velocity
c_T	torsional wave velocity
D	plate rigidity
E	Young's modulus
G	shear modulus
h	thickness
I	centroidal moment of inertia of A
J	polar moment of inertia of A
K	torsional constant of A
L	length
S	membrane tension force/unit edge length
T	string tension force
V_o	volume
κ_b	radius of gyration of A
κ_p	radius of gyration of plate cross section
ν	Poisson's ratio
ω	frequency (radians/time)
ρ	material density

expressions for the modal density, $n(\omega)$, which are generally valid in the range of SEA applicability. These expressions are in terms of material properties and structural dimensions, and only have to be multiplied by bandwidth to yield the number of modes in a frequency band $\Delta\omega$ ($N = n(\omega)\Delta\omega$). The values for a cylinder can be improved by using the value of Figure 3 (Reference 10).

A considerable amount of information has been generated on the subject of damping (see References 8 and 9, for example). However, incorporating this information into the analysis of a structural system is difficult because it is uncertain what added damping contributions may be created by structural joint effects. This study evaluated a simple test technique to provide satisfactory definition of the SEA damping term.

Definitive information on values for the SEA coupling parameter is almost completely nonexistent. Most experimental examinations of SEA to date have utilized only very simple structural specimens with joints that are not typical of aerospace construction. This study evaluated a simple test method for determining coupling parameter values for the joints of general structures.

The input term will generally involve a transfer function to couple a fluctuating pressure field to the structural system. This study developed a method for coupling a reverberant acoustic field to a structure. Use of these expressions for predicting response from other acoustic fields requires the definition of an "equivalent" reverberant field, or the coupling terms must be modified. The development of the reverberant coupling terms will indicate an approach that could be used in defining coupling terms for other pressure fields.

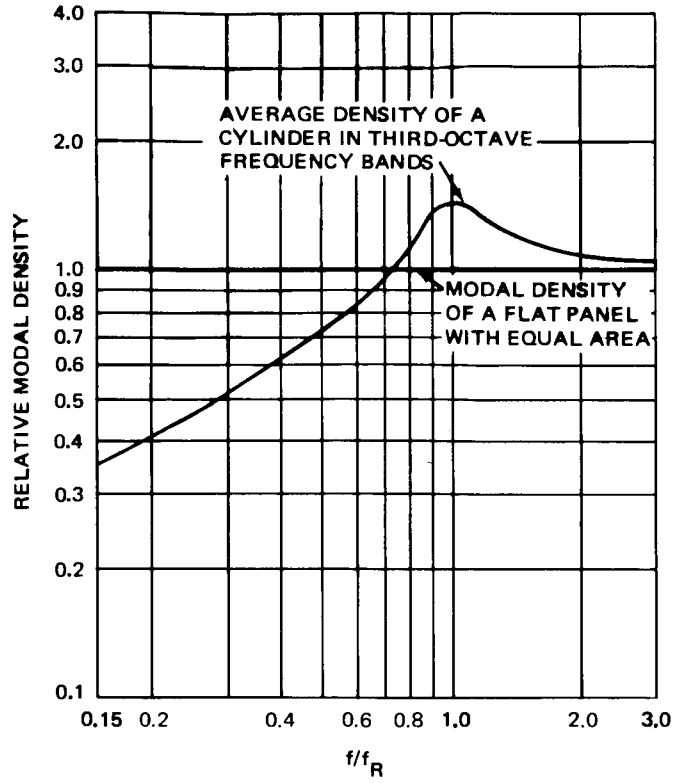

Figure 3. Modal Density of a Cylinder Compared to a Flat Panel (After Reference 10)

ELEMENTARY SYSTEMS

This section presents the results of a theoretical study on elementary systems (few elements) performed to furnish insight into the characteristics of SEA parameters, SEA modeling, and high-frequency vibration in general. Besides aiding in a better understanding of SEA parameters and aspects of modeling, the theoretical results have practical benefit as well.

An energy-per-mode formulation is used in this section because it results in a simplification in the nomenclature. The relationship between energy per mode and some basic response parameters is discussed, as is the use of the linearity of the systems for estimating response.

The section continues with derivations of the effect of couple length on coupling factors and of a method of adding coupling factors. The derivation of the combination of coupling factors did require a fairly stringent assumption concerning damping. A test case is examined to evaluate the effects of this assumption.

A discussion of the effects of damping and coupling factors is presented: the first portion concerning vibration control, and the second portion concerning accuracies required in these parameters.

Energy-per-Mode Expressions

A number of interesting results can be obtained with the basic two-element model utilized for development of the SEA equations. Rewriting the equations for the two-element system in terms of E/N yields

$$(\omega\eta_1 N_1 + \phi_{1,2} N_1 N_2)\frac{E_1}{N_1} - \phi_{1,2} N_1 N_2 \frac{E_2}{N_2} = S_1$$

and

$$-\phi_{1,2} N_1 N_2 \frac{E_1}{N_1} + (\omega\eta_2 N_2 + \phi_{1,2} N_1 N_2) \frac{E_2}{N_2} = S_2$$

Defining

$$\psi_{i,i} = \omega\eta_i N_i$$

$$\psi_{i,j} = \phi_{i,j} N_i N_j$$

$$e_i = \frac{E_i}{N_i}$$

Rewriting the equations in terms of these variables yields

$$(\psi_{1,1} + \psi_{1,2}) e_1 - \psi_{1,2} e_2 = S_1$$

$$-\psi_{1,2} e_1 + (\psi_{2,2} + \psi_{1,2}) e_2 = S_2$$

The form is symmetrical and the nomenclature much less cluttered. Both factors are advantageous when working with closed-form solutions.

The energy-per-mode (e_i) form of the equations is sufficient for observing relative effects since the energy-per-mode ratio is proportional to the square of the response ratio

$$\frac{e_1}{e_2} = \frac{N_2 E_1}{N_1 E_2} = \frac{N_2 m_1}{N_1 m_2} \frac{\overline{<V_1^2>}}{\overline{<V_2^2>}}$$

Some additional observations can be made concerning this form. Both m and N for a given element are proportional to either volume, area, or length depending on whether the element of interest is an acoustic medium, plate, or beam, respectively.

If the elements consist of the same medium, the ratio of e's reduces to a ratio of the mean-squared responses for the systems. The same medium is the fluid for the acoustic case, and the material thickness and curvature for a vibrating plate. For the acoustic case where the mediums are not the same, the expressions reduce to

$$\frac{e_1}{e_2} = \frac{\rho_1 \, c_1^3 \langle \overline{v_1^2} \rangle}{\rho_2 \, c_2^3 \langle \overline{v_2^2} \rangle} = \frac{\rho_1 \, c_1^3 \langle \overline{p_1^2} \rangle}{\rho_2 \, c_2^3 \langle \overline{p_2^2} \rangle}$$

The general expression for a plate reduces to

$$\frac{e_1}{e_2} = \frac{\omega_{r_1}^{2/3} \, h_1 \langle \overline{v}_1^2 \rangle}{\omega_{r_2}^{2/3} \, h_2 \langle \overline{v}_1^2 \rangle}$$

Not only do the above expressions give a more direct means of relating the mean-squared response for systems, but they also serve to emphasize the relationship between acoustic and vibration problems.

General Observations

Of primary interest is the configuration with $S_2 = 0$, similar to an internal element not being directly excited. This leads to

$$- \psi_{1,2} e_1 + (\psi_{2,2} + \psi_{1,2}) e_2 = 0$$

$$\frac{e_1}{e_2} = \frac{\psi_{2,2} + \psi_{1,2}}{\psi_{1,2}} = 1 + \frac{\psi_{2,2}}{\psi_{1,2}} = 1 + \frac{\omega \eta_2 N_2}{\Phi_{1,2} N_1 N_2} = 1 + \frac{\eta_2}{\eta_{2,1}}$$

$\eta_{2,1}$ representing the equivalent damping in Element 2 as a result of energy loss to Element 1. Note that in a general solution to this system, η_2 and $\eta_{2,1}$ have reciprocal effects on e_1/e_2.

A special case of this expression exists when

$$\eta_2 \ll \eta_{2,1}$$

For this case, the solution yields $e_1 = e_2$. This indicates that all system modes within the subject frequency band have identical energies. Both elements of the system are responding as a single element, a situation which will be denoted "reverberant" by analogy to an acoustic field with the energy evenly distributed throughout an enclosed volume. This case results from systems with very low damping or with very large coupling; for example, a continuous panel modeled as two elements coupled by an imaginary joint.

An additional case is where $\eta_2 \gg \eta_{1,2}$. The ratio of responses reduces to

$$\frac{e_1}{e_2} = \frac{\eta_2}{\eta_{2,1}}$$

or

$$e_1 \eta_{2,1} = e_2 \eta_2$$

This often exists when a structure is excited by an acoustic field, and the acoustic damping is small compared to the structural damping.

The low acoustic damping is an inborn assumption in the acoustically induced structural response formulations that neglect the interaction between the acoustic medium and the structure and is a valid assumption for most complex systems excited by airborne acoustic fields. The expression

$$\frac{e_2}{e_1} = 1 + \frac{\text{structural damping}}{\text{acoustical damping}}$$

could be used to evaluate this assumption.

Although only two-element models have been considered, they can furnish insight into more complex models. Consider

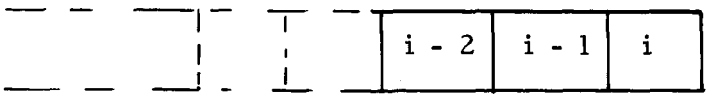

The equation for the i^{th} element of this model is

$$\frac{e_{i-1}}{e_i} = 1 + \frac{\psi_{i,i}}{\psi_{i-1,i}}$$

identical to the two-element result. This is a result of an element being able to "see" only the elements directly coupled to it.

Addition of Responses

SEA describes the response of linear systems. Therefore, the e values resulting from different excitation sources can be summed to yield the total response. An application of this principle is evident when considering the response of the second element of a two-element system when $S_2 \neq 0$. The equation for this element is

$$-\psi_{1,2}\, e_1 + (\psi_{2,2} + \psi_{1,2})\, e_2 = S_2$$

or

$$e_2 = \frac{\psi_{1,2}}{\psi_{2,2} + \psi_{1,2}}\, e_1 + \frac{S_2}{\psi_{2,2} + \psi_{1,2}}$$

The first expression on the right of the equal sign is the contribution of e_1 to e_2, which has already been discussed. The second expression can be simplified to

$$\frac{S_2}{N_2 (\eta_2 + \eta_{2,1})}$$

This is the form obtained for the response of a one-element system excited by S_2, where $\eta_2 + \eta_{2,1}$ represents the total loss factor of the system.

The equation for the second element of the three-element system can be put in the form of

$$e_2 = \frac{\psi_{1,2}\, e_1}{\psi_{2,2} + \psi_{2,3} + \psi_{1,2}} + \frac{\psi_{2,3}\, e_3}{\psi_{2,2} + \psi_{1,2} + \psi_{2,3}} + \frac{S_2}{\psi_{2,2} + \psi_{1,2} + \psi_{2,3}}$$

or

$$e_2 = \frac{e_1}{1 + \dfrac{\psi_{2,2} + \psi_{2,3}}{\psi_{1,2}}} + \frac{e_3}{1 + \dfrac{\psi_{2,2} + \psi_{1,2}}{\psi_{2,3}}} + \frac{S_2}{\psi_{2,2} + \psi_{1,2} + \psi_{2,3}}$$

The denominator of the first expression on the right of the equal sign reduces to

$$1 + \frac{N_2 (\eta_2 + \eta_{2,3})}{\psi_{1,2}}$$

This is identical to the form for the two-element system if the system damping includes $\eta_{2,3}$. In general, the contribution of each coupled system (in this case 1 and 3) can be obtained using two-element theory if the loss factor includes losses to all elements except the coupled system being considered. The response resulting from a direct input can be obtained by combining all the loss factors. The analytical expression for this is

$$e_i = \sum_j \left(\frac{\psi_{i,j}\, e_j}{\psi^j_{i,i} + \psi_{i,j}} \right) + \frac{S_i}{\psi^{j,j}_{i,i}}$$

where

$\psi_{i,j} \neq 0$ for coupled elements and

$$\psi_{i,i}^{j,j} = \sum_{k} \psi_{i,k}$$

$$\psi_{i,i}^{j} = \psi_{i,i}^{j,j} - \psi_{i,j}$$

This expression can be used to gain insight into the environment and control of that environment for a given system when the response of the rest of the system is fairly well defined.

Coupling Factor versus Length

The effect of coupled length for panels, or area for the acoustic case, is examined below.

Consider the two systems

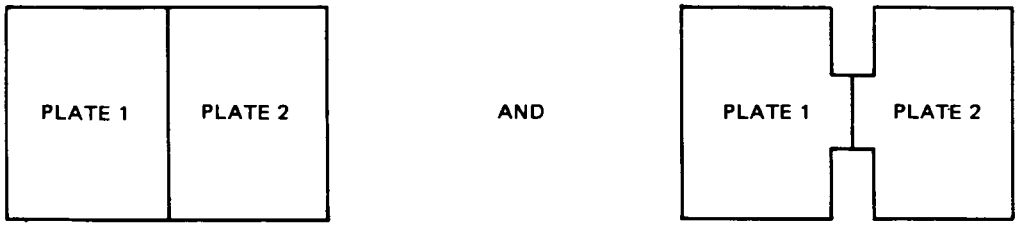

The panels and coupling differ only in that the first panel is coupled along the entire length of common boundary and the second is coupled along one-third of the length.

Plate 2 is modeled as three equal plates and the coupling between them is large so that the response (e) of each is identical. The models for the two systems are

In these systems

$$e_2 = e_3 = e_4$$

$$\psi_{2,2} = \psi_{3,3} = \psi_{4,4}$$

and

$$\psi_{1,2} = \psi_{1,3} = \psi_{1,4}$$

for the first system and the $\psi_{1,3}$'s are the same for both systems.

The equations for the first system can be reduced to

$$(\psi_{1,1} + 3\psi_{1,3})\, e_1 - 3\psi_{1,3}\, e_3 = S_1$$

$$-3\psi_{1,3}\, e_1 + (3\psi_{3,3} + 3\psi_{1,3})\, e_3 = 0$$

by combining the equations for Elements 2, 3, and 4.

If the same procedures are followed for the second system, the following expressions are obtained

$$(\psi_{1,1} + \psi_{1,3})\, e_1 - \psi_{1,3}\, e_3 = S_1$$

$$-\psi_{1,3}\, e_1 + (3\psi_{3,3} + \psi_{1,3})\, e_3 = 0$$

The coupling for the first system is three times that for the second system, or the amount of coupling is proportional to the coupled length.

Combining Coupling and Equivalent Systems

This subsection will derive and evaluate a method of combining the coupling factors for a series of elements. The vehicle for evaluating this will be the

use of "equivalent" systems based on a combination method. The derivation is presented below.

Consider the systems

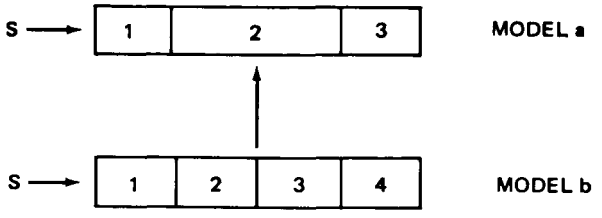

where

$$N_1^a = N_1^b$$

$$N_2^a = N_2^b + N_3^b$$

$$N_3^a = N_4^b$$

The equations of Elements 2 and 3 of the first system are

$$-\psi_{1,2}^a e_1^a + \left(\psi_{2,2}^a + \psi_{1,2}^a + \psi_{2,3}^a\right) e_1^a - \psi_{2,3}^a e_3^a = 0$$

$$-\psi_{2,3}^a e_2^a + \left(\psi_{3,3}^a + \psi_{2,3}^a\right) e_3^a = 0$$

If

$$\psi_{2,2}^a \ll \psi_{1,2}^a + \psi_{2,3}^a$$

then

$$\frac{e_1^a}{e_3^a} = \frac{\psi_{1,2}^a + \psi_{2,3}^a}{\psi_{1,2}^a} \frac{e_2^a}{e_3^a} - \frac{\psi_{2,3}^a}{\psi_{1,2}^a}$$

and

$$\frac{e_2^a}{e_3^a} = \frac{\psi_{3,3}^a + \psi_{2,3}^a}{\psi_{2,3}^a}$$

Therefore

$$\frac{e_1^a}{e_3^a} = \frac{\left(\psi_{1,2}^a + \psi_{2,3}^a\right)\left(\psi_{3,3}^a + \psi_{2,3}^a\right)}{\psi_{1,2}^a \psi_{2,3}^a} - \frac{\psi_{2,3}^a}{\psi_{1,2}^a}$$

$$= \frac{\left(\psi_{1,2}^a + \psi_{2,3}^a\right)\psi_{3,3}^a + \psi_{1,2}^a \psi_{2,3}^a}{\psi_{1,2}^a \psi_{2,3}^a}$$

$$= 1 + \frac{\psi_{3,3}^a}{\dfrac{\psi_{1,2}^a \psi_{2,3}^a}{\psi_{1,2}^a + \psi_{2,3}^a}} = 1 + \frac{\psi_{3,3}^a}{\psi_{1,3_e}^a}$$

where

$$\frac{1}{\psi_{1,3_e}^a} = \frac{1}{\psi_{1,2}^a} + \frac{1}{\psi_{2,3}^a}$$

The equations for Sections 2, 3, and 4 in the b system are

$$-\psi_{1,2}^b e_1^b + \left(\psi_{1,2}^b + \psi_{2,3}^b\right) e_2^b - \psi_{2,3}^b e_3^b = 0$$

$$-\psi_{2,3}^b e_2 + \left(\psi_{2,3}^b + \psi_{3,4}^b\right) e_3^b - \psi_{3,4}^b e_4^b = 0$$

$$-\psi_{3,4}^b e_3^b + \left(\psi_{4,4} + \psi_{3,4}\right) e_4^b = 0$$

Solving for e_2 in the second and substituting into the first of the above equations yields

$$-\psi^b_{1,2}\, e^b_1 + \left(\psi^b_{1,2} + \psi^b_{2,3}\right)\left(\frac{\left[\psi^b_{2,3} + \psi^b_{3,4}\right] e_3}{\psi_{2,3}} - \frac{\psi_{3,4}\, e_4}{\psi^b_{2,3}}\right) - \psi^b_{2,3}\, e^b_3 = 0$$

or

$$-\psi^b_{1,2}\, e^b_1 + \frac{\psi^b_{1,2}\,\psi^b_{2,3} + \psi^b_{1,2}\,\psi^b_{3,4} + \psi^b_{2,3}\,\psi^b_{3,4}}{\psi_{2,3}}\, e_3 - \frac{\psi_{3,4}\left(\psi^b_{1,2} + \psi^b_{2,3}\right)}{\psi_{2,3}}\, e_4 = 0$$

and

$$\frac{e^b_1}{e^b_4} = \frac{\psi^b_{1,2}\,\psi^b_{2,3} + \psi^b_{1,2}\,\psi^b_{3,4} + \psi^b_{2,3}\,\psi^b_{3,4}}{\psi^b_{1,2}\,\psi^b_{2,3}}\,\frac{e^b_3}{e^b_4} - \frac{\psi^b_{3,4}\left(\psi^b_{1,2} + \psi^b_{2,3}\right)}{\psi^b_{1,2}\,\psi^b_{2,3}}$$

The equation for the fourth subset gives

$$\frac{e^b_3}{e^b_4} = \frac{\psi_{4,4} + \psi_{3,4}}{\psi_{3,4}}$$

Therefore

$$\frac{e^b_1}{e^b_4} = \frac{\left[\psi^b_{1,2}\,\psi^b_{2,3} + \psi^b_{3,4}\left(\psi^b_{1,2} + \psi^b_{2,3}\right)\right]}{\psi^b_{1,2}\,\psi^b_{2,3}\,\psi^b_{3,4}}\left[\psi^b_{4,4} + \psi^b_{3,4}\right] - \frac{\psi^b_{3,4}\left(\psi^b_{1,2} + \psi^b_{2,3}\right)}{\psi^b_{1,2}\,\psi^b_{2,3}}$$

$$= \frac{\psi_{4,4}\left(\psi^b_{1,2}\,\psi^b_{2,3} + \psi^b_{1,2}\,\psi^b_{3,4} + \psi^b_{2,3}\,\psi^b_{3,4}\right) + \psi_{1,2}\,\psi_{2,3}\,\psi_{3,4}}{\psi^b_{1,2}\,\psi^b_{2,3}\,\psi^b_{3,4}} = 1 + \frac{\psi^b_{4,4}}{\psi^b_{1,4_e}}$$

where

$$\frac{1}{\psi^{b}_{1,4_e}} = \frac{1}{\psi^{b}_{1,2}} + \frac{1}{\psi^{b}_{2,3}} + \frac{1}{\psi^{b}_{3,4}}$$

This reasoning can be extended to the system shown below

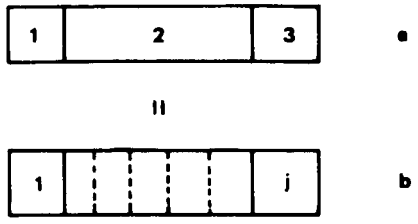

When

$$N_2 = \sum_{i=2}^{j-1} N_i$$

$$\psi_{i,i} \ll \psi_{i-1,i} + \psi_{i,i+1} \qquad \text{for } i = 2 \text{ to } j-1$$

The result is

$$\frac{1}{\psi^{a}_{1,2}} + \frac{1}{\psi^{a}_{2,3}} = \frac{1}{\sum_{i=1}^{j-1} \psi^{b}_{i,i+1}} = \frac{1}{\psi_e}$$

The assumption of negligible damping is required to reduce the algebra to a manageable form. The assumption of small damping does not eliminate damping from consideration.

Addition of the initial equations for the b system yields

$$S = \psi_{1,1}\, e_1 + \sum_{i=2}^{j-1} \psi_{i,i}\, e_i + \psi_{j,j}\, e_j$$

The e's are approximately the same if the elements are the same, and $\psi_{i,i} \ll \psi_{i-1,i} + \psi_{i,i+1}$. The above equation reduces to

$$S = \psi_{1,1}\, e_1 + e_i \sum_{i=2}^{j-1} \psi_{i,i} + \psi_{j,j}\, e_j$$

Therefore

$$\psi^a_{2,2} = \sum_{i=2}^{j-1} \psi^b_{i,i}$$

The test cases shown in Figure 4 were run on the computer to test these results. The equivalent number of modes, damping, and coupling factors were established for a five- and equivalent three-element system. The damping ($\psi_{i,i}$) was then varied from 0.01 to 10 times the coupling ($\psi_{i,j}$). The results are tabulated in Table 2 and presented graphically in Figure 5.

The first observation from Figure 5 is that the agreement in the first element is excellent between the two models, good in the center element, and may or may not be acceptable for the last element at the higher values of $(\psi_{i,i})/(\psi_{i,j})$, depending on the accuracy required and the significance of the computed values. The system analyzed could represent only one of many vibration paths or sources for an actual system.

The equivalent system does give a conservative (high) estimate of the response in the last section. The comparison of the predicted values is better demonstrated in Figures 6 and 7. These figures indicate the equivalent

FIVE-ELEMENT SYSTEM	EQUIVALENT THREE-ELEMENT SYSTEM
S → [1] [2] [3] [4] [5]	S → [1'] [2'] [3']
$N_1^a = N_2^a = N_3^a = N_4^a = N_5^a$	$N_1^b = N_3^b = N_{2/3}^b = N_1^a$
$\psi_{1,2}^a = \psi_{2,3}^a = \psi_{3,4}^a = \psi_{4,5}^a$	$\psi_{1,2}^b = \psi_{2,3}^b$
	$\frac{1}{\psi_{1,2}^b} + \frac{1}{\psi_{2,3}^b} = \frac{1}{\psi_{1,2}^a} + \frac{1}{\psi_{2,3}^a} + \frac{1}{\psi_{3,4}^a} + \frac{1}{\psi_{4,5}^a}$
	$\frac{2}{\psi_{1,2}^b} = \frac{4}{\psi_{1,2}^a}$
	$\psi_{1,2}^b = \frac{\psi_{1,2}^a}{2}$
$\psi_{1,2}^a = 1$	$\psi_{1,2}^b = 1/2$
$\psi_{i,i}^a = 1$	$\psi_{1,1}^b = \psi_{3,3}^b = 1$
$(\omega\eta N_i)$	$\psi_{2,2}^b = 3\psi_{i,i}^a$

Figure 4. Comparative Systems

Table 2

RESPONSE VALUES FOR COMPARATIVE SYSTEMS

Damping / Coupling $(\psi_{1,1}/\psi_{1,2})$	e_1^a e_1^b	e_2^a	e_3^a e_2^b	e_4^a	e_5^a e_3^b
0.01	21 21	20	20 20	19	19 19
0.05	5.1 5.2	4.3	3.8 3.8	3.5	3.3 3.4
0.1	3.0 3.2	2.3	1.8 1.8	1.5	1.4 1.5
0.25	1.6 1.7	1.0	0.63 0.62	0.44	0.35 0.41
0.5	1.0 1.1	0.50	0.26 0.25	0.14	0.094 0.12
1.0	0.62 0.70	0.24	0.09 0.091	0.036	0.018 0.03
2.0	0.37 0.40	0.098	0.026 0.029	0.0072	0.0024 0.0059
4.0	0.21 0.22	0.036	0.0061 0.0086	0.0011	0.00021 0.00096
10.0	0.092 0.095	0.077	0.00065 0.00065	0.000054	0.0000049 0.000077

system is adequate up to a value of one, and may or may not be acceptable at higher values for $(\psi_{i,i})/(\psi_{i,j})$. It is also clear that if levels are desired in the intermediate section, care must be taken in applying this equivalent system.

The overestimate of the response in the last section is the result of an underestimate of the energy dissipated by damping. This suggests a modification to the equivalent system if enough is known concerning the original system.

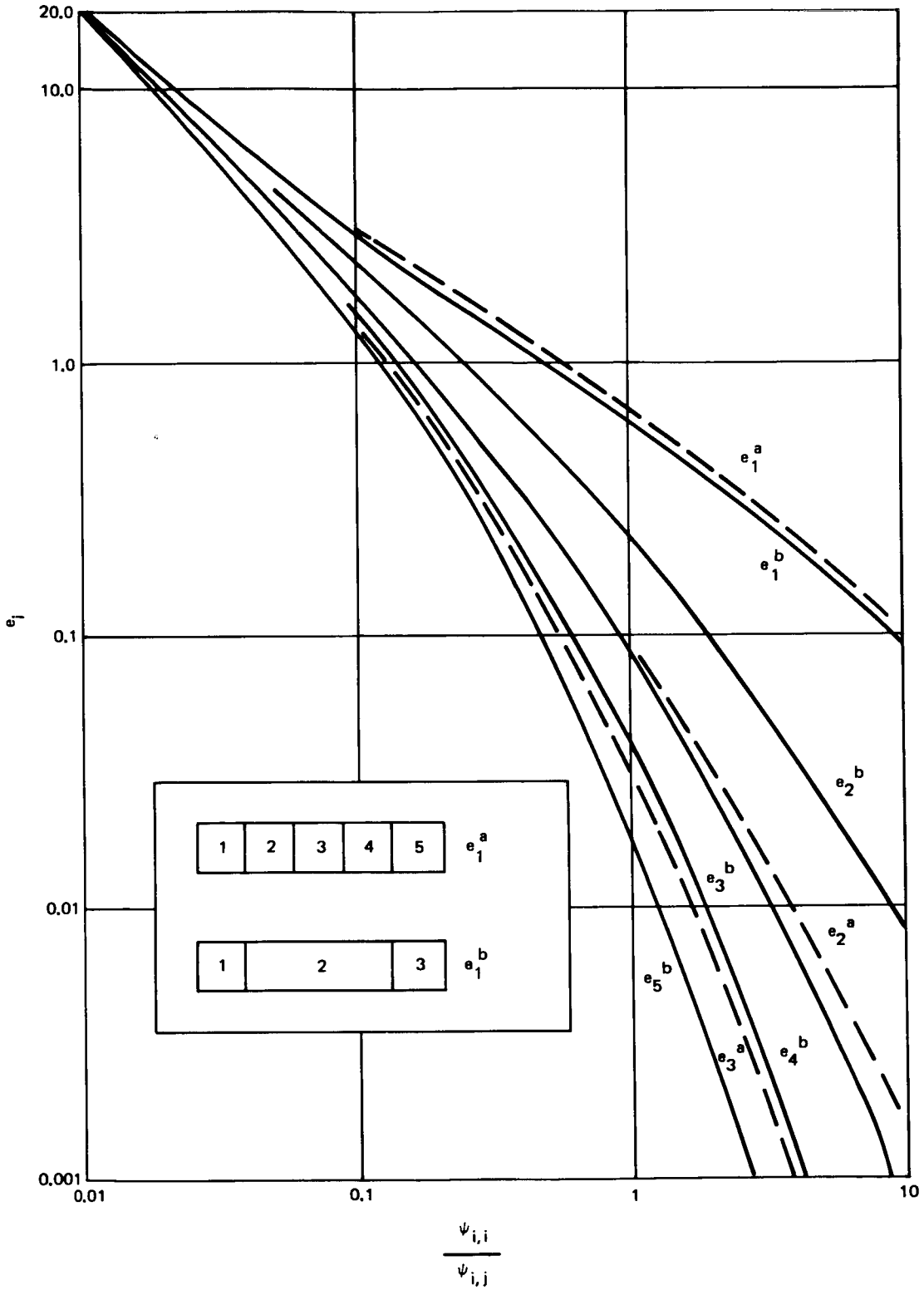

Figure 5. Evaluation of Equivalent Model

CR103

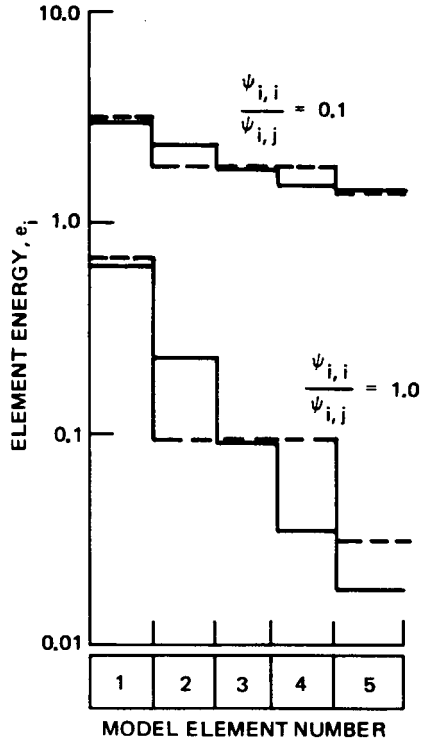

Figure 6. Evaluation of Equivalent Model

CR103

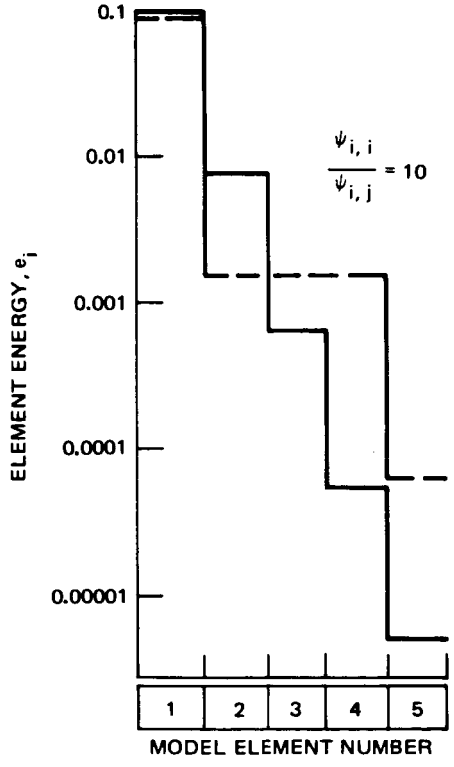

Figure 7. Evaluation of Equivalent Model

To test this, the damping in Subsystem 2 of the equivalent model was adjusted using the following expression

$$\psi^{b}_{2,2} = \sum_{L=2}^{4} \psi^{a}_{i,i} \frac{e^{a}_{i}}{e^{a}_{3}}$$

This resulted in adjusted values of $\psi^{b}_{2,2}$ of

$\frac{\psi^{a}_{1,1}}{\psi^{a}_{1,2}}$	$\frac{\psi^{b}_{2,2}}{\psi^{a}_{1,2}}$ (Adjusted) Damping	$\frac{\psi^{b}_{2,2}}{\psi^{a}_{1,2}}$ (Original) Damping
0.25	0.81	0.75
0.50	1.74	1.5
1.0	4	3
2	10	8
4	28	12
10	130	30

The results obtained using the adjusted damping are shown in Table 3 and Figure 8 where System a represents the original system, Model 1 represents the original model of System 1, and Model 2 represents the model using the corrected damping. The corrected damping results in a marked improvement in predicted levels for the last section as they should, since additional information has been incorporated into the model. The prediction is still conservative. In addition, the agreement in the first subset is still excellent, but the value for the center section of the equivalent is now lower than for the center section of the original model. Again this indicates the need for caution in combining elements in an area where environmental information is required.

Damping

The two-element model can be used to furnish insight on adding damping material to a system in order to lower the response levels. Recall that

Table 3

RESPONSE VALUES FOR COMPARATIVE SYSTEMS WITH ADJUSTED DAMPING

Damping/Coupling $\psi_{1,1}/\psi_{1,2}$	e_1^a e_1^1 e_1^2	e_3^a e_2^1 e_2^2	e_5^a e_3^1 e_3^2
0.25	1.6 1.7 1.7	0.63 0.62 0.58	0.35 0.41 0.39
0.5	1.0 1.1 1.1	0.26 0.25 0.22	0.094 0.12 0.11
1.0	0.62 0.70 0.69	0.09 0.091 0.071	0.018 0.030 0.024
2.0	0.37 0.40 0.40	0.026 0.029 0.019	0.0024 0.0059 0.0037
4.0	0.21 0.22 0.22	0.0061 0.0086 0.0038	0.00021 0.00096 0.00043
10	0.092 0.095 0.095	0.00065 0.0015 0.00036	0.000004 0.000073 0.000017

$\eta_{2,1}$ represents the energy lost from System 2 to System 1 and rewrite the e ratio as

$$\frac{e_2}{e_1} = \frac{\eta_{2,1}}{\eta_{2,1} + \eta_2}$$

In the case where η_2 is on the order of $\eta_{2,1}$ or greater, the ratio of e_2/e_1, and therefore e_2, can be reduced by increasing η_2 (or decreasing $\eta_{2,1}$).

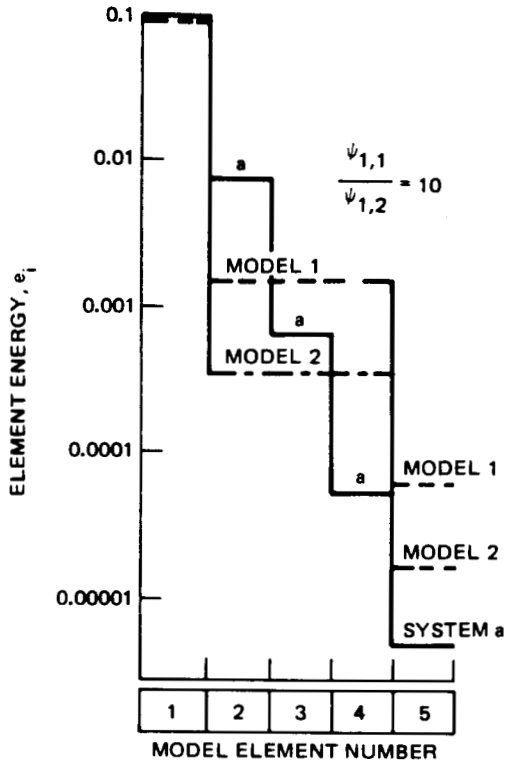

Figure 8. Evaluation of Equivalent Model

As η_2 become smaller compared to $\eta_{2,1}$ the effect of increasing η_2 diminishes. This is often the case for a component or component-carrying structure attached to a large structure such as a vehicle. This should be considered, by simple test if necessary, before damping is added to a component in hopes of reducing its environment. An example of this is the addition of microballoons or foam to the interior of a component for the sole purpose of increasing damping.

The addition of damping will yield a general reduction in response according to

$$S_1 = \psi_{1,1} e_1 + \psi_{2,2} e_2$$

as well as changes in e_1/e_2. This should also be kept in mind when damping is added to reduce vibration.

Additional insight can be obtained by examining the expression

$$\frac{S_1}{e_2} = \psi_{1,1}\left(\frac{\psi_{2,2} + \psi_{1,2}}{\psi_{1,2}}\right) + \psi_{2,2}$$

or

$$\frac{S_1}{e_2} = \frac{\psi_{1,1}\,\psi_{1,2} + \psi_{1,1}\,\psi_{2,2} + \psi_{2,2}\,\psi_{1,2}}{\psi_{1,2}}$$

This expression is symmetric with respect to 1 and 2. Therefore, neither location is intrinsically preferred for an increase in $\psi_{i,i}$ (the addition of damping) when a reduction in e_2 is desired. Rewriting the above equation yields

$$\frac{S_1}{e_2} = \omega\eta_1 N_1 + \omega\eta_2 N_2 + \frac{\omega^2\eta_1\eta_2}{\phi_{1,2}}$$

This form of the expression suggests that damping be added to areas of high modal density and where the increase in damping can be maximized. This is a fairly good description of large thin plates or shells with low damping (the outer skin of a typical flight vehicle).

The form also shows that increasing $\omega^2\eta_1\eta_2/\phi_{1,2}$ may be the best means of reducing e_2. This would be particularly true when System 2 is small and the damping can be increased or $\phi_{1,2}$ decreased (with an isolator) by an appreciable amount. This is the most common method presently used for component environment control but at times it does not yield the desired or expected results.

The general effects of damping on more complex systems can be examined by replotting the response data previously computed for the equivalent systems. The combined effect of damping is that the energy levels (e) will be inversely proportional to damping. This is the general trend observed in

Figure 5. The deviations from this for the case shown in Figure 5 can be examined by multiplying e by the damping ($\psi_{i,i}$) and replotting. The case where e is inversely proportional to damping becomes a horizontal line. This is shown in Figure 9 for the equivalent system.

At low values of $\psi_{i,i}$ the responses of the three elements converge and are proportional to $\psi_{i,i}$ (constant $e\psi_{i,i}$), as expected. As damping is increased, the value of $e_1\psi_{i,i}$ increases, and $e_2\psi_{i,i}$ and $e_3\psi_{i,i}$ start to decrease. As the value of $e_2\psi_{i,i}$ and $e_3\psi_{i,i}$ become small, little energy is dissipated in 2 and 3, and as a result $e_1\psi_{i,i}$ begins to flatten out as its value approaches five times its original value. The value of five is the result of only one-fifth of the damping being contained in Mode Set 1. The figure shows that the general application of damping is very effective for structure away from the source of vibration, but the response in the excited system will be reduced at a rate less than $1/\psi_{i,i}$.

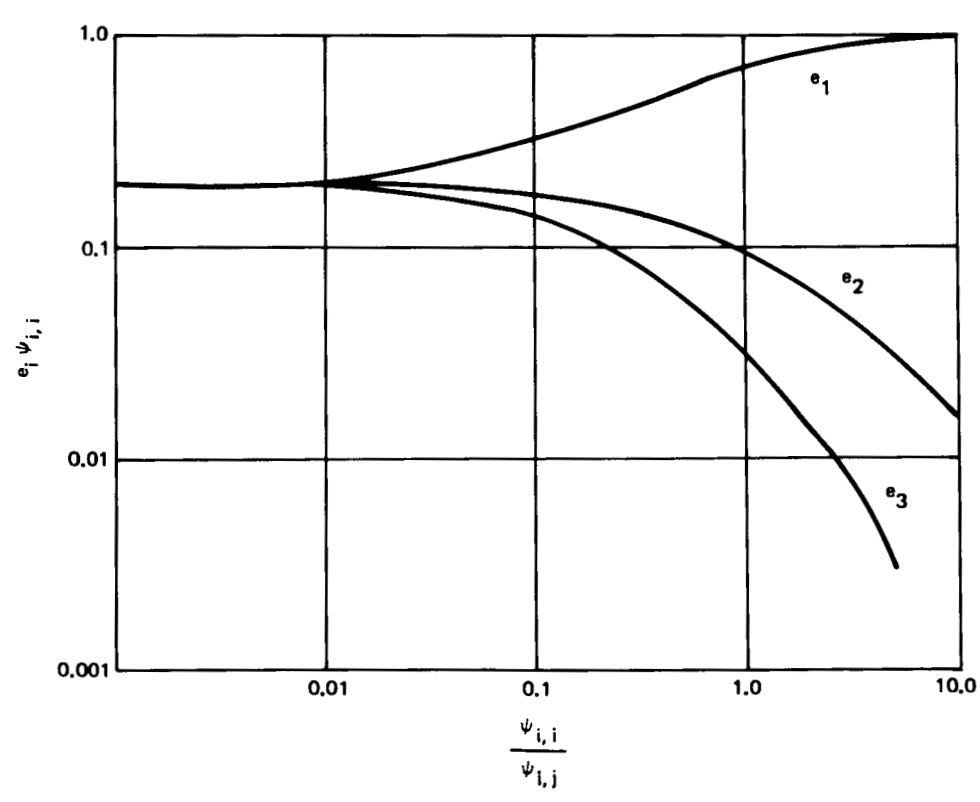

Figure 9. Effect of Damping

The effect of damping location was also examined using the five-element model. This was done by solving for the e's using the model previously discussed with $\psi_{i,i}$ equal to 0.25 and 1.0 times the coupling $\psi_{i,j}$. The damping was increased in one element by an order of magnitude for each run. The elements chosen for the increase were 2, 3, and 4. The results are shown in Table 4. The general observations from the two test runs are basically the same.

First the value of e at or behind the location of higher damping (higher number element) is basically independent of the damping location. The e values in front of the highly damped mode set increased as the damping moved further away. This effect appears to be insignificant for a highly damped system but is significant at the lower values of damping. Again the conclusion is reached that damping is more effective, in an overall sense, close to the point of excitation.

Table 4

EFFECT OF DAMPING LOCATION FOR TWO DAMPING VALUES

S → | 1 | 2 | 3 | 4 | 5 |

$\psi_{11} = \psi_{55} = 0.25$

ψ_{22}	ψ_{33}	ψ_{44}	e_1	e_2	e_3	e_4	e_5
2.5	0.25	0.25	1.00	0.262	0.166	0.116	0.0925
0.25	2.5	0.25	1.33	0.674	0.177	0.122	0..0975
0.25	0..25	2.5	1.48	0.847	0.428	0.116	0.0925

$\psi_{11} = \psi_{55} = 1.0$

ψ_{22}	ψ_{33}	ψ_{44}	e_1	e_2	e_3	e_4	e_5
10.0	1.0	1.0	0.577	0.0450	0.0173	0.00697	0.00346
1.0	10.0	1.0	0.604	0.207	0.0179	0.00714	0.00357
1.0	1.0	10.0	0.616	0.232	0.0796	0.00692	0.00346

Parameter Accuracy

The accuracy of the parameters used in any analysis is of primary importance. In the case of SEA, the modal densities should be, by far, the best-defined parameter included in the model and, therefore, will not be included in the following discussion. The accuracy required for the parameters will be related to the accuracies required from the analysis. A 3-dB analysis accuracy will be assumed for most of the discussion.

First, the average response energy for a total system is inversely proportional to the damping of that system. This leads to root-mean-squared response being inversely proportional to the damping. Therefore, if 3-dB accuracy is desired from analysis, then, in general, a 6-dB accuracy is required in the definition of damping.

Distribution of energy will also be affected by the damping as well as the coupling, as shown in

$$\frac{e_1}{e_2} = 1 + \frac{\eta_2}{\eta_{2,1}} = 1 + \frac{\omega \eta_2}{\phi_{1,2} N_1}$$

where e_1 is the excited section.

This shows that as far as energy distribution is concerned, the same accuracy is required for both η_2 and $\eta_{2,1}$. The effect of deviation of the ratio $\eta_2/\eta_{2,1}$ is insignificant for $\eta_2 \ll \eta_{2,1}$ and maximizes at

$$\frac{e_1}{e_2} = \frac{\overline{V}_1^2}{\overline{V}_2^2} = \frac{\eta_2}{\eta_{2,1}}$$

for $\eta_2 \gg \eta_{2,1}$.

The general result is that damping must be better defined than coupling, since errors in damping affect both the general energy content and energy distribution, while errors in coupling affect only the energy distribution.

For the two extremes (from $\eta \gg \eta_{1,2}$ to $\eta \ll \eta_{1,2}$), the accuracy required in damping to yield response predictions within 3 dB varies from 6 to 3 dB. Over the same range, the accuracy required in coupling varies from infinity to 6 dB. From this, it appears that a reasonable accuracy criterion would be to define the damping to within 6 to 3 dB, depending on the case, and to set the coupling accuracy requirement to a level of 3 dB above the damping accuracy requirement.

This approach for damping can be tested by examining the curves presented in Figure 5. The 6- and 3-dB requirements would yield the desired accuracy of 3 dB. The effect of the general variation due to damping is removed from Figure 5 by replotting the results in the form of Figure 9. The 9- to 6-dB accuracy in $\eta_{1,2}$ again would yield the desired accuracy of 3 dB.

Because of this agreement, it is recommended that the damping values should be defined to within 6 to 3 dB, and that the coupling factor should be defined to within 9 to 6 dB. The choice of a higher or lower accuracy depends on the case of specific interest. It is felt that these guidelines will yield response levels to within 3 dB.

ANALYTICAL MODEL OF UpSTAGE SPECIMEN

Modeling

The UpSTAGE acoustic test specimen was a design configuration of the flight vehicles consisting of the load-carrying structure up to Station 14.5 (i.e., external skin, field joints, and internal bulkheads) without internal components, except for a model of a laser gyro. The specimen, shown in Figure 10, is an elliptical cone, which is separated into four sections by three field joints. Internally the specimen has 12 bulkheads, the 3 field joints, and a closure plate at each end. The skin thicknesses of the sections vary, decreasing from the rear to the front.

The mathematical model used initially for the present analysis is identical to the model used for the earlier UpSTAGE predictions (see Reference 2). This

CR103

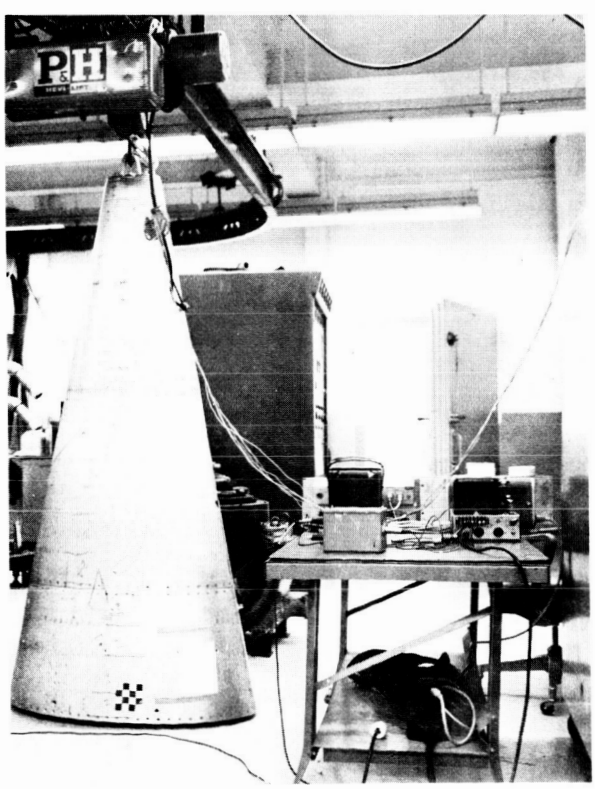

Figure 10. UpSTAGE Acoustic Test Specimen

model separates the specimen lengthwise at the field joints into four basic elliptical sections. The aft section was further divided into four elliptical subsections to allow for localized acoustic inputs at locations that simulate the positions of the UpSTAGE aerodynamic control forces.

The external skin of each section was modeled with four elements, junctions occurring at the points where the two radii of curvature coincide. Since there are seven sections and subsections, this modeling resulted in 28 skin elements as indicated in Figure 11. Each of the internal bulkheads, field-joint bulkheads, and closure plates was modeled as a single element. The complete mathematical model therefore consists of 45 elements. Table 5 presents the elements of the complete model. Because this 45-element model does not treat the aft section consistently with the other sections, an alternate model was also utilized. This alternate model was developed from the original 45-element model by greatly increasing the coupling factor between the subsections within the aft section. This change caused the four subsections to respond as if they were only one section and resulted in a model with essentially 37 elements. This modeling is more consistent with that for the three forward sections; however, it does cause the local acoustic excitation to be effectively spread over a larger area although the total input acoustic power remains the same.

Equation Format

The matrix format developed for SEA systems is

$$\left\{\langle \overline{a^2} \rangle\right\} = \omega^2 \left[m\right]^{-1} \left(\left[D\right]\right) + \left(\left[C\right]\right)^{-1} \left\{S\right\}$$

with $[C]$ formed from $[\Phi]$ and $[N]$ matrices. This format will now be adapted to the current analysis.

The diagonal matrix $[N]$ must be formed in order to obtain $[C]$. The number of modes in a given element is

$$N(\omega) = n(\omega) \cdot (\Delta\omega)$$

where $n(\omega)$ = modal density

FOLDOUT FRAME

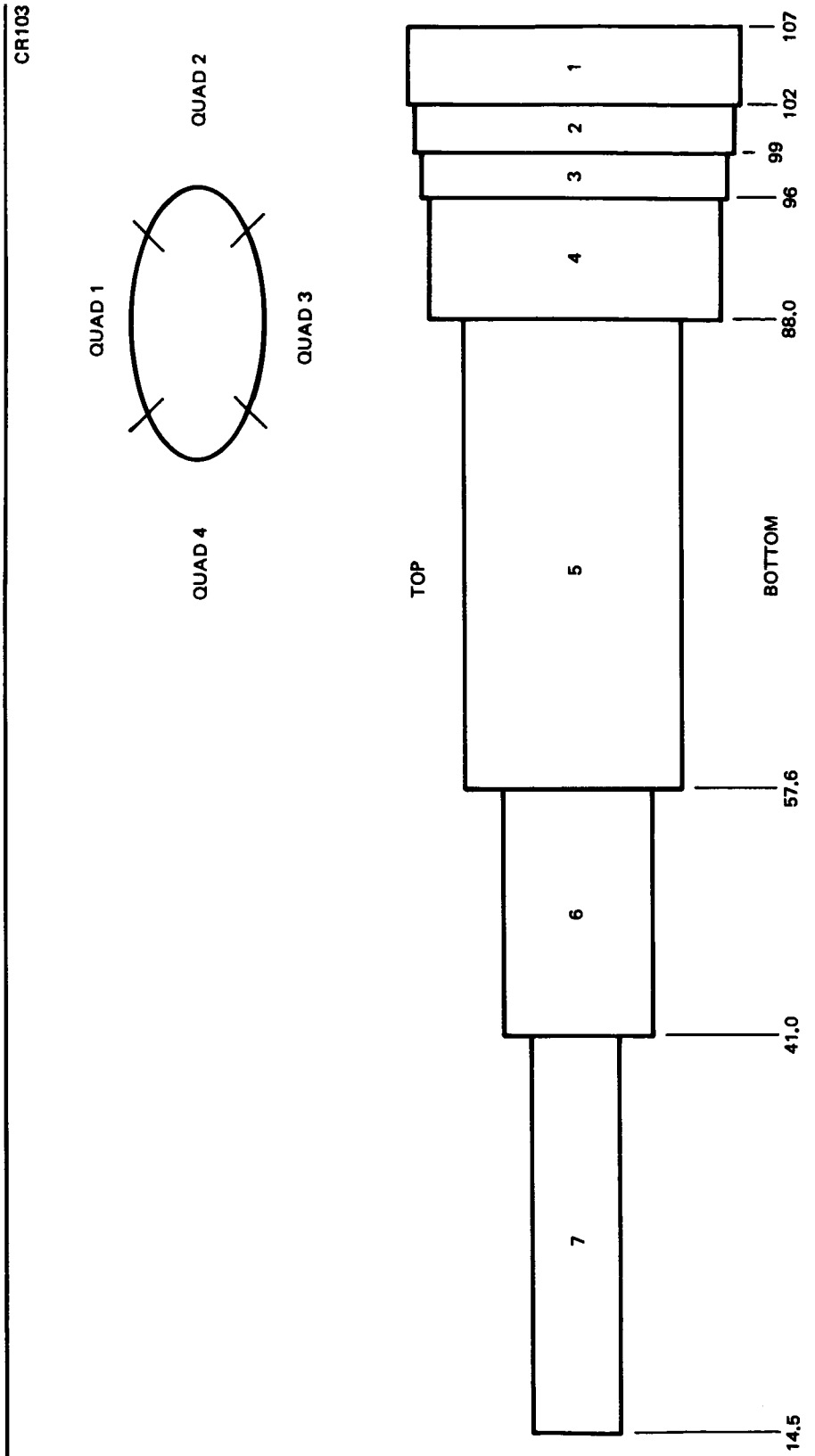

Figure 11. Skin Elements

FOLDOUT FRAME

FOLDOUT FRAME

Table 5

UpSTAGE MODEL ELEMENTS

Sec. No.	Description	Region No.	Quad. No.
1	Skin	1	1
2	Skin	1	2
3	Skin	1	3
4	Skin	1	4
5	Skin	2	1
6	Skin	2	2
7	Skin	2	3
8	Skin	2	4
9	Skin	3	1
10	Skin	3	2
11	Skin	3	3
12	Skin	3	4
13	Skin	4	1
14	Skin	4	2
15	Skin	4	3
16	Skin	4	4
17	Skin	5	1
18	Skin	5	2
19	Skin	5	3
20	Skin	5	4
21	Skin	6	1
22	Skin	6	2
23	Skin	6	3
24	Skin	6	4
25	Skin	7	1
26	Skin	7	2
27	Skin	7	3
28	Skin	7	4

Sec. No.	Description	Sta.	Region No.
29	Aft Bulkhead (B. H.)	107.0	1
30	Forward B. H.	14.5	7
31	Field Joint B. H.	88.2	4-5
32	Field Joint B. H.	57.6	5-6
33	Field Joint B. H.	41.0	6-7
34	Internal B. H.	97.0	3
35	Internal B. H.	92.0	4
36	Internal B. H.	83.5	
37	Internal B. H.	76.3	5
38	Internal B. H.	68.0	
39	Internal B. H.	51.2	6
40	Internal B. H.	46.2	
41	Internal B. H.	36.7	
42	Internal B. H.	31.9	
43	Internal B. H.	28.0	7
44	Internal B. H.	24.0	
45	Internal B. H.	19.4	

Table 6

CONSTANTS FOR MATHEMATICAL MODEL

Section	Area (A)	Thickness (t)	$(t)^2$	Ring Freq (Hz)	A/t^2	A/t	At
1 and 3	172.5	0.31	0.096	1,025	1,795	557	53.5
2 and 4	70.5			4,250	733	227	21.8
5 and 7	107.0	0.16	0.026	1,065	4,180	670	17.1
6 and 8	43.5			4,425	1,700	272	6.95
9 and 11	108.5	0.16	0.026	1,100	4,240	678	17.35
10 and 12	44.5			4,550	1,740	278	7.13
13 and 15	250.5	0.16	0.026	1,165	9,800	1,770	40.0
14 and 16	102.0			4,820	4,000	638	16.3
17 and 19	757.0	0.125	0.013	1,530	57,400	6,150	94.6
18 and 20	309.0			6,370	23,300	2,460	38.5
21 and 23	269.0	0.125	0.013	2,225	21,500	2,150	33.7
22 and 24	109.5			9,250	8,250	875	13.7
25 and 27	254.0	0.090	0.008	5,000	31,400	2,820	22.9
26 and 28	103.0			21,000	12,700	1,145	9.27
29	733.0	0.25	0.063	NA	NA	2,940	183.2
30	13.5	0.09	0.008	NA	NA	150	1.21
31	497.0	0.125	0.013	NA	NA	4,000	62.0
32	213.0	0.08	0.0064	NA	NA	2,660	17.0
33	108.0	0.09	0.0081	NA	NA	1,200	9.7
34	573.0	0.09	0.0081	NA	NA	6,370	51.3
35	550.0	0.09	0.0081	NA	NA	6,120	49.5
36	450.0	0.08	0.0064	NA	NA	5,520	36.0
37	375.0	0.08	0.0064	NA	NA	4,630	30.0
38	298.0	0.08	0.0064	NA	NA	3,770	31.8
39	169.0	0.07	0.0049	NA	NA	2,420	11.9
40	138.0	0.07	0.0049	NA	NA	1,970	9.6
41	86.5	0.09	0.0081	NA	NA	950	7.7
42	65.3	0.07	0.0049	NA	NA	930	4.2
43	50.3	0.07	0.0049	NA	NA	720	3.5
44	37.0	0.07	0.0049	NA	NA	578	2.6
45	24.2	0.07	0.0049	NA	NA	346	1.7

The structure presently being analyzed is made up of flat plates (end plates and internal bulkheads) and curved plates (external skin). The modal density of a plate is given as

$$n_b = A_s \Big/ \left[4\pi \sqrt{\frac{D}{\rho h}} \right]$$

where

A_s = area
D = bending stiffness
ρ = density in mass/volume
h = thickness

The modal density for a curved plate is

$$n_c = n_p \cdot (CF)$$

CF is a correction factor that accounts for the curvature effects of the panel. An approximate value used for CF is

$$CF = \left(\frac{\omega}{\omega_r} \right)^{2/3} \quad \text{for } \omega < \omega_r$$

$$= 1 \quad \text{for } \omega > \omega_r$$

where $\omega_r = C_L/r$ is the ring frequency of the system. A more exact CF is presented in Figure 3. This type of correction could be easily incorporated in a generalized computer program for SEA. Both CF forms have been incorporated into the UpSTAGE model. The results of these calculations are presented and discussed in a later section.

For the UpSTAGE specimen analysis, the damping factor and the base value for the coupling parameter were evaluated by a series of tests, which will be examined in the following section.

The relative values of coupling in the $[\Phi]$ matrix were initially assigned on the basis of engineering judgment. The aspect will be further examined as the computed response is compared with test measurements in a later section of this report. The base coupling value (from the test program) was considered to apply to the coupling across the field joints between the four sections. The other element coupling is between skin and internal bulkheads (and endplates), and circumferentially around the skin. The initial coupling values relative to the field joints were selected as 1/3 for the bulkhead/skin coupling and 10 for the circumferential coupling.

The acoustic input term is developed by considering a separate acoustic field coupled to each excited model element. The power flow terms for the acoustic element are:

$$\phi_{j,ac}\ N_j\ E_{ac} - \phi_{j,ac}\ N_{ac}\ E_j$$

The first of these terms represents the acoustic power input to the element. The second term is the power radiated from the element to the acoustic field and will be accounted for in the damping term for the element. However, this term can be used to evaluate the acoustic coupling element $\phi_{j,ac}$.

Reference 4 presents an expression for the acoustic power radiated in terms of the radiation efficiency. Equating the given value to the radiation term above gives

$$\phi_{j,\ ac}\ N_{ac}\ E_j = \sigma_j\ A_j\ \rho_o\ c_o\ \langle \overline{V_j^2} \rangle$$

where

σ_j = radiation efficiency

Substituting for E_j and solving for the acoustic coupling factor

$$\phi_{j,\ ac} = \frac{\sigma_j\ A_j\ \rho_o\ c_o}{N_{ac}\ m_j}$$

This expression may now be substituted into the acoustic input term, giving

$$\phi_{j,ac} \; N_j \; E_{ac} = \frac{\sigma_j \; A_j \; \rho_o \; c_o}{N_{ac} \; m_j} \; N_j \; E_{ac}$$

Reference 5 provides useful expressions for the number of modes, N_{ac}, and total energy, E_{ac}, of a reverberant chamber:

$$N_{ac} = \frac{\omega_o^{\,2} \; V \; (\Delta\omega)}{2\pi^2 \; c_o^{\,3}}$$

$$E_{ac} = \frac{<\overline{P^2}> V}{\rho_o \; c_o^{\,2}}$$

Consequently the acoustic input term will be expressed as

$$S_j = \phi_{j,\,ac} \; N_j \; E_{ac} = \frac{2\pi^2 \; c_o^{\,2} \; A_j <\overline{P_j^{\,2}}> \sigma_j}{\omega_o^{\,2} \; (\Delta\omega) \; m_j} \; N_j$$

or

$$\{S\} = \frac{2\pi^2 \; c_o^{\,2}}{\omega^2 \; \Delta\omega} \left[A\right]\left[\frac{1}{m}\right]\left[\sigma\right]\left[N\right] \left\{<\overline{P^2}>\right\}$$

The values for radiation efficiency were obtained from data in Reference 4. These data were scaled on both the ring and the critical frequencies of the elements.

The properties relating to acoustic medium that appear in this expression for the input are c_o, $<\overline{p}^2>$, and σ. The only one of these terms that is unique to the assumed reverberant field is σ. Therefore, this input representation

would seem to be valid for nonreverberant acoustic fields if a proper value for σ can be determined for the field.

Performing all the indicated substitutions changing from rad/sec to Hz, and expressing the solution for the system response in power spectral density [PSD(g^2/Hz)] form, the complete matrix formulation for the SEA response solution in a single frequency band of a general system is

$$\left\{ \frac{\langle \overline{a^2} \rangle}{(\Delta f)\, g^2} \right\} = \left[W \right]^{-1} \left(\left[D \right] + \left[C \right] \right)^{-1} \frac{\pi c_o}{(\Delta f)^2} \left[\sigma \right] \left[N \right] \left[\frac{A}{W} \right] \left\{ \langle \overline{P^2} \rangle \right\}$$

This format was utilized for response solutions during the study. The following section will consider the elements of the two matrices not yet defined, $[D]$ and $[C]$.

Solutions were obtained for each of the one-third-octave bands from 500 Hz to 3,150 Hz. The evaluation of this analysis, which appears later in this report, will utilize root-mean-squared values for the one-third-octave-band accelerations that correspond to the power spectral densities obtained in the solutions.

TEST PROGRAM

Tests were performed during the program to:

A. Determine SEA parameter values for the damping and coupling for use in analyzing the UpSTAGE acoustic test specimen.

B. Provide general insight into the characteristics of the SEA coupling parameter.

C. Establish a method of determining SEA damping and coupling parameters by performing tests on simplified structures.

The test program was carried out with three basic test specimens, each one consisting of two panels with connecting tee-joint fabricated to simulate the aft joint of the UpSTAGE acoustic specimen. Figure 12 shows the general specimen configuration and Figures 13, 14 and 15 detail the test parts.

CR103

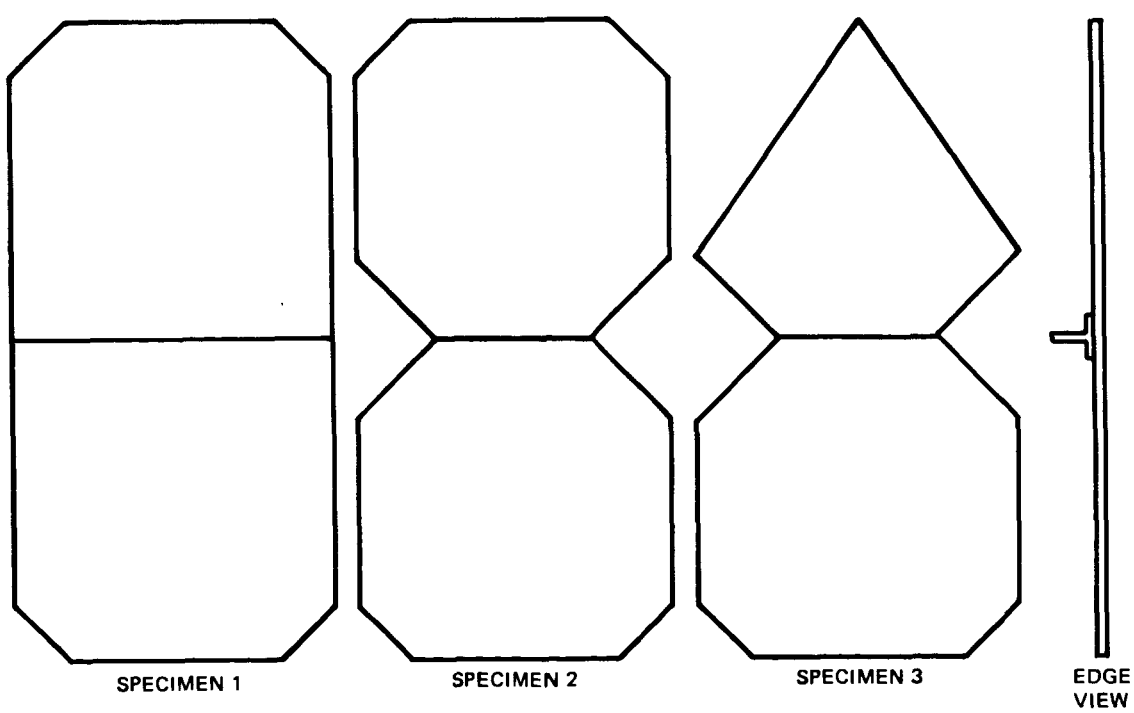

Figure 12. Panel Test Configurations

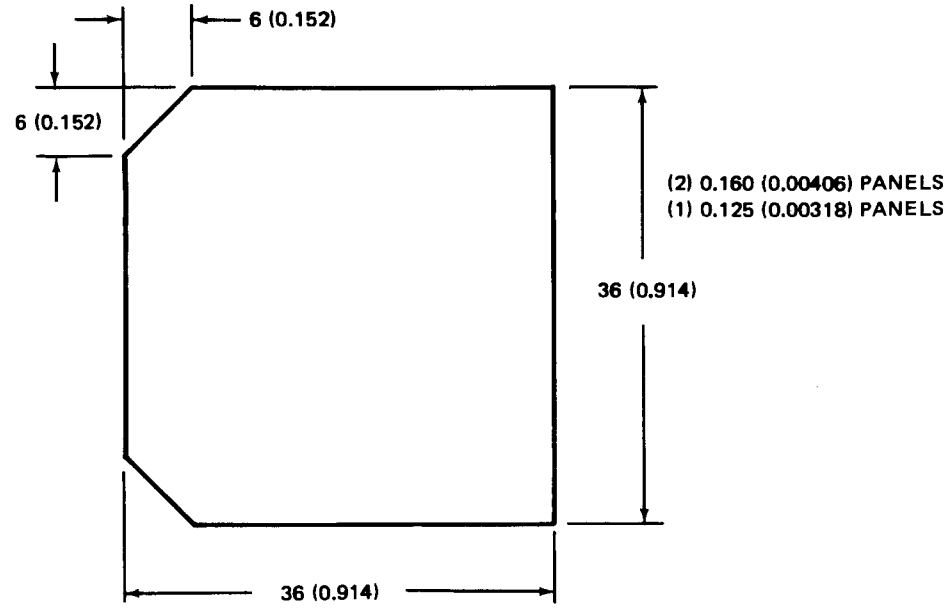

SPECIMEN 1

ALL MATERIAL 6061-T6A1, ALL DIMENSIONS IN INCHES (METERS)

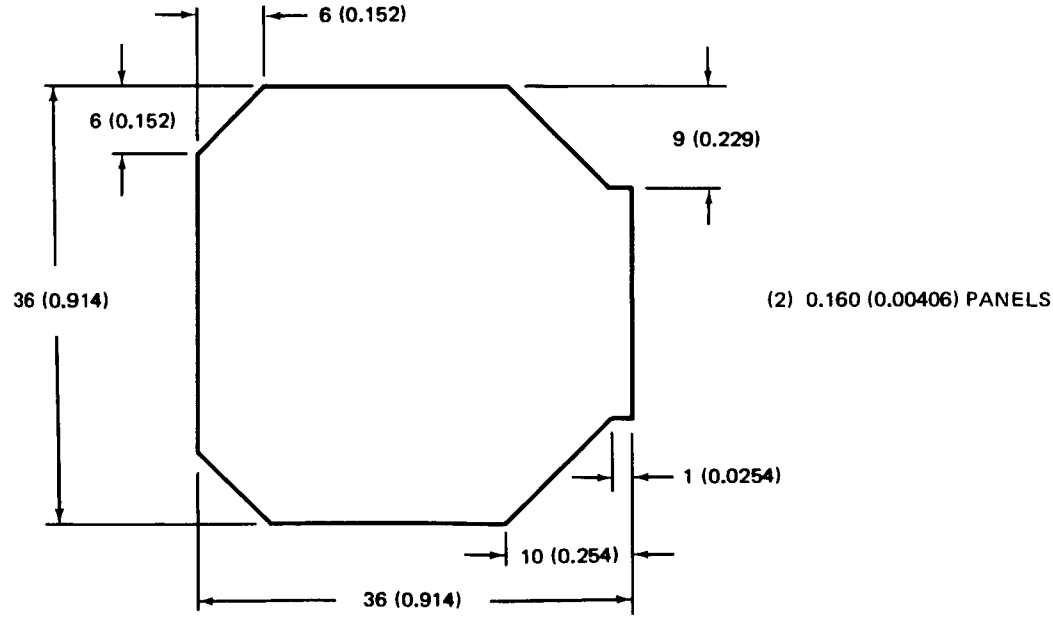

SPECIMEN 2

Figure 13. Test Panel Dimensions

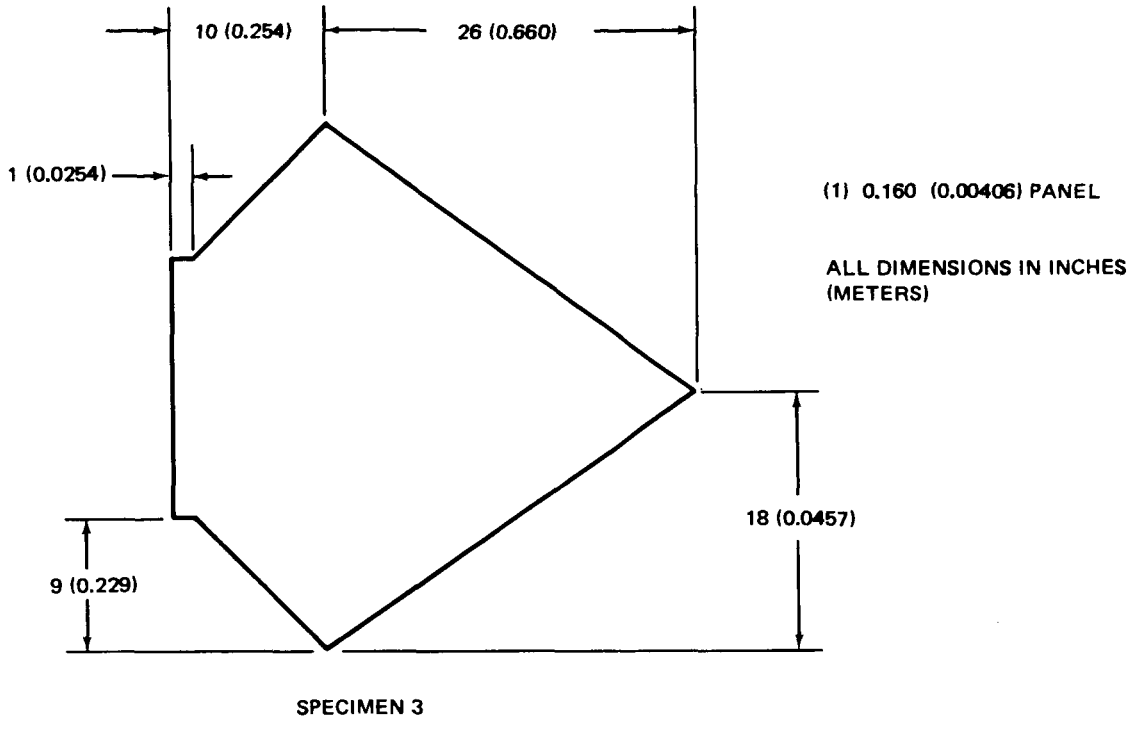

Figure 14. Test Panel Dimensions

Specimens 1 and 2 were designed to furnish information on the effects of joint length on the coupling parameter, while Specimen 3 was designed to evaluate an unsymmetric configuration. The panels were made of aluminum with a basic size of 3 feet by 3 feet (0.914 meter by 0.914 meter). Because the skin thickness is different on the two sides of the UpSTAGE joint being simulated, three panels were fabricatedfor Specimen 1, two with a thickness of 0.160 inch (0.00406 meter) and one with a thickness of 0.125 inch (0.00318 meter), so that a joint with the appropriate skin thickness variation could be examined, as well as a joint that was completely symmetric. Specimens 2 and 3 used only panel thicknesses of 0.160 inch (0.00406 meter).

The primary purpose of the tests is to evaluate the coupling parameter ϕ. This is done by exciting one panel, measuring the response in both panels, and solving for $\eta_{1,2}$ or ϕ in the expression

$$\frac{E_1}{E_2} = \frac{N_1}{N_2} \cdot \frac{\eta_{1,2}}{\eta_{1,2} + \eta_1}$$

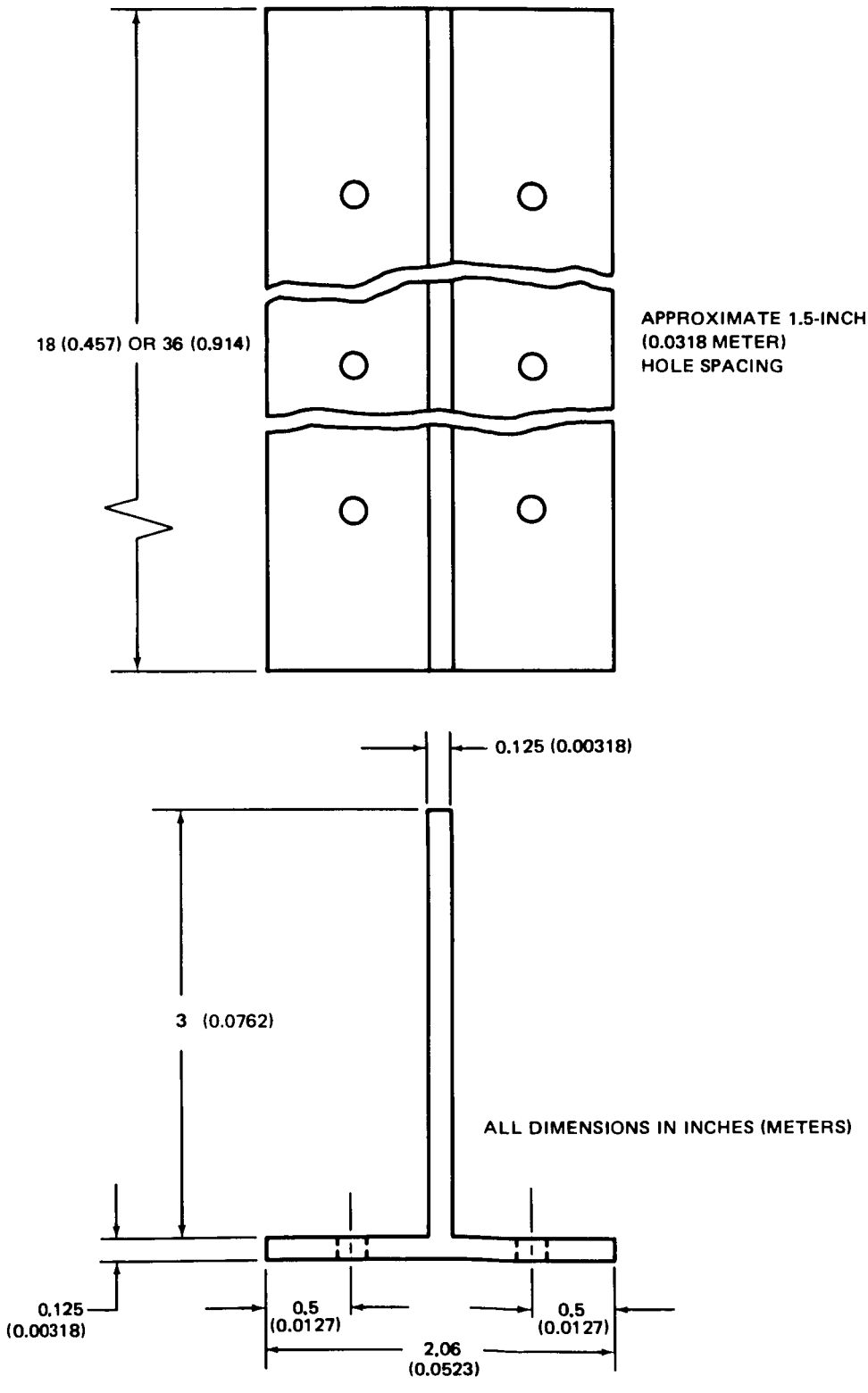

Figure 15. Test Panel Joint Configuration

where

$$\eta_{1,2} = \frac{\phi N_2}{\omega}$$

The damping of the panels (η) must be evaluated before ϕ can be obtained. In addition, η is required in the analysis of the total system. This leads to two types of testing, the first to determine damping, and the second to determine ϕ.

The original intent was to support the test panels in a specially constructed test frame. It was found that the frame transmitted too much vibratory energy between the panels to allow the coupling through the tee joint to be evaluated. Consequently, all testing was accomplished with the panels suspended on elasticized cords (bungees). Figures 16 and 17 show these two test configurations.

Endevco 2226 accelerometers were used for all testing. These accelerometers weigh 2.8 grams and furnish ±5 percent accuracy to 5,000 Hz, with a first resonance at 24,000 Hz. The accelerometers and the shaker itself were attached to the panels with double-sided adhesive tape. The use of this tape was evaluated initially by mounting two accelerometers at the same location but on opposite sides of a panel, one attached with a dental cement and the other with the adhesive tape. The indicated vibration responses of the two accelerometers were identical throughout the measured frequency spectrum (up to 8,000 Hz). The accelerometers were checked for security of mounting prior to each test. No apparent difficulties were noted with this mounting technique.

Damping Test

Damping was determined by exciting the system of interest and observing the response. These tests are referred to as "bop tests" and were performed by striking the panel with a steel hammer or wooden stake and recording a decay trace of the panel vibration response with an oscillograph. The response signal from an accelerometer mounted on the panel was routed through an

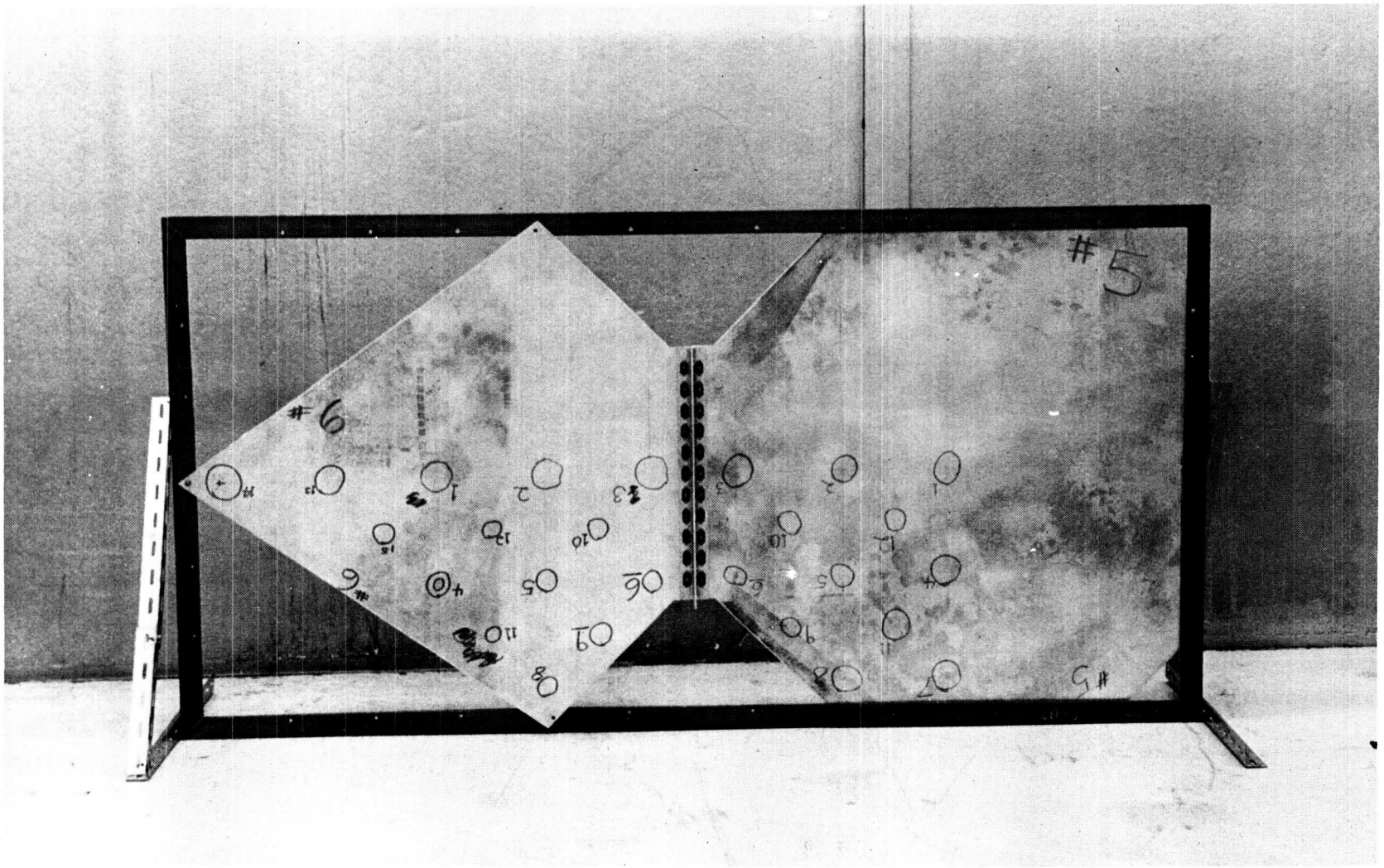

Figure 16. Panels in Frame

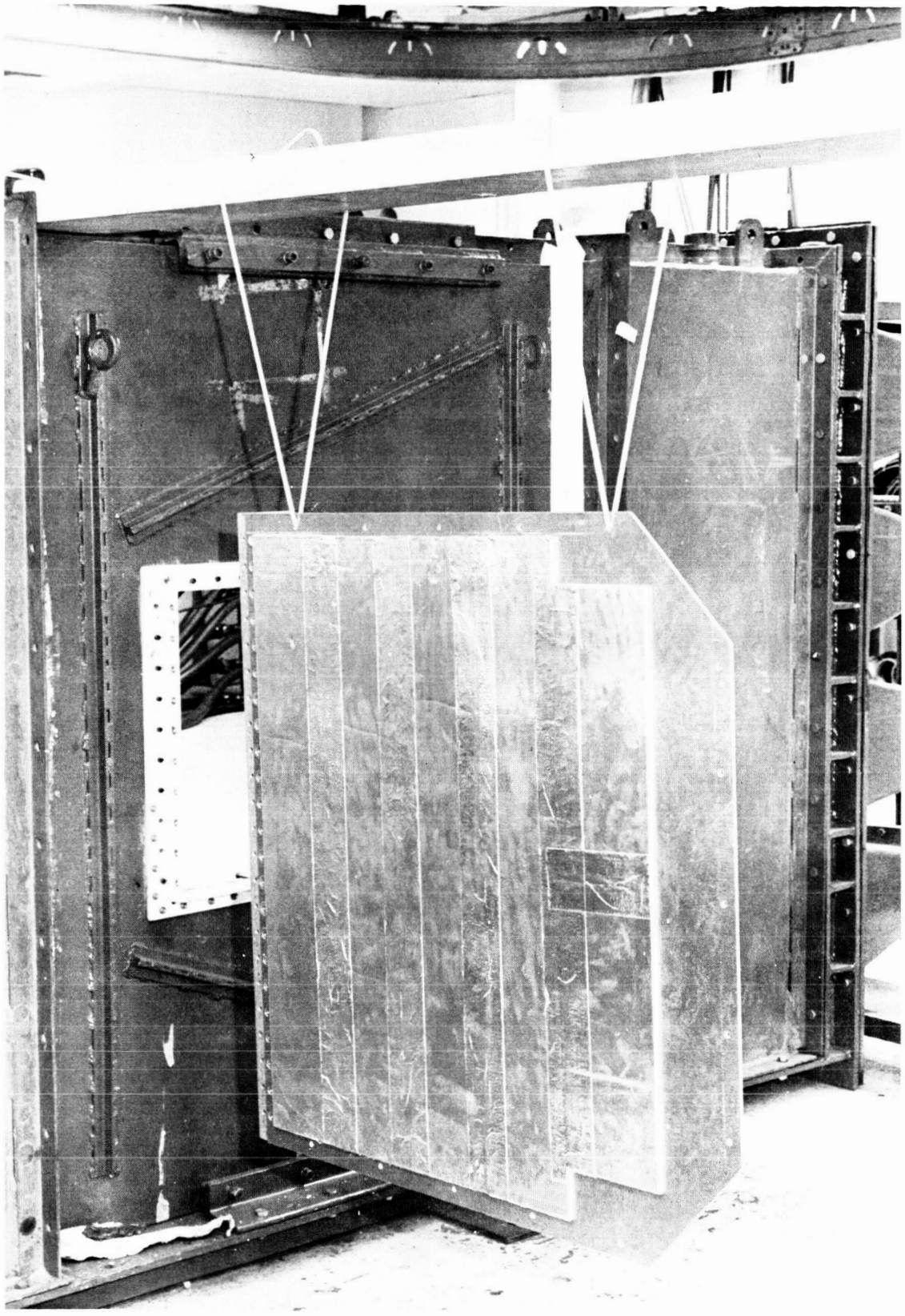

Figure 17. Panel on Bungees

adjustable bandpass filter prior to being recorded with the oscillograph. This filter permitted various bandwidths and center frequencies to be selected. The data obtained from the testing consisted of decay traces using both octave and third-octave bandwidths with center frequencies encompassing the range of 400 to 4,000 Hz. This method permitted the vibration response of the panels to be observed graphically as it decayed to about one-tenth of the initial level (in g's). This decay was plotted on semi-logarithmic paper and a straight line drawn to approximate the decay slope.

This approximate decay slope permitted the fraction of critical damping to be evaluated for an assumed exponential type of decay. The damping for each specimen was measured with both octave and third-octave bandwidths at two locations on the specimen.

Typical decay traces and plots on logarithmic paper are shown in Figures 18 and 19.

Early in the test program it became evident that the damping of the system would have to be increased to obtain meaningful values of the coupling parameter (see below). This was accomplished by applying a single layer of Scotchfoam damping tape to the panels (see Figure 20). This material is essentially a 1/4-inch (0.000635-meter)-thick polyurethane foam pad with an aluminum foil protective cover. The Scotchfoam is self-adhering to metal surfaces. The majority of the observations made concerning damping were made on the damped panels. The values obtained with and without damping, and also data consistency, for two locations on a given panel are presented in Table 7 for a test panel of Specimen 2 configuration. The primary effect of the added Scotchfoam was to raise the damping by a factor of approximately 8. It should be noted that the base panel was 0.16-inch (0.00406-meter)-thick aluminum and that the addition of Scotchfoam to panels of different gage would result in different changes in damping.

The damping values are averaged values of all the data taken at each center frequency. Since two locations were used for each panel together with two analysis bandwidths, the averages are of four values at the octave center

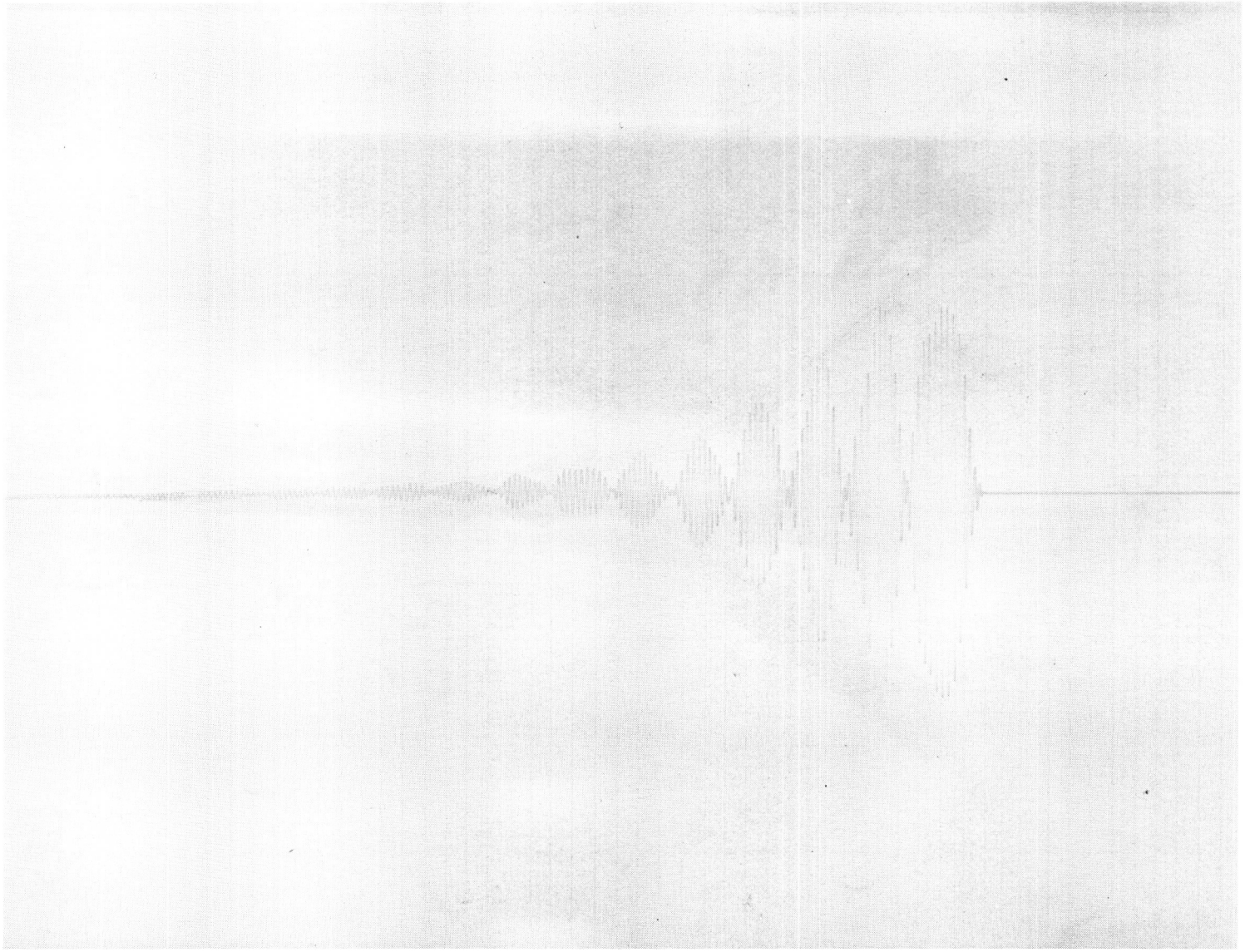

Figure 18. Decay Trace

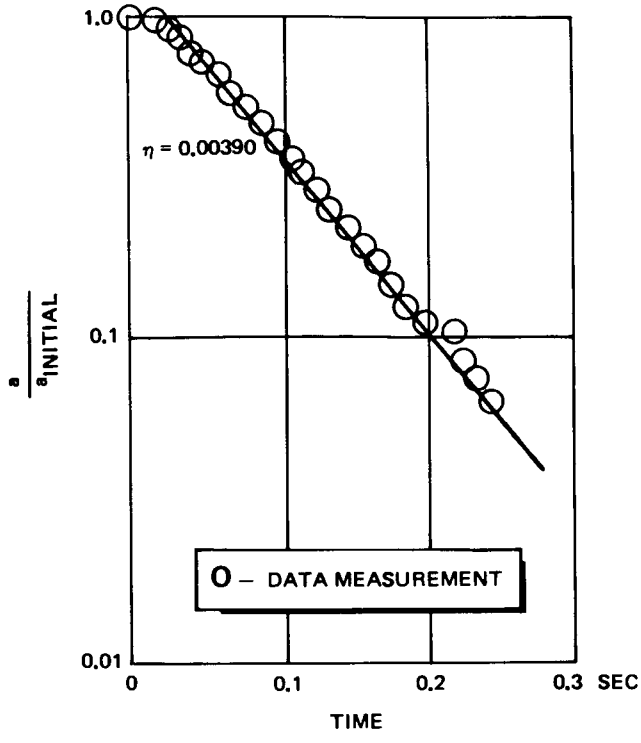

Figure 19. Graphic Determination of Decay Slope

frequencies (400, 800, 1,600, 3,200 Hz) and two values for each of the other frequencies.

Figure 21 presents the damping data obtained for a damped 0.160 panel of each of the three configurations. The range of values for the damping parameter is from 0.005 to 0.015. Two phenomena are shown in the graph. First, close examination reveals a peaking effect which occurs for the Specimen 1 and 2 panels near 2,000 Hz, but not for the Specimen 3 panel. The effect is greater for the Specimen 1 panel. This seems to indicate a shape effect which diminishes as the panels become less square. The frequency of this peaking effect corresponds to a bending wave speed of about 3,000 ft/sec (914 m/sec) or 1.5 ft/cycle (0.457 m/cycle) (half the width of the panel). The second phenomenon is evident when the 2,000 Hz peaking is removed from the data; namely, the reduction in damping as frequency increases.

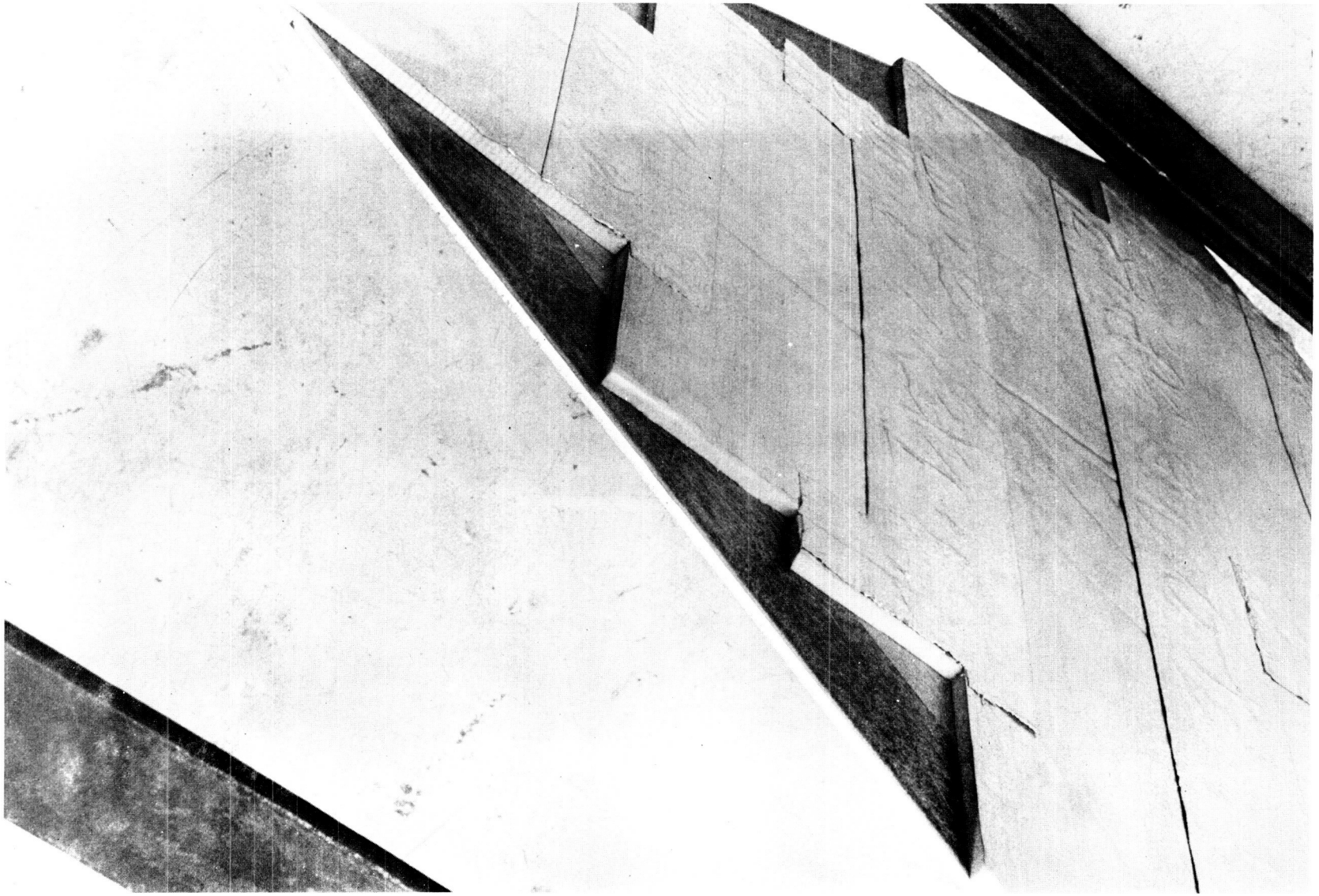

Figure 20. Closeup of Scotchfoam Application

Table 7

DAMPING DATA OBTAINED FOR A SINGLE PANEL OF SPECIMEN 2 CONFIGURATION

	Panel with Damping Tape Applied						
	Measured Damping (C/Cc)				Average Value	Standard Deviation	Fractional Error
	Location 1		Location 3				
f	1/3 Octave	Octave	1/3 Octave	Octave	μ	σ	σ/μ
400	0.00531	0.00442	0.00504	0.00497	0.00494	0.000326	0.0655
500	0.00434		0.00471		0.00452	0.000185	0.0409
630	0.00150		0.00520		0.00335	0.00185	0.552
800	0.00394	0.00395	0.00420	0.00452	0.00415	0.000236	0.0570
1000	0.00497		0.00337		0.00417	0.000800	0.192
1250	0.00566		0.00432		0.00499	0.000670	0.134
1600	0.00663	0.00448	0.00585	0.00389	0.00521	0.00108	0.208
2000	0.00556		0.00572		0.00564	0.0000800	0.0142
2500	0.00318		0.00354		0.00336	0.000180	0.0536
3150	0.00297	0.00303	0.00235	0.00207	0.00260	0.000408	0.157

Bare Panel

One-third octave, 1000 Hz only, three measurements gave
C/Cc = 0.000137, 0.000119, 0.000117; average = 0.000124

Octave, 800 Hz only, three measurements gave
C/Cc = 0.000182, 0.000175, 0.000165; average = 0.000174

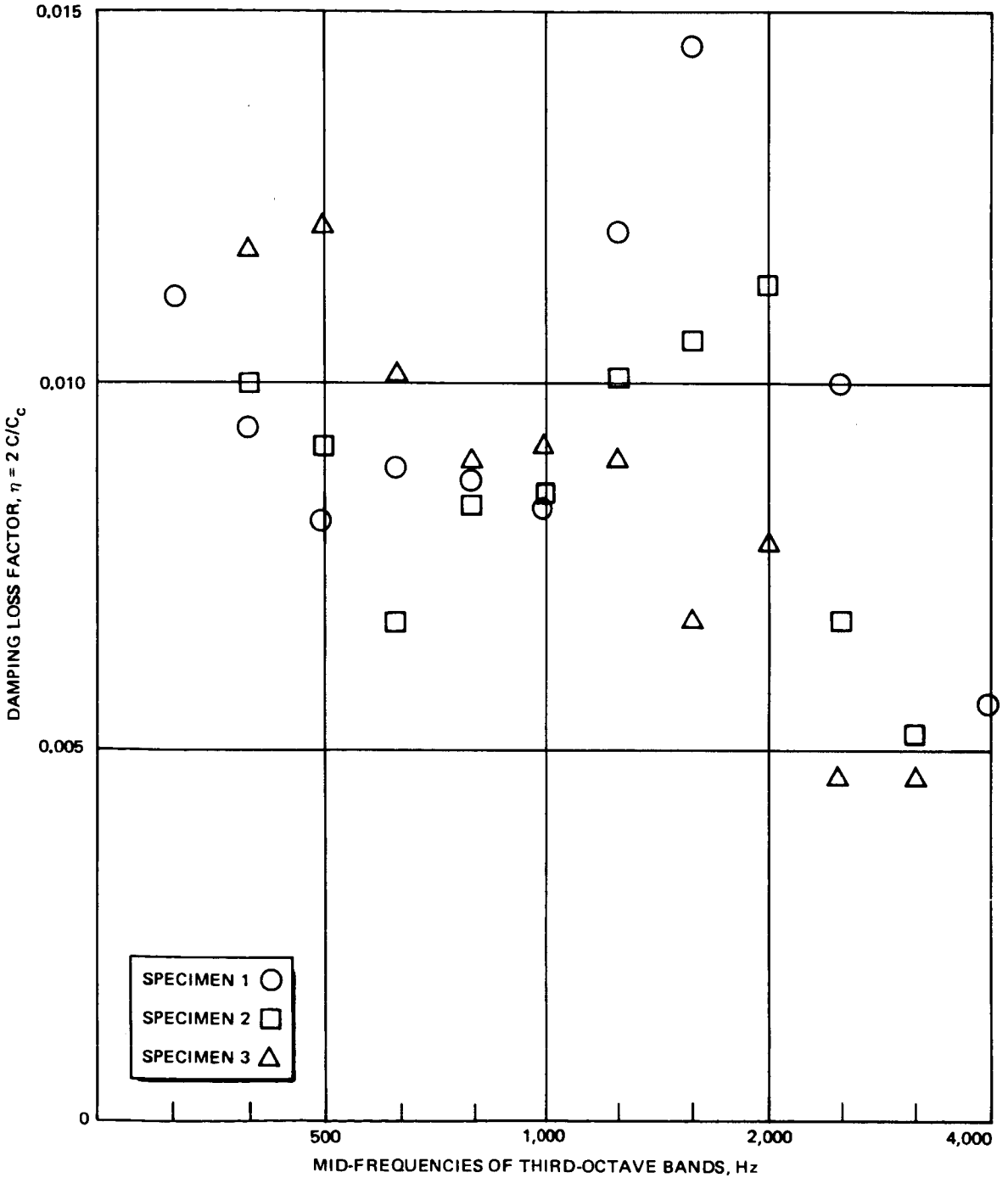

Figure 21. Damping Loss Factor for 0.160 Panels (with Damping Tape Applied)

Figure 22 presents a comparison of the damping data for the 0.125 and 0.160 panels of Specimen 1. These data illustrate the greater effect of the damping tape on the thinner panel. The same type of peaking and frequency rolloff is evident for the 0.125 panel as was found for the 0.160 panels.

Figure 23 presents the damping data for the undamped panels. It is noteworthy that these damping values agree with data published in Reference 9 (and summarized in Reference 8) for the 6061-T6 aluminum alloy panel material. The addition of the damping tape is noted to have increased the damping by a factor of 8.

Vibration Tests

The vibration portion of the testing was accomplished by exciting the panels with a 1-pound (4.45 Newton) force Goodman shaker. The input spectrum for the testing was furnished by a random noise generator. The evaluation of joint coupling required only that the relative level of vibration on the two panels of a specimen be determined; consequently, no specific input was required. Input control was achieved by operating consistently at an overall level of 5 G_{rms}.

Vibration data was reduced with a Spectral Dynamics SD301B Real-Time Analyzer using approximately 15-second samples of steady-state data. A complementary filter set allowed this data to be reduced in the form of G_{rms} in third-octave bands

The accuracy of the approach can be established by considering the expression

$$\frac{\sigma}{\mu} = \frac{1}{\sqrt{\text{bandwidth x sample time}}}$$

This defines the standard deviation of the reduced value (Reference 6). This is a 3σ data reduction accuracy within 0.5 dB for the narrowest bandwidth used during this study.

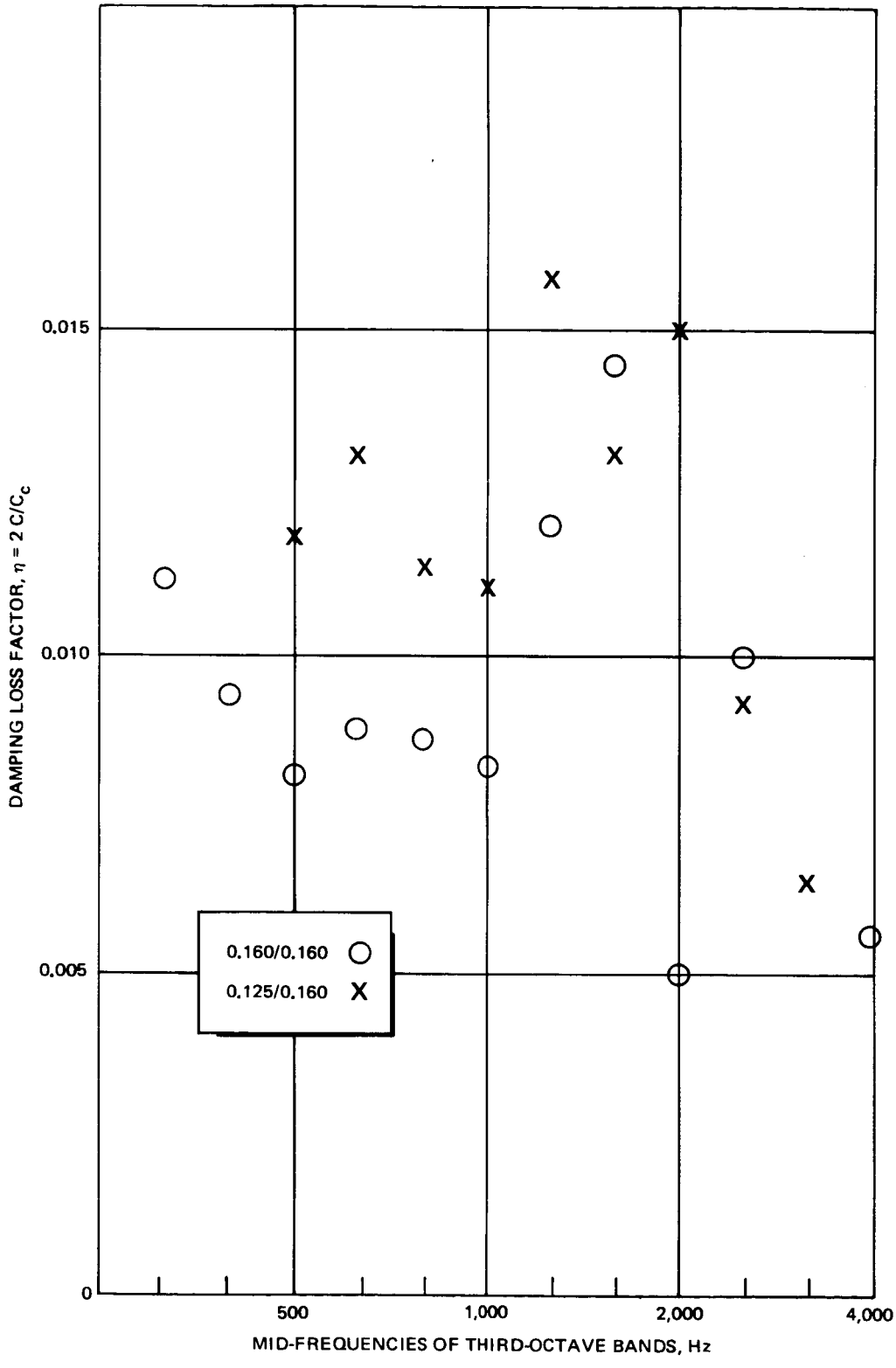

Figure 22. Damping Loss Factor for Two Configurations of Specimen 1 (with Damping Tape Applied)

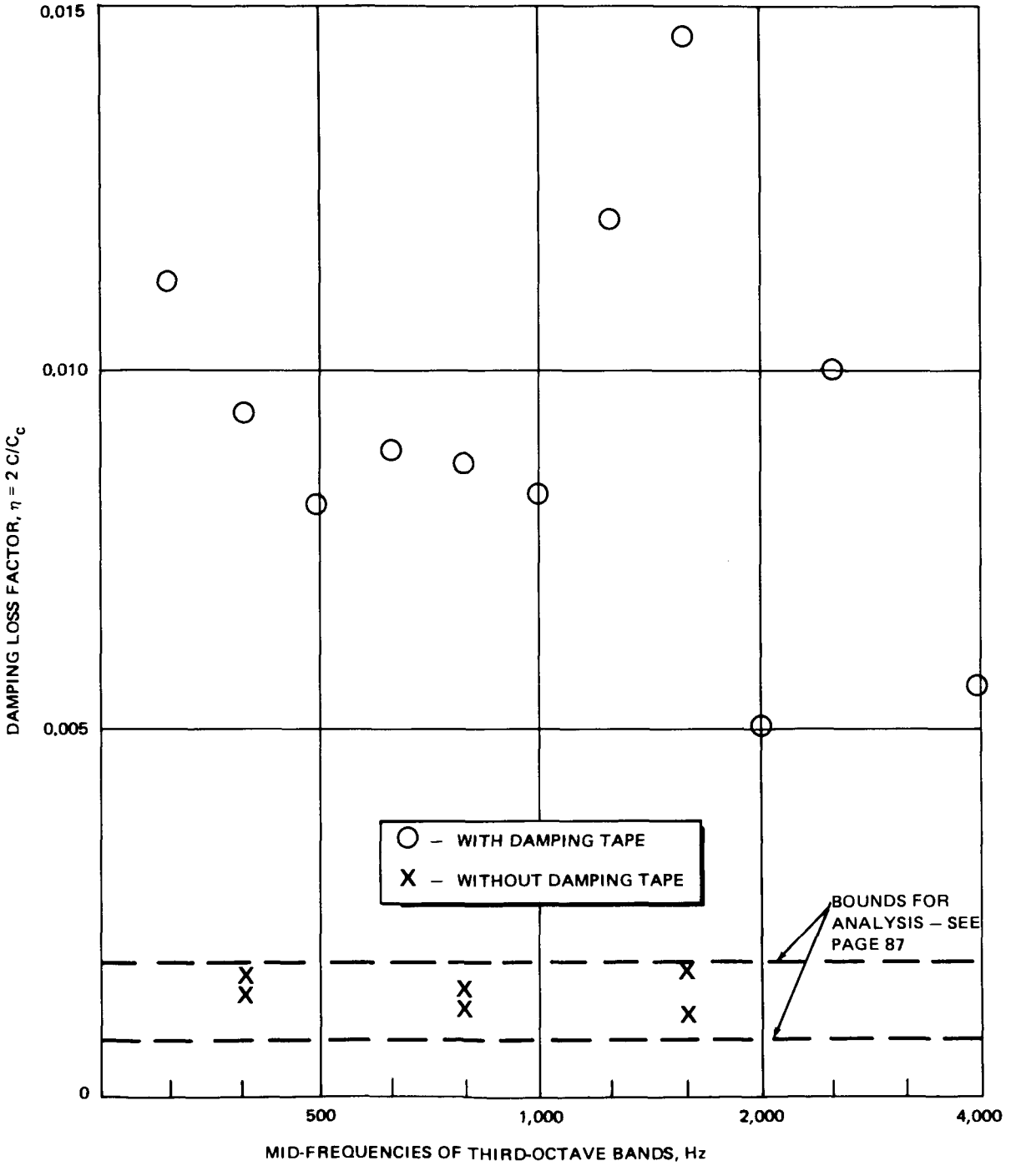

Figure 23. Damping Loss Factor for Specimen 1 Panels with and without Damping Tape

As was stated, the average mode-to-mode coupling parameter, ϕ, was evaluated with the equation for the relative energies of a two-element system:

$$\frac{E_1}{E_2} = \frac{m_1}{m_2} \frac{\overline{<a_1^2>}}{\overline{<a_2^2>}} = \frac{N_1}{N_2} \frac{\eta_{1,2}}{\eta_{1,2} + \eta_1} = \frac{N_1}{N_2} \frac{\frac{\phi N_2}{\omega_o}}{\frac{\phi_{1,2} N_2}{\omega_o} + \eta_1}$$

This equation indicates that for a very small damping

$$\left(\frac{\phi_{1,2} N_1}{\omega_o} \gg \eta_1 \right)$$

the ratio E_1/E_2 will be very close to unity. This situation occurred when attempting to evaluate the coupling parameter before adding Scotchfoam to the panels, and measurement inaccuracy made it impossible to obtain reliable coupling values.

For the symmetric Specimens 1 and 2, the coupling relation reduced to

$$\frac{\overline{<a_1^2>}}{\overline{<a_2^2>}} = \frac{\frac{\phi N_2}{\omega_o}}{\frac{\phi N_2}{\omega_o} + \eta_1}$$

while the element masses and modal density ratios were required for Specimen 3 (also for the 0.160/0.125 configuration of Specimen 1). The modal density was calculated with the relation

$$A_s / \left[4\pi \sqrt{\frac{D}{\rho h}} \right]$$

valid for plates.

A survey was made to determine the uniformity of response across the panels. Several shaker input locations were tried in an attempt to minimize the response variation. The optimum shaker location that could be determined resulted in an approximate average variation of 6 dB across a panel, with a maximum of about 10 dB within the frequency range of interest. In order to minimize the effects of this variation, acceleration was measured at a number of points on each panel for every test configuration. Six locations were used for the symmetric specimens (including the 0.125/0.160 configuration of Specimen 1). Figure 24 indicates these accelerometer locations and also the shaker input location. The measured values for one of the Specimen 1 configuration panels are presented in Table 8.

The indicated alternate input location was also utilized with each specimen. This alternate location was chosen to keep the input as far as possible from the accelerometers and thus minimize any input effects. The data obtained using this alternate location did not differ significantly from that for the initial input location.

CR103

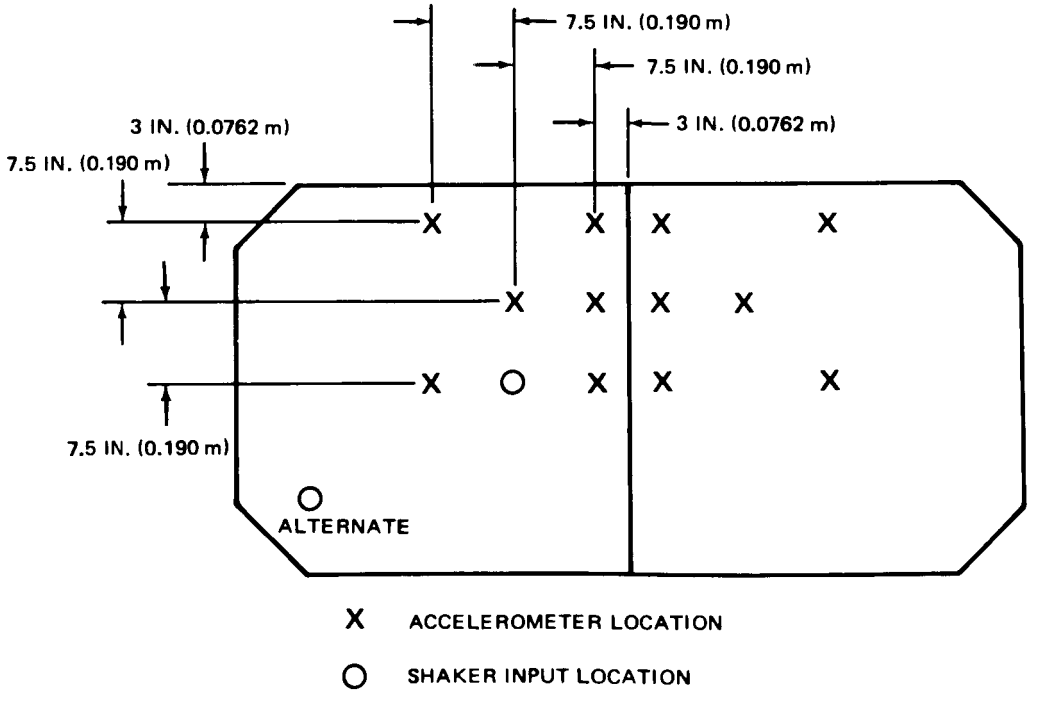

Figure 24. Accelerometer and Shaker Input Locations for Panel Tests

Table 8

VARIATION IN RELATIVE VIBRATION LEVEL AT DIFFERENT LOCATIONS ON A PANEL ASSEMBLY

0.16-inch (0.00406 meter) Panels with Damping Tape (Specimen 1)

$\frac{E_1}{E_2}$ (dB)

	Location Reference Number					
f	1	2	3	4	5	6
125	3	4.2	0.9	0.95	-1.2	1.5
160	2.5	6.2	1.4	2.2	0.3	-1
200	2	2.7	0.4	1.7	-0.2	1
250	2.5	11.2	-0.1	5.2	-0.2	4.5
315	1	5.7	1.15	1.2	3.8	0.5
400	2	2.2	3.4	5.2	6.3	4.5
500	4	9.2	0.15	0.2	1.8	2.25
630	7	10.7	6.9	5.7	5.8	3
800	4	7.2	4.4	4.7	2.8	11
1,000	2	7.2	7.4	2.7	2.8	3.5
1,250	3.5	9.2	5.4	3.7	6.8	9.5
1,600	8	8.2	10.9	6.2	9.8	5.5
2,000	12.5	9.7	8.4	9.7	14.8	13
2,500	11	9.2	10.4	8.7	12.3	11.5
3,150	10	10.7	7.9	8.7	7.8	11
4,000	12.5	10.2	12.9	10.2	5.8	8.5
5,000	7.5	7.7	9.9	7.45	10.3	10.5
6,300	9	7.7	11.9	8.2	10.3	14
8,000	9	10.2	11.9	10.7	7.8	10.75
10,000	7	8.2	9.4	8.7	8.8	9.25

The averaging to determine the response levels for the symmetric specimens was established by

$$\frac{\overline{\langle a_1^2 \rangle}}{\overline{\langle a_1^2 \rangle}} = \left[\frac{\overline{\langle a_{1,1}^2 \rangle}}{\overline{\langle a_{2,1}^2 \rangle}} + \frac{\overline{\langle a_{1,2}^2 \rangle}}{\overline{\langle a_{2,2}^2 \rangle}} + \cdots \frac{\overline{\langle a_{1,6}^2 \rangle}}{\overline{\langle a_{2,6}^2 \rangle}} \right] \Big/ 6$$

where

$$\overline{\langle a_{2,1}^2 \rangle}$$

is the acceleration measured at location 1 on the panel with shaker attached. The corresponding acceleration values,

$$\overline{\langle a_{1,j}^2 \rangle} \quad \text{and} \quad \overline{\langle a_{2,j}^2 \rangle}$$

were always determined from data recorded simultaneously. These two techniques for the averaging and testing insured maximum data consistency without requiring the use of 12 accelerometers at all times. Table 8 presents data from the individual accelerometer locations which was used to determine the relative acceleration response for the 0.160/0.160 configuration of Specimen 1 for one of the input locations.

For the nonsymmetric Specimen 3, an average value of the acceleration on each panel was obtained using ten points. The equation used for this averaging was

$$\frac{\overline{\langle a_1^2 \rangle}}{\overline{\langle a_2^2 \rangle}} = \frac{\sum_{j=1}^{10} \left\{ \dfrac{\overline{\langle a_{1,j}^2 \rangle}}{\overline{\langle a_{\text{control}}^2 \rangle}} \right\}}{\sum_{j=1}^{10} \left\{ \dfrac{\overline{\langle a_{2,j}^2 \rangle}}{\overline{\langle a_{\text{control}}^2 \rangle}} \right\}}$$

The damping values utilized in calculating the mode-to-mode coupling for each center frequency for each specimen were from the data points shown in Figures 21 and 22.

Figure 25 presents the values determined for the average mode-to-mode coupling of the 0.160 panel specimens. Specimen 3 exhibits the highest value at each frequency, while Specimen 2, except at one frequency, has always the lowest value. Comparing values for Specimens 1 and 2, the doubling of the joining length causes the coupling parameter value to increase by a factor ranging from two to five. The same type of comparison for Specimens 2 and 3 indicates that this type of nonsymmetry causes the coupling parameter to increase by a factor of 5 to 20 over the symmetric configuration.

Figure 26 presents comparisons of the mode-to-mode coupling for the two configurations of Specimen 1. The data for the 0.125/0.160 configuration demonstrate much less frequency dependence than is apparent for the other configurations. The data is, in fact, remarkably flat. Comparison of these

CR103

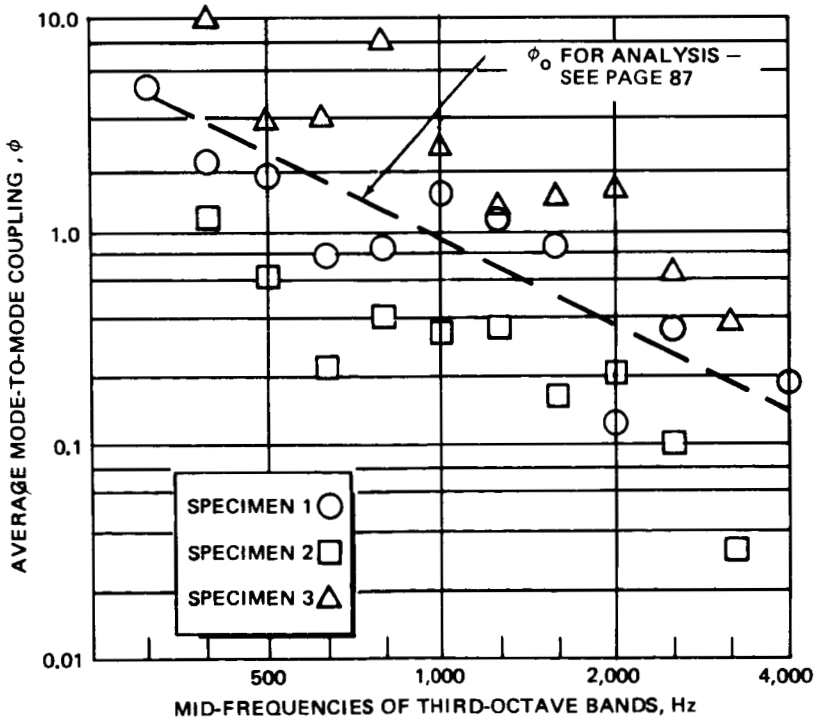

Figure 25. Mode-to-Mode Coupling of 0.160 Panel Specimens

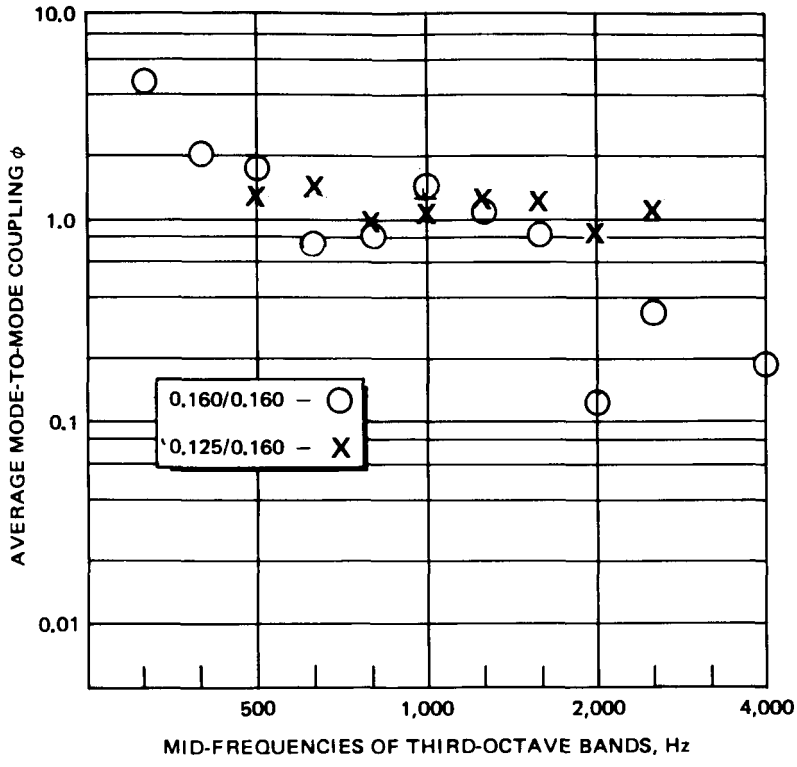

Figure 26. Mode-to-Mode Coupling of Two Specimen I Configurations

data with those for Specimens 2 and 3 indicates that two different effects of nonsymmetry are present with the panels. The nonsymmetry effect of shape (Specimen 2 and 3 data) causes a shift in coupling, while no such shift is evident for nonsymmetry in modal density (data for the two configurations of Specimen 1).

The data from the panel tests was examined statistically to evaluate accuracy. The fractional error, defined as the standard deviation divided by the average value of the quantity being evaluated (fractional error = σ/μ), was chosen as the measure of accuracy. For the damping measurements, the fractional error in the data is about 0.1. The value is approximately 0.35 for the panel vibration measurements, corresponding to a standard deviation of about 2 dB on the panels. These values result in a fractional error for the calculated coupling factors of 0.48. An initial series of tests was repeated and an attempt made to increase the accuracy of the vibration measurements without success.

The UpSTAGE acoustic test specimen was made available, so testing was performed to establish the damping of the specimen and also to attempt a direct evaluation of the joint coupling values. The UpSTAGE specimen was separated at the three joints into the four basic sections. Bop tests were performed with each individual section suspended on bungees. Decay data in octave and third-octave bandwidths was reduced for both an external skin and an internal bulkhead location on each of the sections. A graph of the average values obtained for Sections II, III, and IV is presented in Figure 27. Section I had been fitted with a wooden bulkhead for use as a wiring mockup and was therefore not considered a valid dynamic test specimen.

In order to evaluate the SEA coupling factors for this complex specimen, a very gross four-element SEA system was assumed with each of the four sections representing one element. The specimen was suspended on bungees and Section I excited by the 100-pound (445-Newton) force CALIDYNE shaker shown in Figure 28. Three configurations consisting of Sections I and II; I, II, and III; and I, II, III, and IV were tested. With the four-element modeling, coupling values were obtained by using an average response determined from

CR103

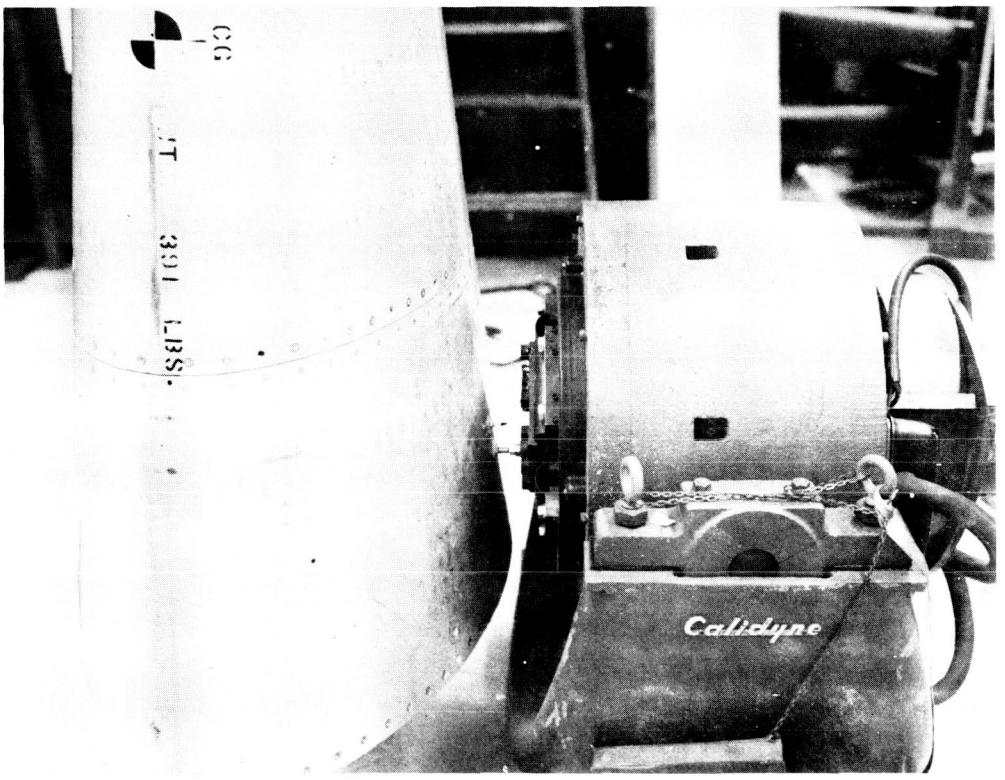

Figure 27. Calidyne Shaker

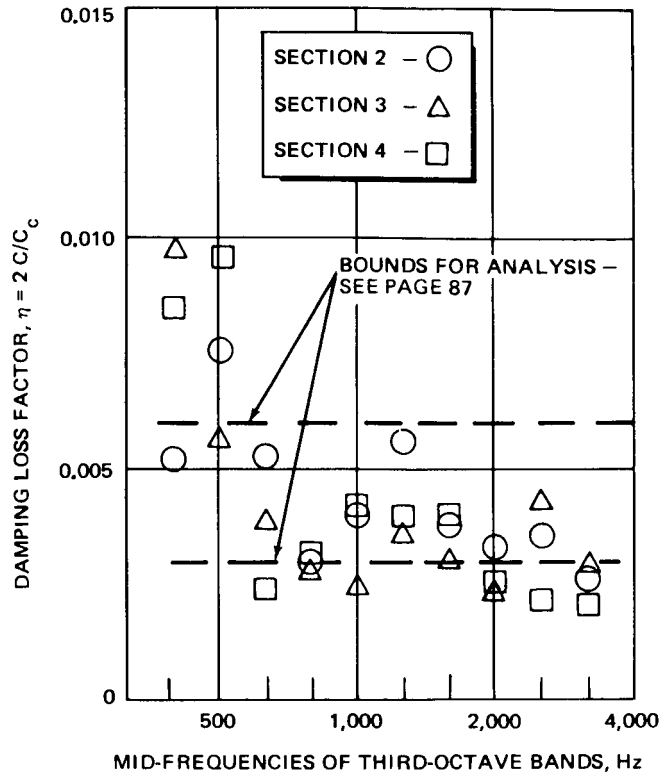

Figure 28. Damping Loss Factor for Sections of the UpSTAGE Acoustic Test Specimen

a survey of each element and assuming this average response to be valid for the total mass of the element. This method permits the coupling parameter values to be evaluated for the forwardmost joint of each configuration (for example, in the configuration with Sections I, II, and III, the parameter values for the joint between Sections II and III may be evaluated) with the simple relation:

$$\frac{m_1}{m_2} \frac{\overline{<a_1^2>}}{\overline{<a_2^2>}} = \frac{N_1}{N_2} \frac{\eta_{1,2}}{\eta_{1,2} + \eta_1}$$

since this model appears as a two-element system about the joint with an input to the system from an outside source. The modal densities were taken as calculated for the computer model of the specimen.

The resulting values obtained for the average mode-to-mode coupling by this technique are shown in Figure 29 with a comparison of the values obtained with panel Specimen 1. This approximation technique resulted in a few negative values which are omitted from the graph.

CR103

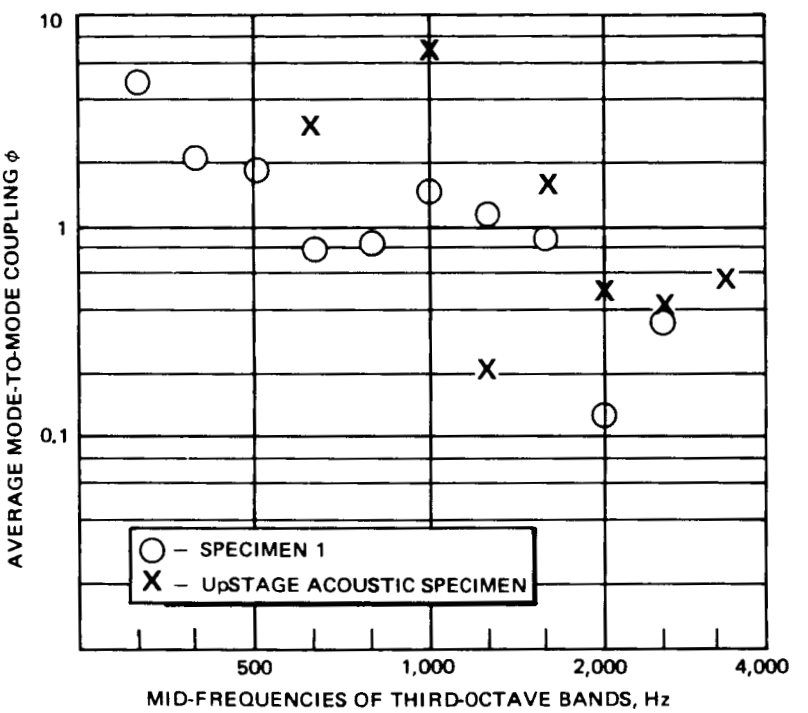

Figure 29. Approximate Mode-to-Mode Coupling Measured for UpSTAGE Acoustic Test Specimen

RESULTS OF COMPLEX ANALYSIS

The computer analysis of the UpSTAGE acoustic specimen provides two types of useful information. First, the comparison between computed and measured values will indicate the accuracy of SEA in conjunction with simple test methods, in predicting vibration response. Second, the parameterization study of the computer model will indicate the sensitivity of a complex system to errors in selection of SEA parameter values for a model.

Before making the comparison of test data with the analytical predictions, the test configurations will be discussed. Two basic test configurations were utilized. The first of these configurations simply mounted the test specimen on bungees in a reverberant chamber so that the entire exterior surface of the specimen was exposed to a uniform acoustic field. This configuration will be referred to as "Reverberant."

The second configuration for testing was attained by mounting the specimen through the wall between the reverberation chamber and an adjoining anechoic chamber. The space between the specimen and the wall was sealed with a lead sheet and lightly packed with fiber glass, as shown in Figure 30. This test configuration achieved a reduction in sound pressure level across the wall of at least 24 dB throughout the frequency range of interest and furnished a convenient means of localizing the acoustic input.

Two types of testing were accomplished with this second configuration. The first type was performed by mounting the specimen flush with the wall so that only the aft closure plate of the specimen was excited. A reverberant field was used for this testing and it will be referred to as "Reverberant (aft plate only)."

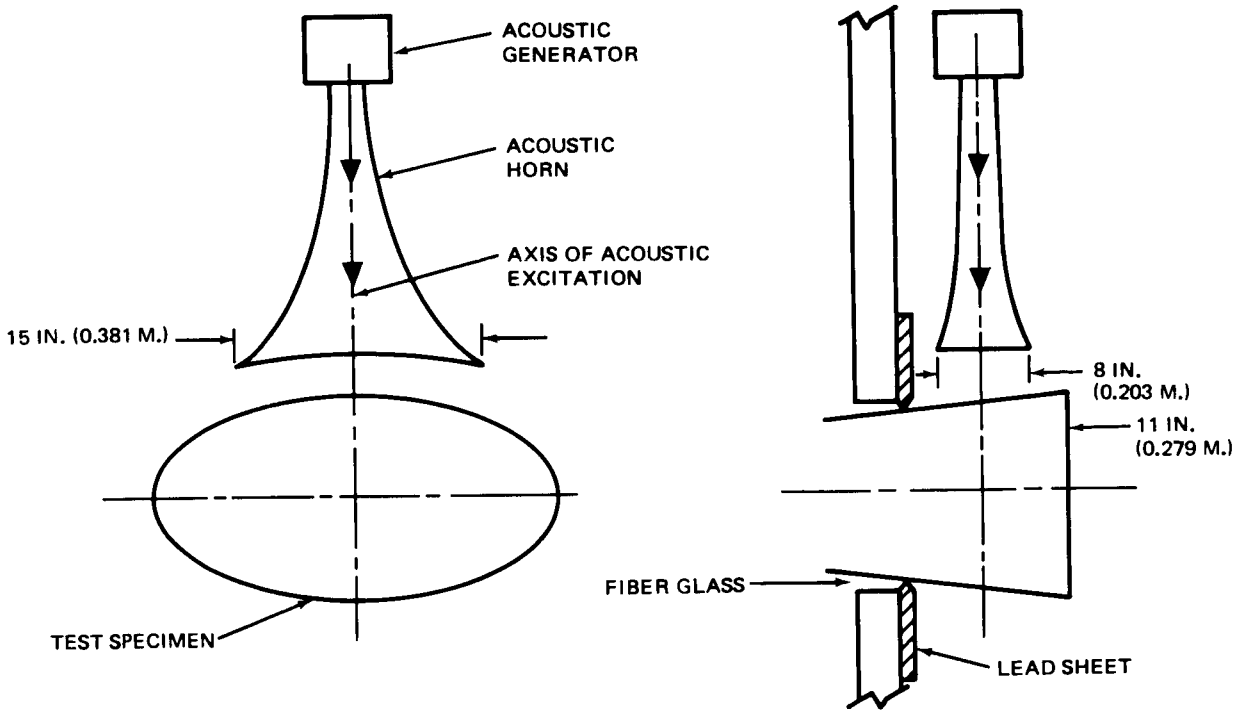

Figure 30. Configuration for Direct Impingement Acoustical Test

The second type of testing with this configuration was accomplished by positioning the sepcimen so that the aft 11 inches (0.279 meter) protruded into the reverberation chamber as shown in Figure 30. Acoustic input was accomplished with an acoustic horn directed at the aft section of the specimen. This setup permitted a localized nonsymmetric input to be attained for the specimen. The side of the specimen which was excited in this configuration will be referred to as the "top" and the opposite side as the "bottom." This test configuration will be referred to as "Direct Impingement." These tests and the specimen are discussed in detail in Reference 2.

To reiterate, three types of specimen acoustic testing will be considered. These are:

A. Reverberant – specimen exterior uniformly excited in a reverberant chamber.

B. Reverberant (aft plate only) – reverberant acoustic field input only to aft closure plate of specimen.

C. Direct Impingement – specimen excited directly with an acoustic horn on one side of the aft section.

The indicated nomenclature will be used to describe test configurations throughout the remainder of this report.

The values used for the basic coupling parameter (ϕ_o) of the field joints of the model were taken from Figure 25 as was previously noted. The coupling values are not parameterized directly during the prediction comparisons, but will be examined at the end of this section.

Two basic sets of values were available for the damping parameter. One set of values was from the tests on bare (prior to applying Scotchfoam) aluminum panels, while the other set resulted from tests on the actual acoustic specimen. The predictions are parameterized on these two sets of values. Each set of data was enveloped with two values as indicated in Figures 23 and Figure 28. These bounds are $\eta = 0.0005$ and 0.001 for the panel test data, and $\eta = 0.003$ and 0.006 for the acoustic specimen data. These bounds for the two sets of data differ by a factor of six.

In order to avoid cluttering the prediction comparisons with unnecessary information, predictions for each of the four damping values will not be shown for all comparisons. These values are omitted when a straightforward interpolation is indicated for the additional values.

The exterior skin levels are considered the more significant aspect of the comparison. The test program was designed to establish coupling parameter values between skin segments and the majority of the acoustic test measurements were made on the external skin. Internal transmission of vibration through bulkheads and substructures is directly analogous to the Reverberant (aft plate only) configuration, which will be examined.

Consequently, the apparent neglect of internal response in the present study (in order to concentrate the test effort) does not diminish the validity or usefulness of SEA throughout an aerospace vehicle.

The predictions for the completely reverberant excitation will be considered first. Because each of the exterior elements of the specimen is being directly excited in this configuration, the computed response should be most directly controlled by the damping values selected for the model elements and the acoustic-structure coupling factor (radiation efficiency) rather than the coupling values between the structural sections.

Figures 31 to 34 provide comparisons of the external skin response in each of the four major regions for this fully reverberant configuration. For this case, the damping based on the panel tests yields predicted responses that agree very well with test data at frequencies above 1,600 Hz, except for a single data point at 2,000 Hz in region IV. The damping obtained from the UpSTAGE specimen results in a computed response which is consistently lower in the high frequencies than the measured values.

The computed values are higher than measured values in the lower frequencies except in Region II. A peak is also indicated by the measurements at 1,250 Hz which does not show up in the computations. These values were obtained with the 45-element modeling of the specimen (this acoustic input configuration should be insensitive to aft section modeling).

The next configuration to be considered is Reverberant (aft plate only). Figures 35 to 38 present a comparison between computed and measured values for both 37- and 45-element models with only one value of damping. It was the very low predicted response for the 45-element model with this lowest value of damping which led to the development of the 37-element model. The constraint of energy flow toward the front of the model by the additional joints of the 45-element model is very obvious in these figures. Likewise, this configuration is the most dependent upon selection of suitable coupling values since energy must flow the entire length of the specimen to excite Section IV.

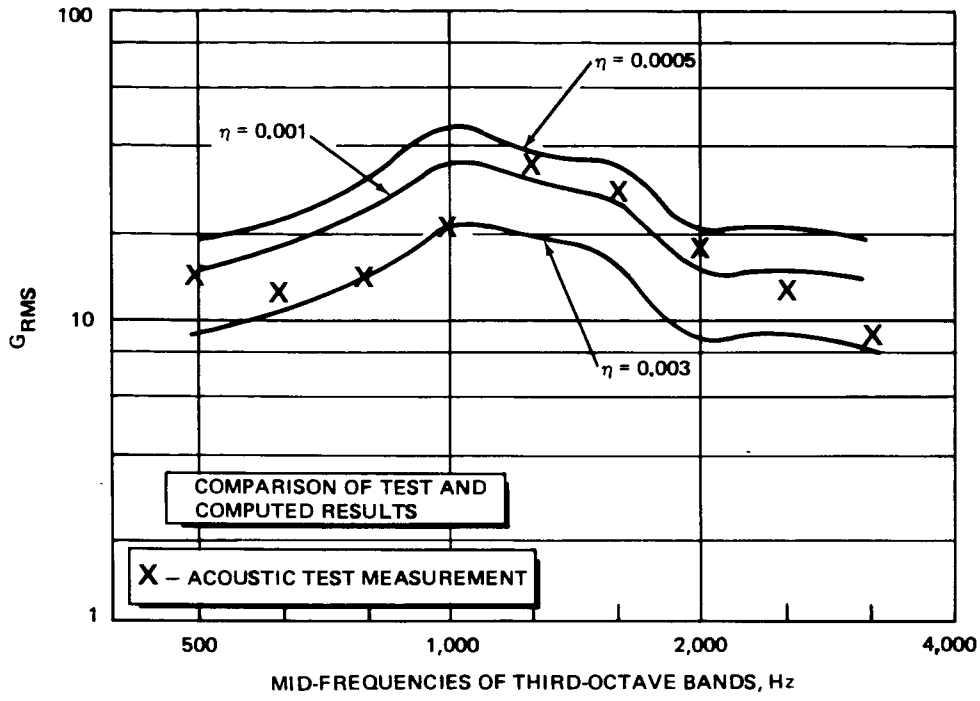

Figure 31. Reverberant – Section I

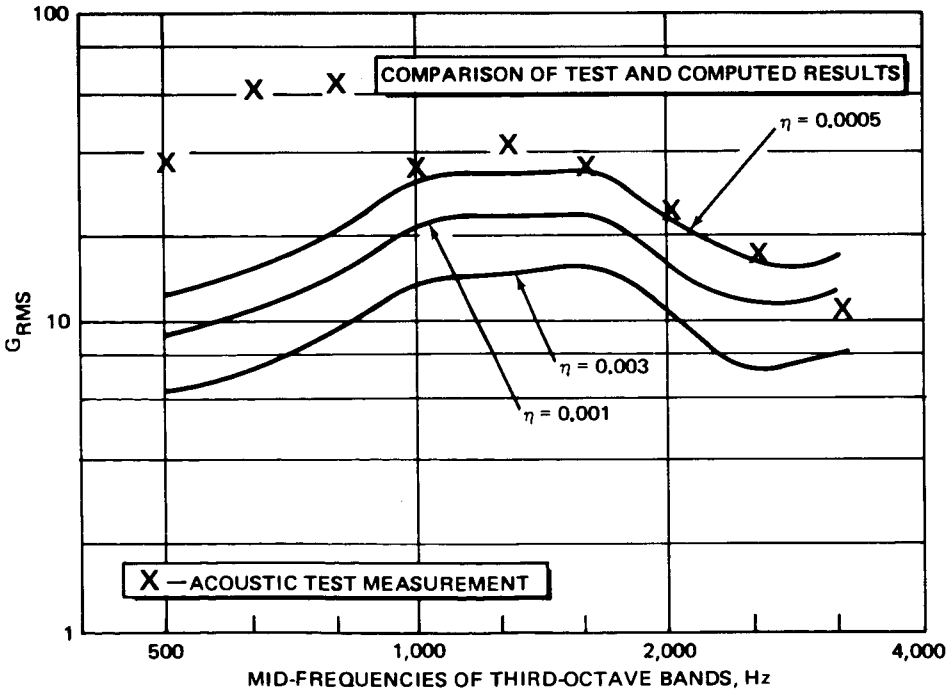

Figure 32. Reverberant – Section II

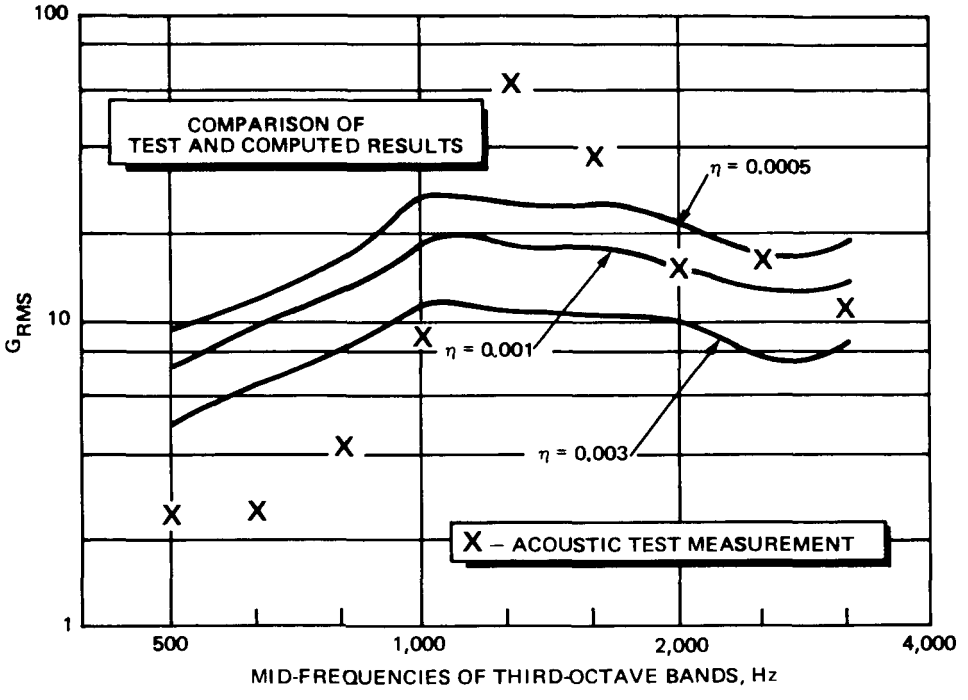

Figure 33. Reverberant – Section III

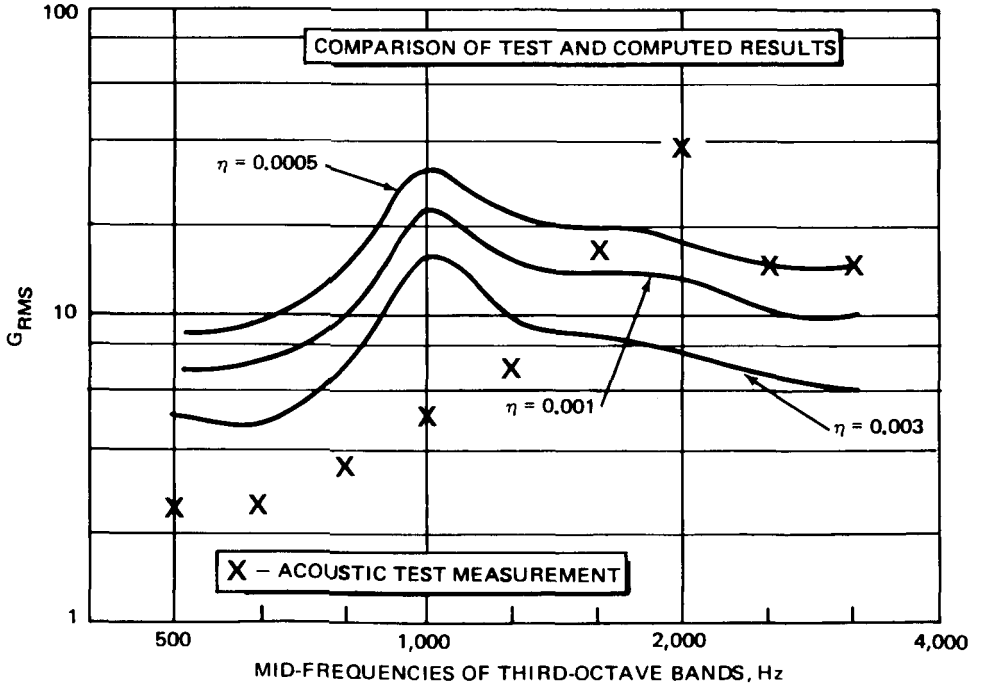

Figure 34. Reverberant – Section IV

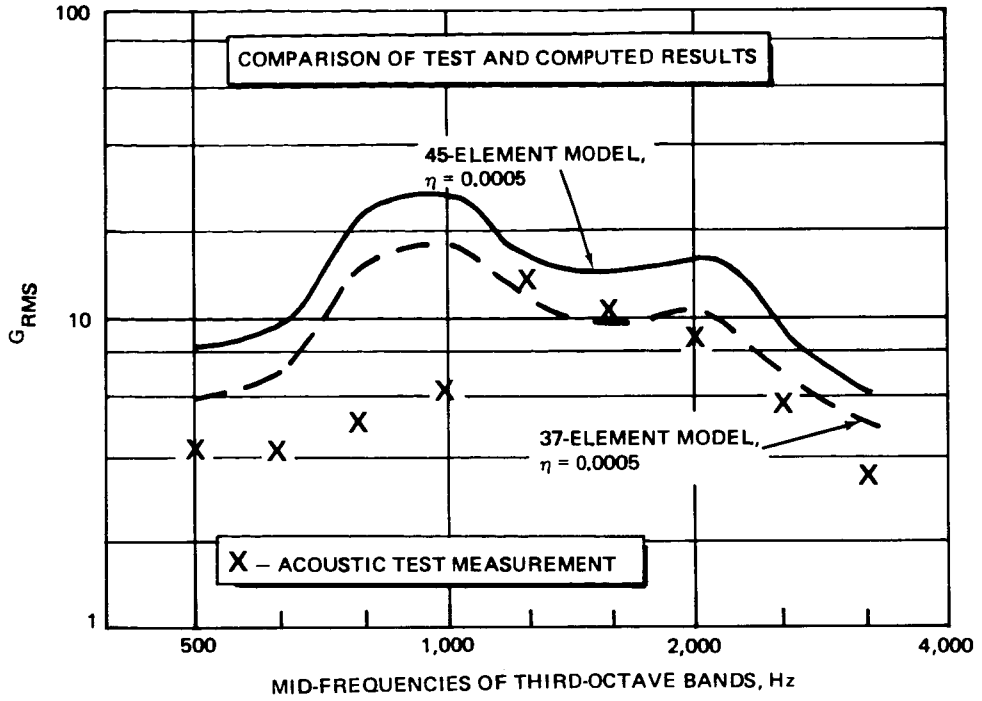

Figure 35. Reverberant – Aft Plate Only – Section I

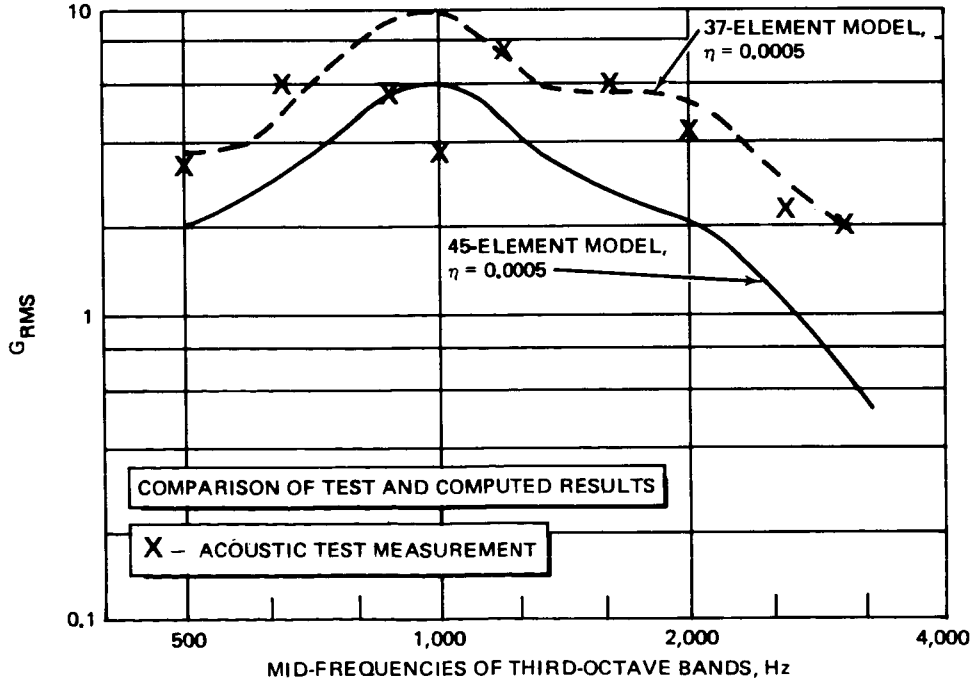

Figure 36. Reverberant – Aft Plate Only – Section II

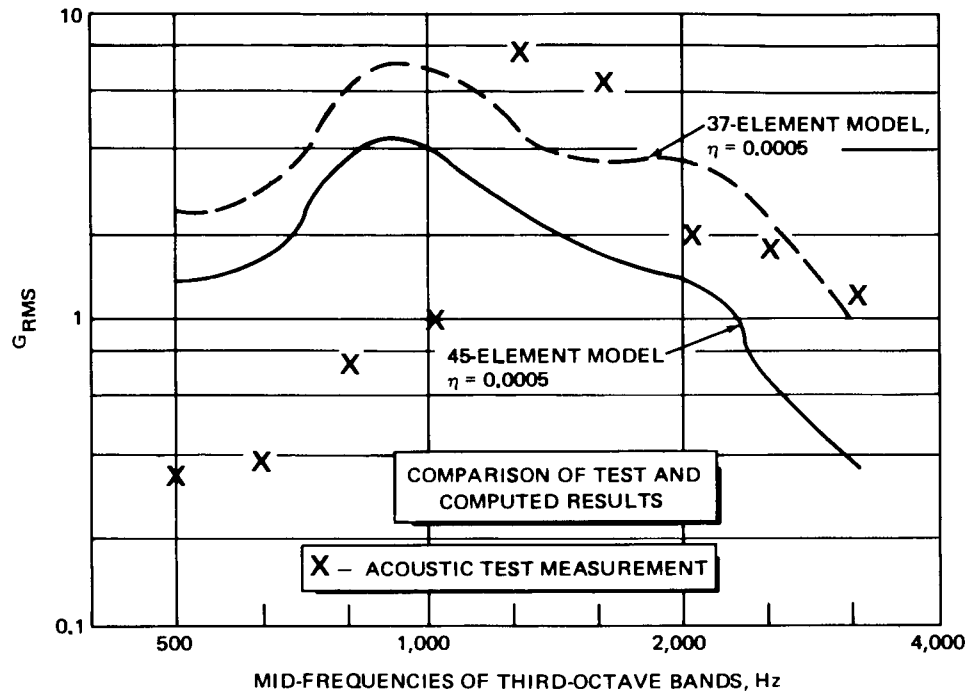

Figure 37. Reverberant – Aft Plate Only – Section III

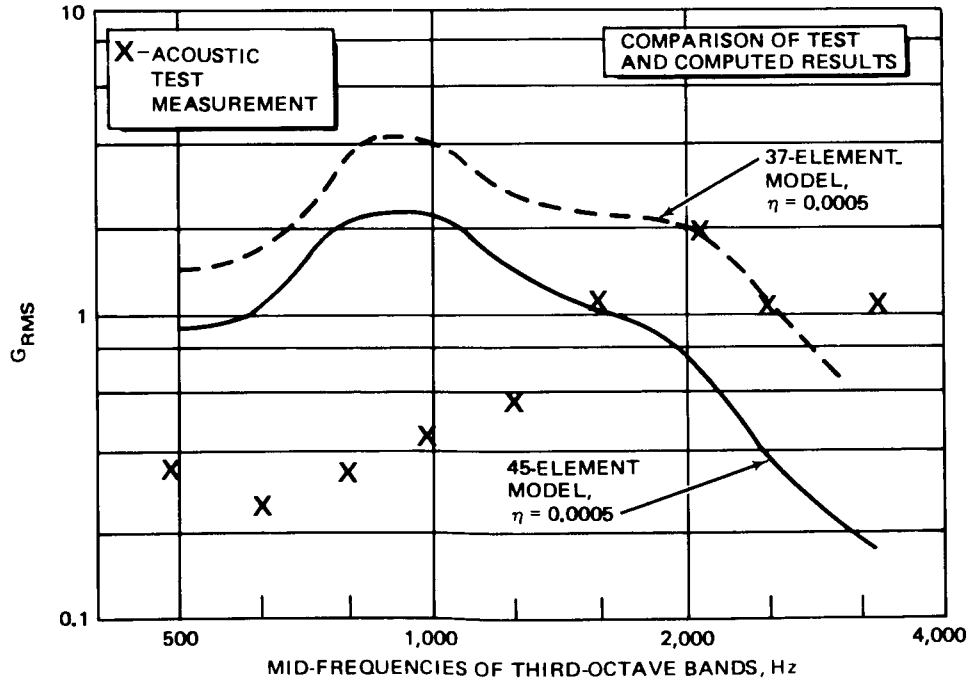

Figure 38. Reverberant – Aft Plate Only – Section IV

Figures 39 to 42 present the measured data and the response computations for the Reverberant (aft plate only) configuration using $\eta = 0.0005$, 0.001, and 0.003 with the 37-element model. The primary observation here is the agreement of the predicted values with the $\eta = 0.0005$ computations.

The remainder of the prediction comparisons are for the Direct Impingement configuration. Three cases were examined for this configuration. These cases correspond to tests performed with varying applications of Scotchfoam damping tape to the test specimen.

Figures 43 to 47 present the initial response comparison for this Direct Impingement configuration with no damping tape applied to the specimen. Test measurements were made on the top and bottom of the aft two sections and these are shown in the figures since the circumferential distribution of response is of interest. These values indicate that the initial estimate of the circumferential coupling, ϕ_c, as ten times the basic field joint coupling value was too low. The computed response in the high frequencies using $\eta = 0.0005$ is high.

Figures 48 to 52 indicate the results of increasing ϕ_c to 50 times the field joint value. The curves on these figures represent the predicted values for $\eta = 0.0005$ and $\eta = 0.003$ as well as a curve labeled $\eta = 0.0005$ corrected. The corrected curve is discussed below.

This configuration is excited by nearly normally incident acoustic energy and the exciting field is not as well defined as it was in the original case. In addition, the analysis of the first two configurations confirmed the damping and axial structural coupling factors for the model. For these reasons it was assumed that the discrepancy resulted because of improper definition of the energy input. To test this assumption the predicted value for $\eta = 0.0005$ was reduced until acceptable agreement was achieved for both measurements in Section I. This reduction was applied to the $\eta = 0.0005$ predicted values for all of the sections. The general agreement between the measured and the corrected prediction values substantiate the assumption of the discrepancy being in the input.

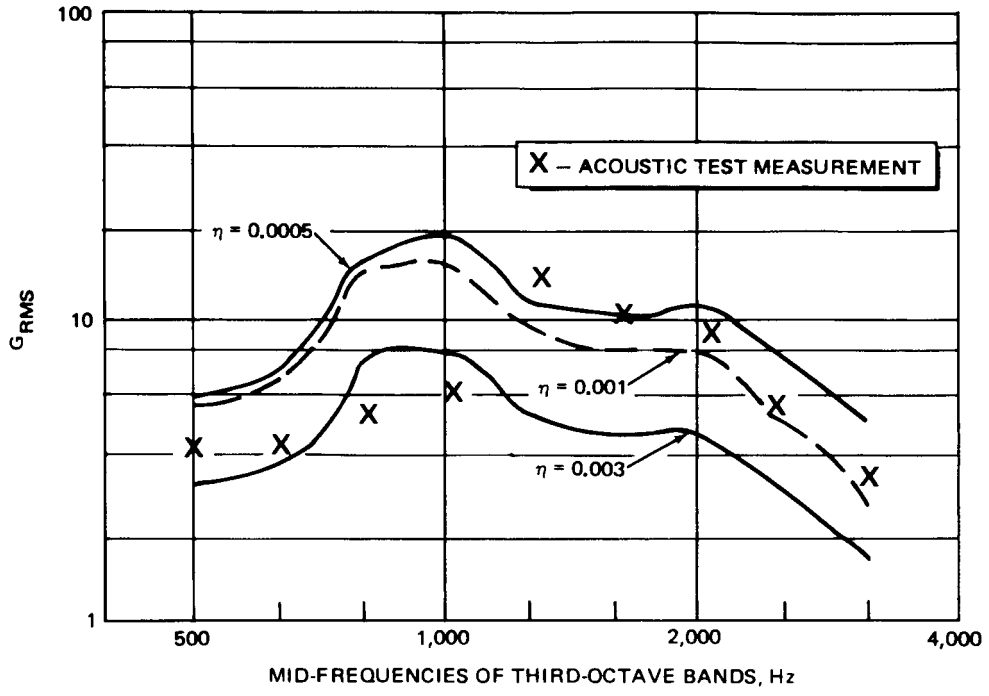

Figure 39. Reverberant (Aft Plate Only) – Section I – 37-Element Model

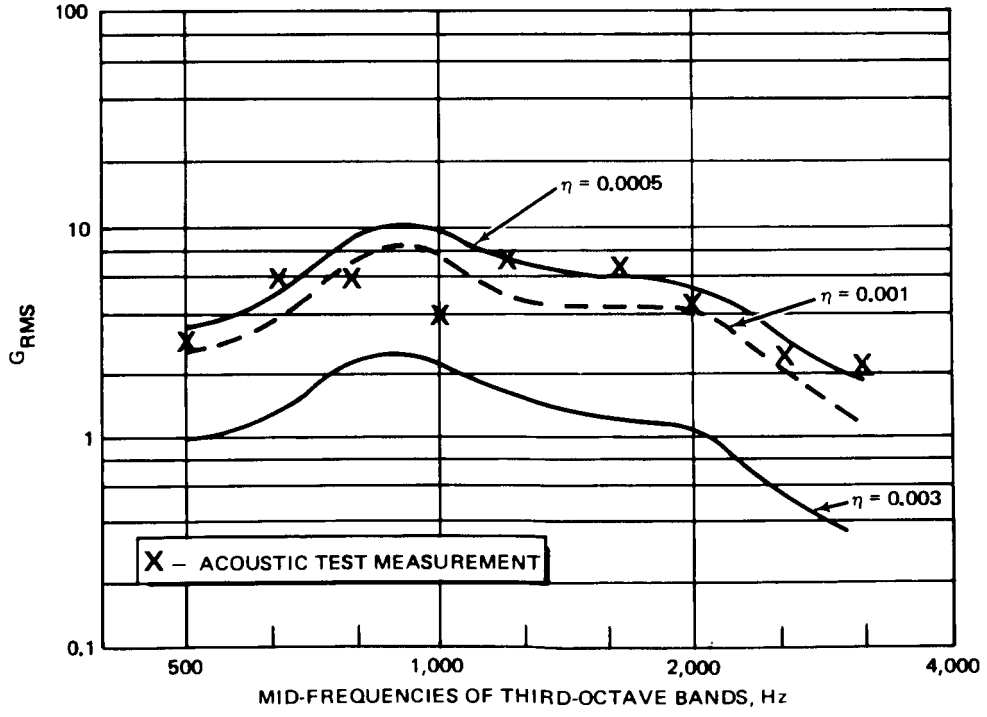

Figure 40. Reverberant (Aft Plate Only) – Section II – 37-Element Model

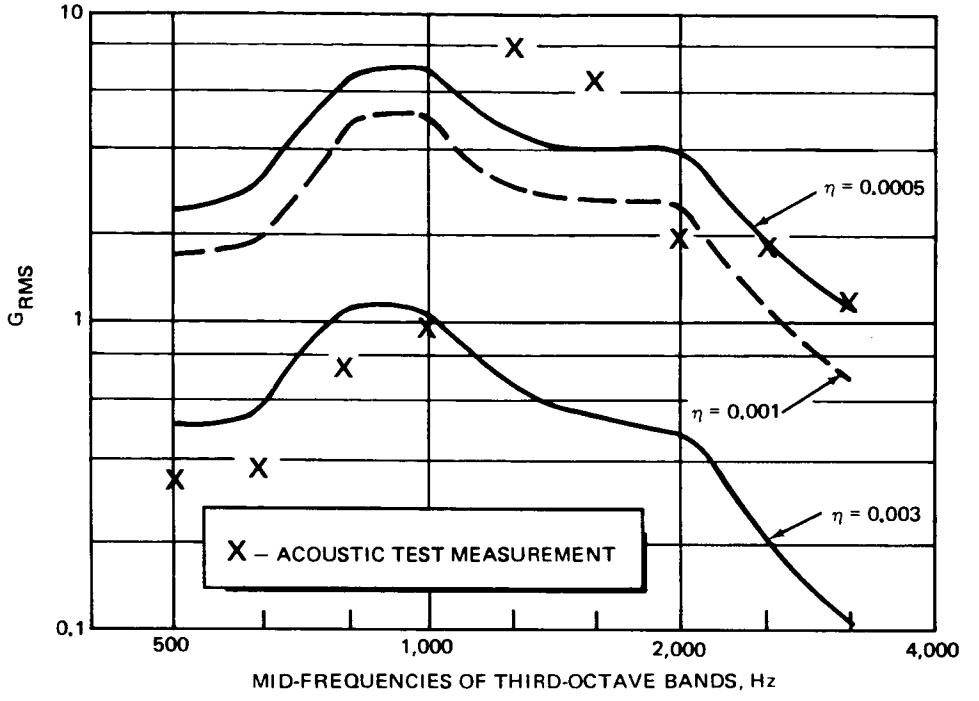

Figure 41. Reverberant (Aft Plate Only) – Section III – 37-Element Model

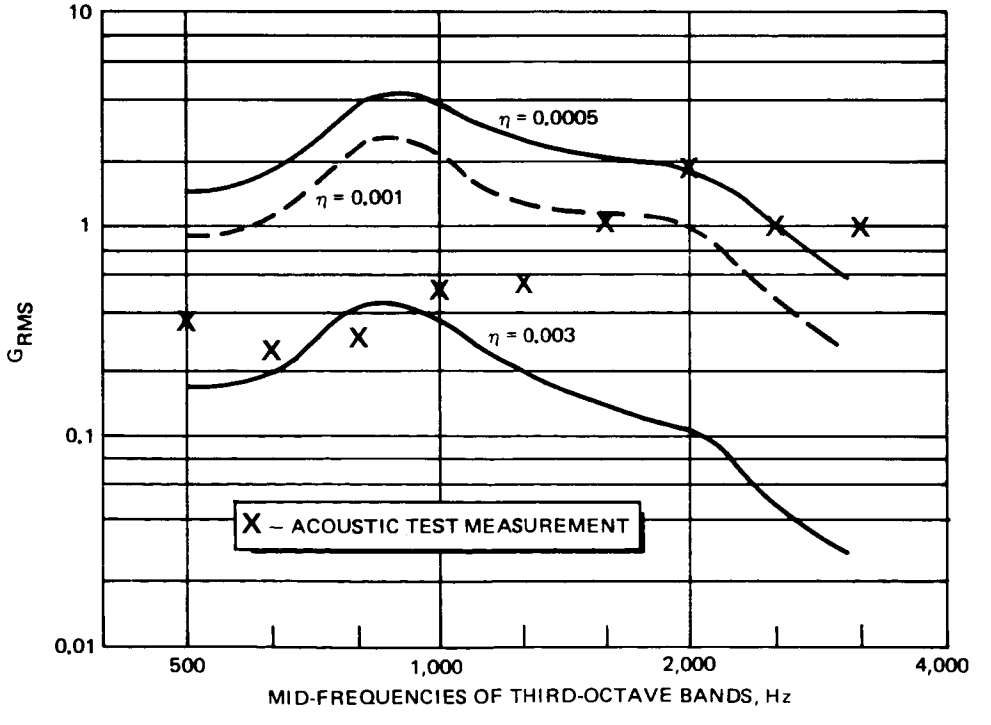

Figure 42. Reverberant (Aft Plate Only) – Section IV – 37-Element Model

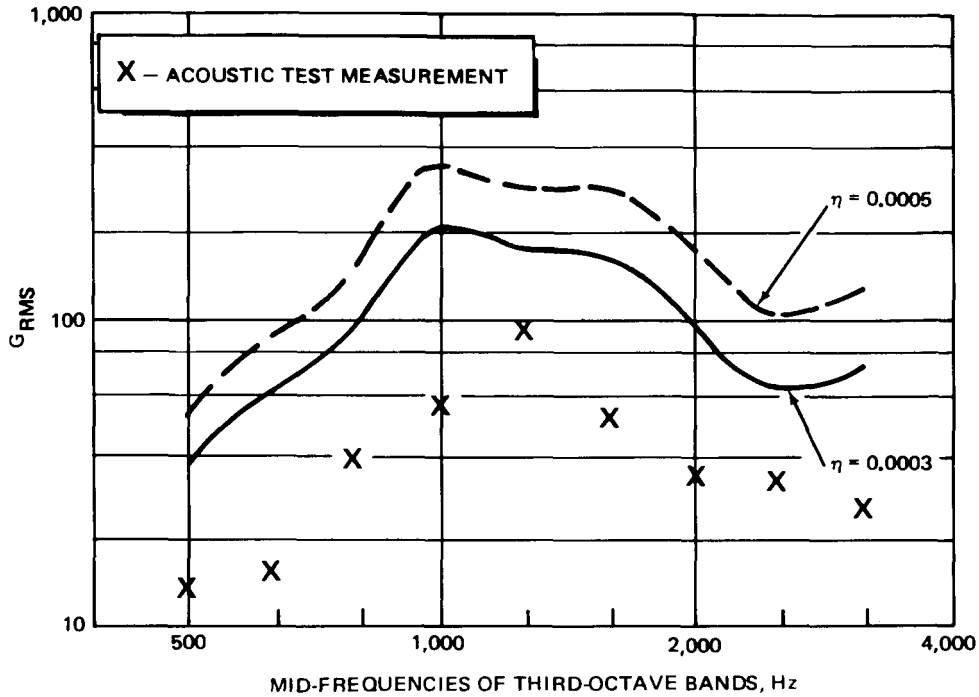

Figure 43. Direct Impingement – Section I – Top, 37-Element Model

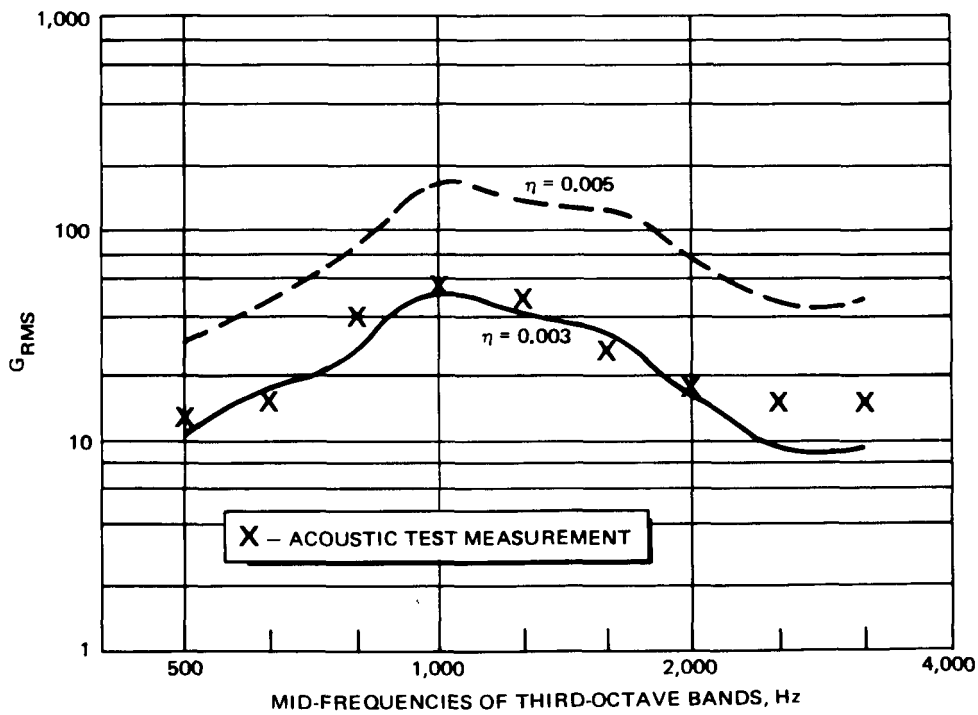

Figure 44. Direct Impingement – Section I – Bottom, 37-Element Model

CR103

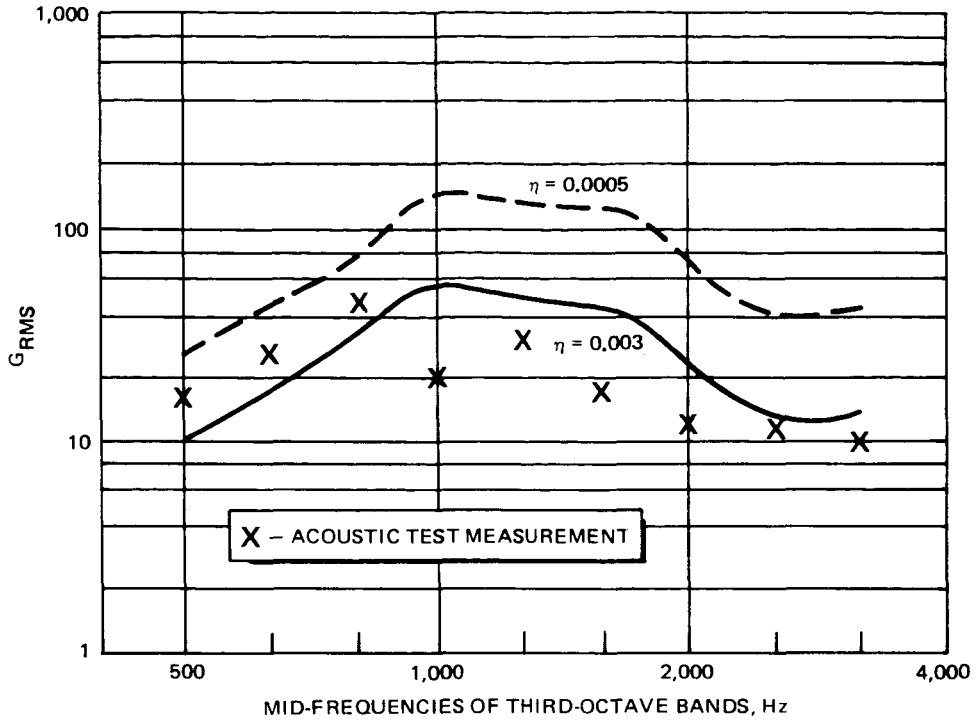

Figure 45. Direct Impingement – Section II – Top, 37-Element Model

CR103

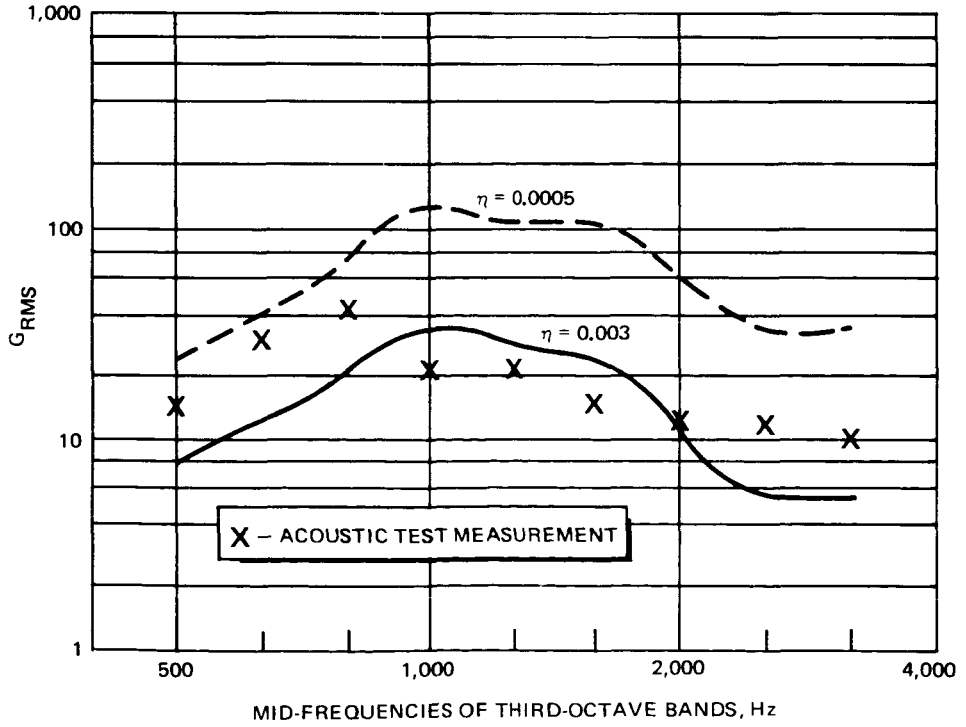

Figure 46. Direct Impingement – Section II – Bottom, 37-Element Model

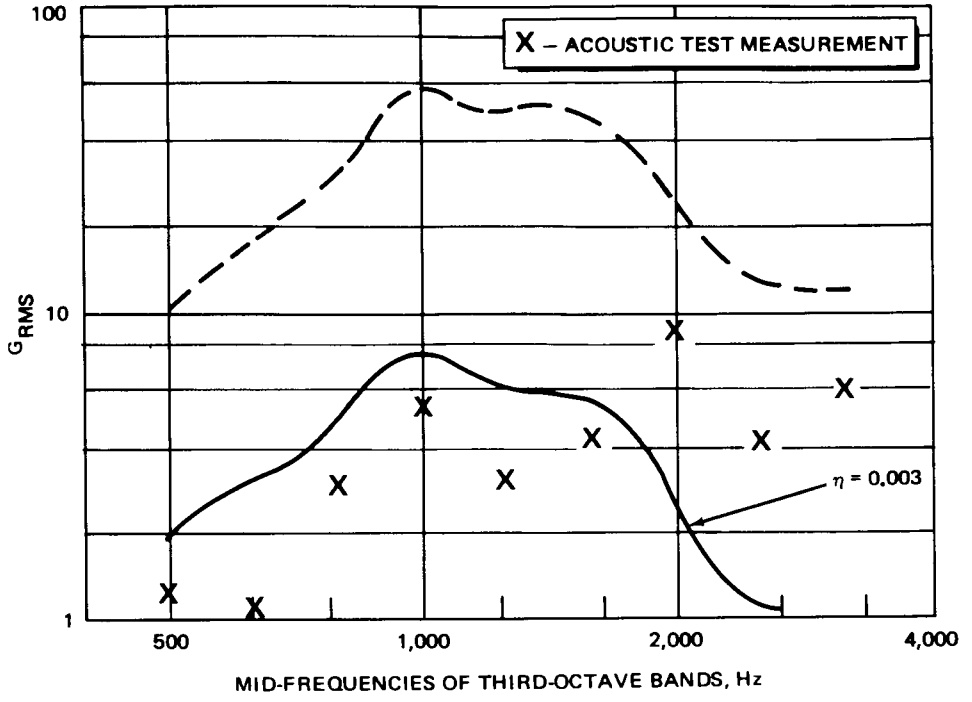

Figure 47. Direct Impingement – Section IV – Top – 37-Element Model

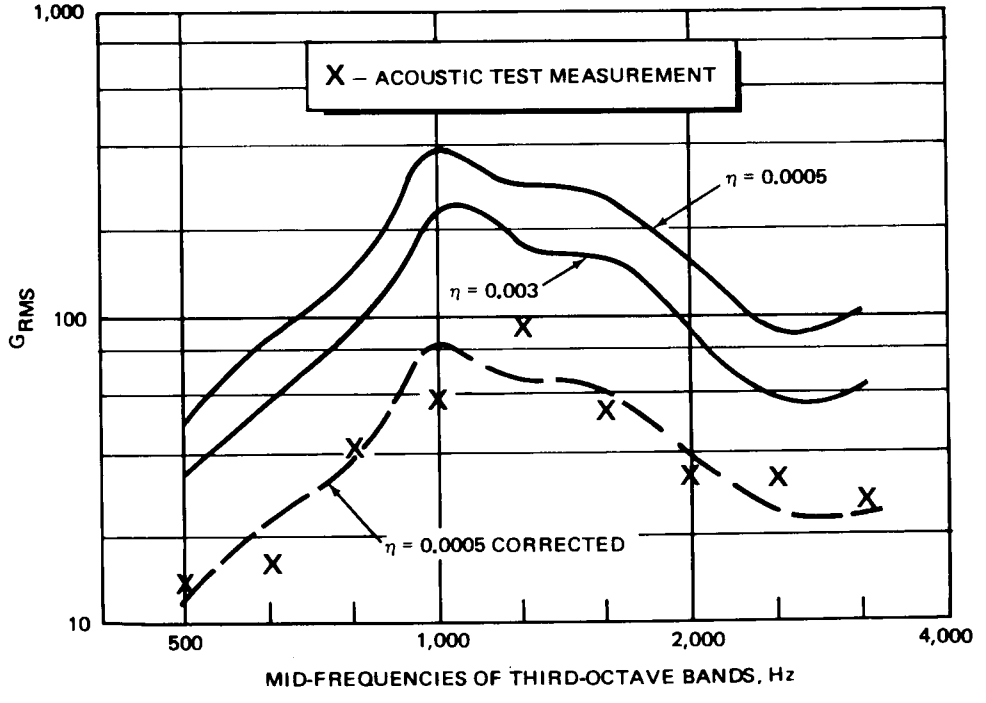

Figure 48. Direct Impingement – Section I – Top – 37-Element Model – $\phi_c = 50\,\phi_o$

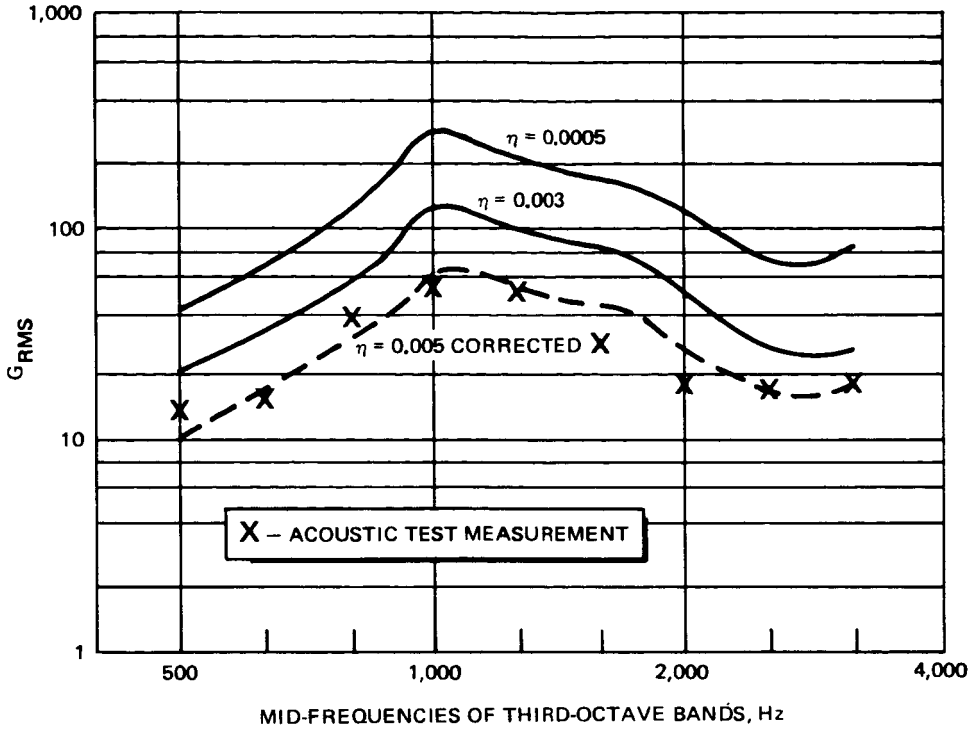

Figure 49. Direct Impingement – Section I – Bottom – $\phi_c = 50\ \phi_o$

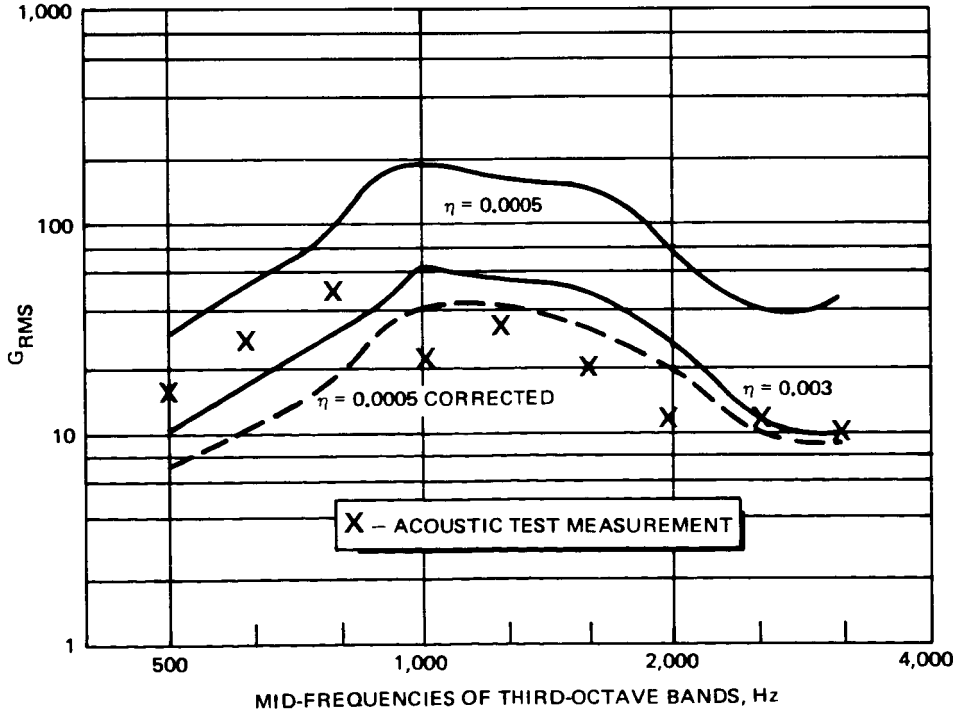

Figure 50. Direct Impingement – Section II – Top – $\phi_c = 50\ \phi_o$

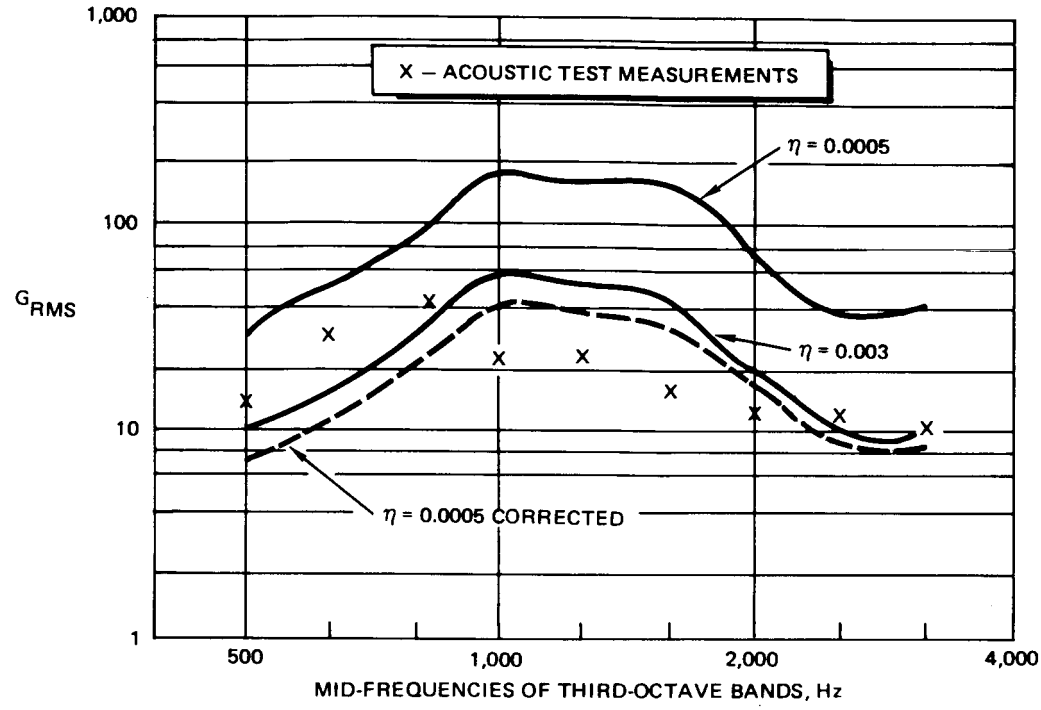

Figure 51. Direct Impingement–Section II–Bottom – $\phi_c = 50\ \phi_o$

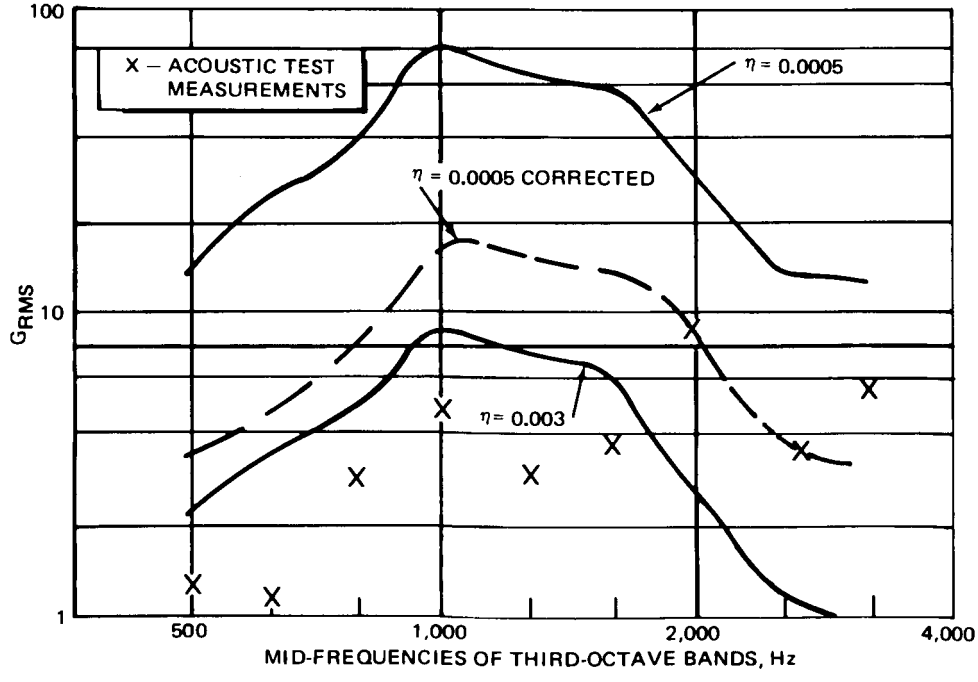

Figure 52. Direct Impingement – Section IV – Top – $\phi_c = 50\ \phi_o$

Figures 53 to 57 present the same type of comparison for a case with damping tape applied to the aft three subsections of Section I. Based on experience with the panels, the addition of the damping tape was assumed to increase the damping by a factor of eight over bare structure. The two values of damping noted on the figures are for the bare structural areas and the damped areas of the specimen. The circumferential coupling for the computed values was 50 times the field joint value.

The results for this case are essentially the same as for the bare specimen.

The final case adds damping tape over a portion of Section II, which is assumed to increase the damping by a factor of three. The Section I damping is retained as in the preceding case, and circumferential coupling is likewise 50 times field joint coupling. The results are shown in Figures 58 to 60. From these figures it appears that the effectiveness of the damping tape was slightly underestimated in Section II. The effect of damping on the predicted response is presented in Figures 61 and 62 for the top of Section I and Section IV for the three cases just discussed.

The comparisons which have been made were all parameterized on damping values. The effect of coupling variation will now be examined.

The configuration which is most directly affected by the coupling is the Reverberant (aft plate only). Figures 63 to 66 indicate the effect on computed response of changing the coupling by an order of magnitude in either direction for two values of coupling. Sections I and IV are used to indicate the effect near and distant from the input.

The figures indicate that near the input the effect is relatively small, but can be very large several elements away from the source. The Section IV responses change by orders of magnitude with the coupling.

The crossover which occurs at the lower frequencies in Figure 65 for the two higher values of coupling illustrates a phenomenon which also occurs in Figure 35 (compare with Figures 36, 37, and 39). At very large values of

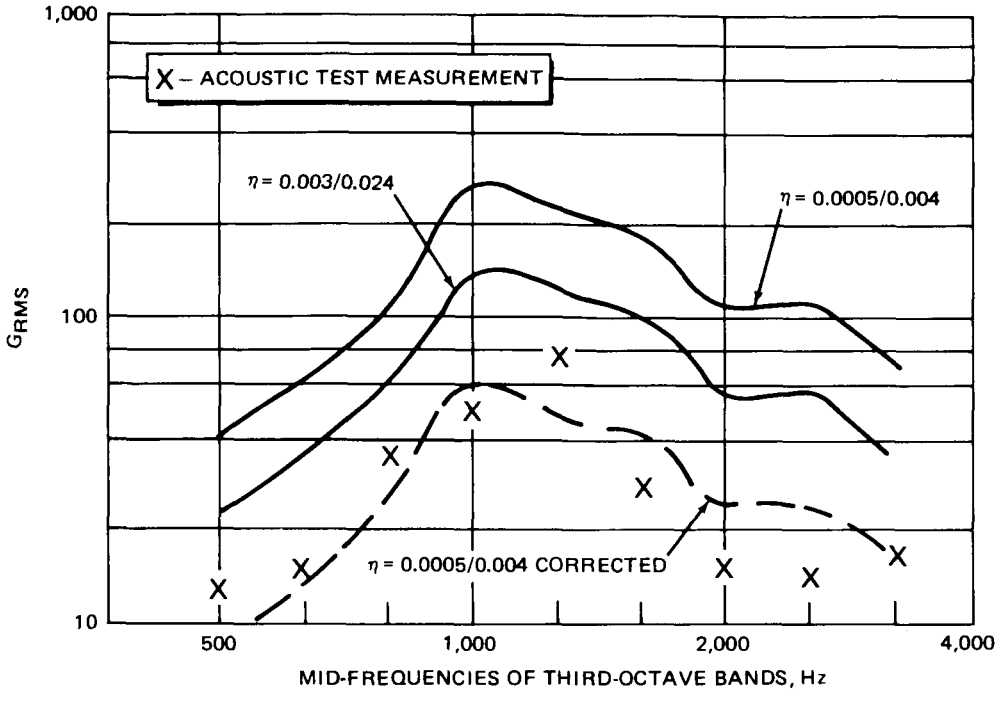

Figure 53. Direct Impingement – Section I – Top – $\phi_c = 50\ \phi_o$ – Damping Tape Applied to Section I

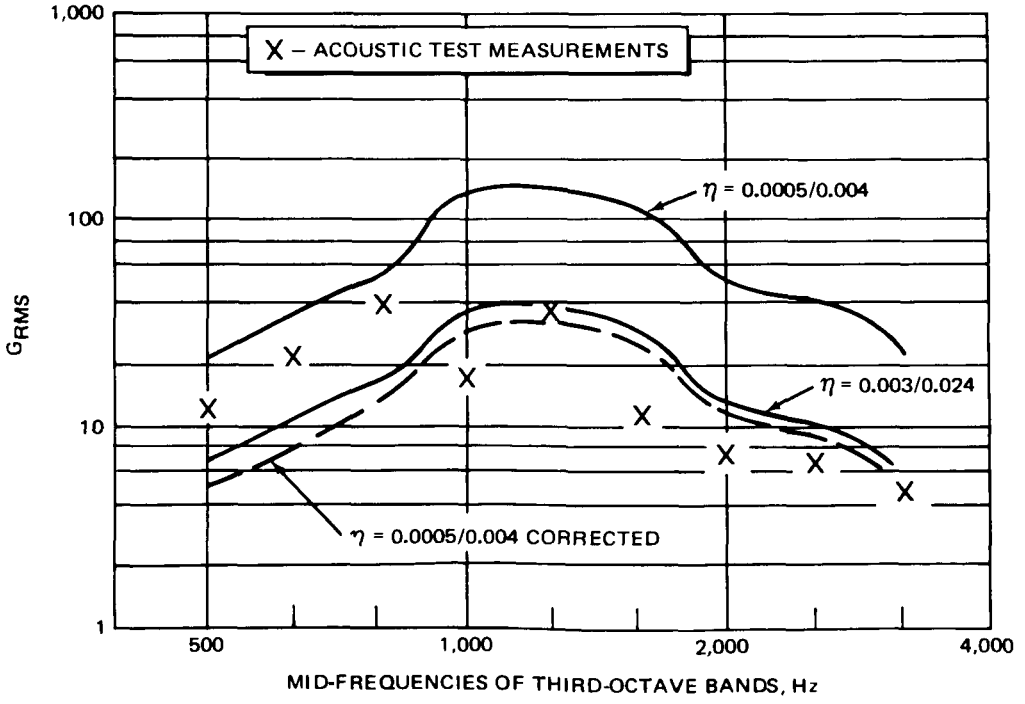

Figure 54. Direct Impingement – Section I – Bottom – $\phi_c = 50\ \phi_o$ – Damping Tape Applied to Section I

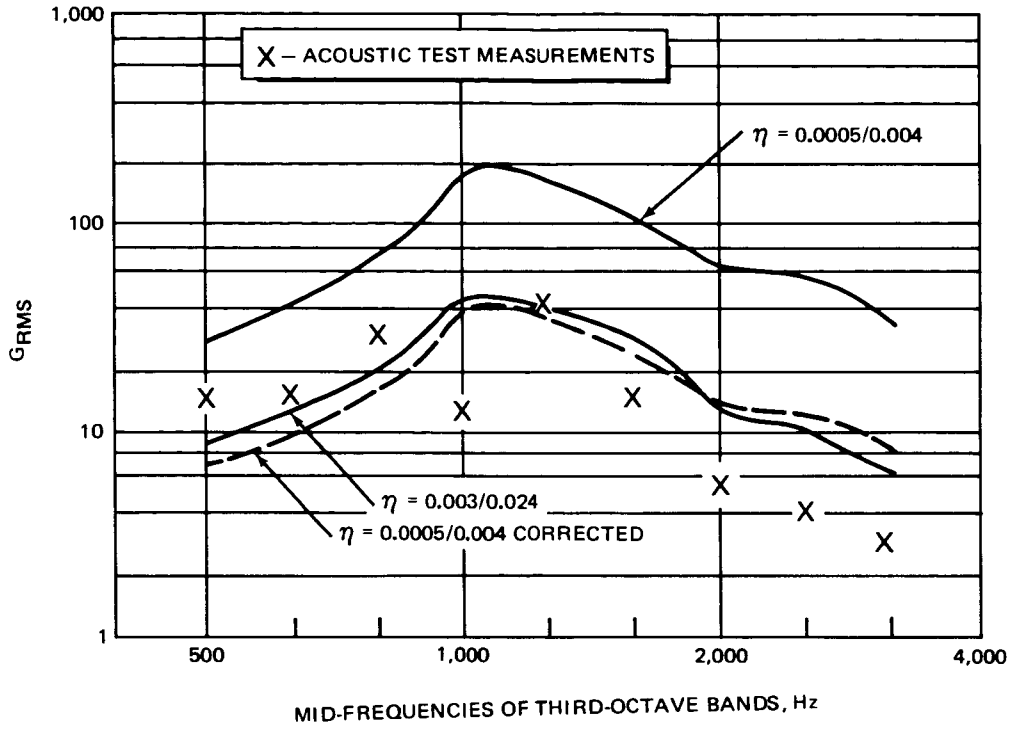

Figure 55. Direct Impingement – Section II – Top – $\phi_c = 50\,\phi_o$ – Damping Tape Applied to Section I

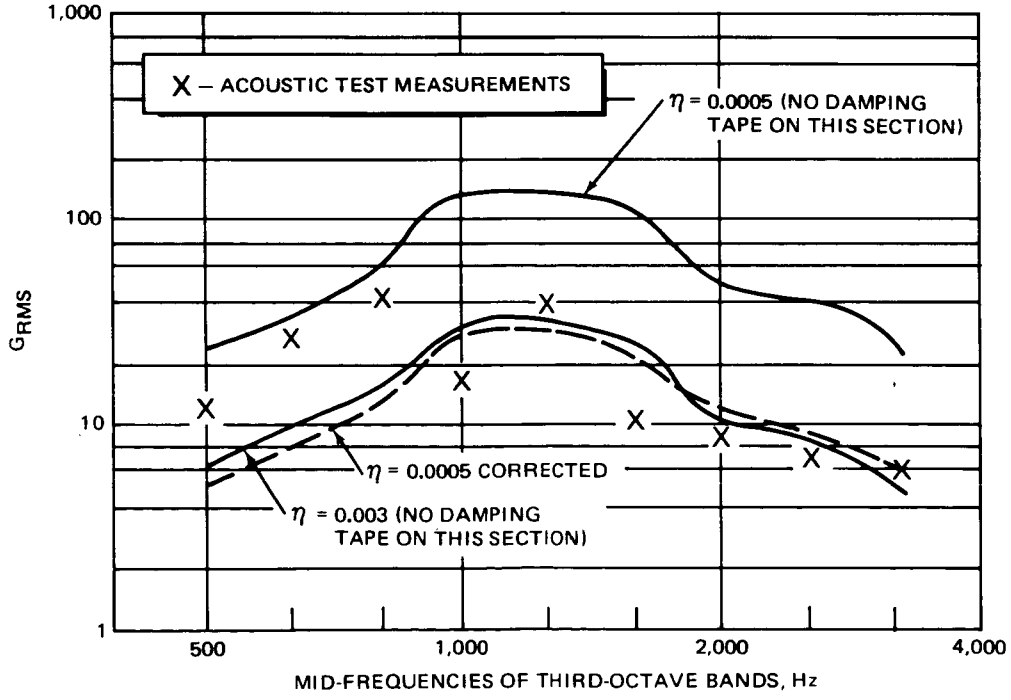

Figure 56. Direct Impingement – Section II – Bottom – $\phi_c = 50\,\phi_o$ – Damping Tape Applied to Section I

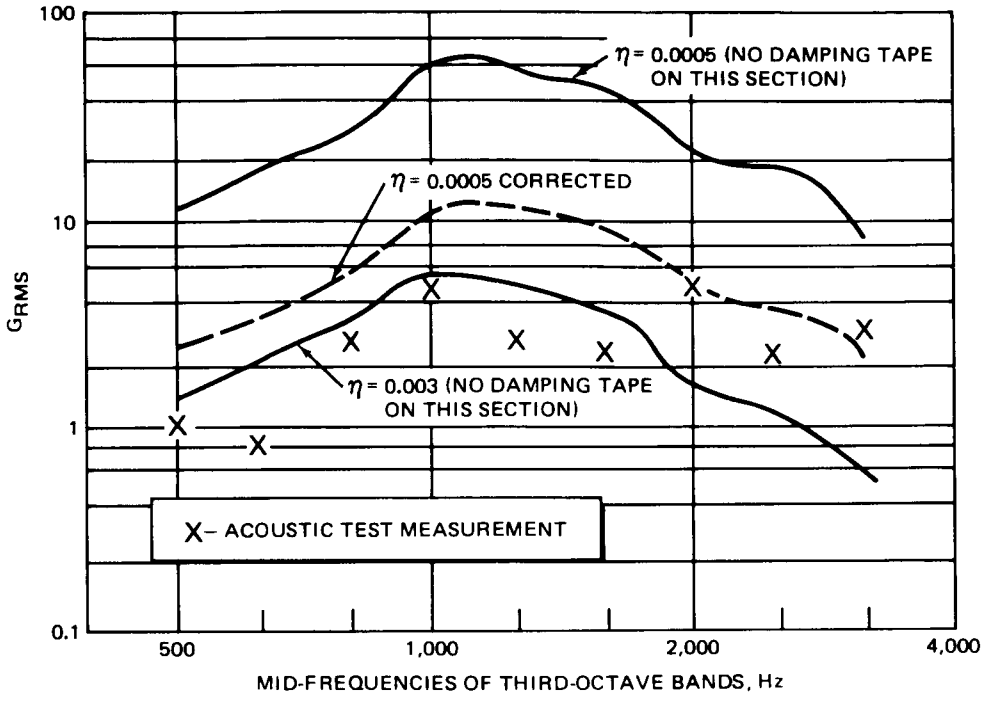

Figure 57. Direct Impingement – Section IV – Top – $\phi_c = 50\ \phi_o$ – Damping Tape Applied to Section I

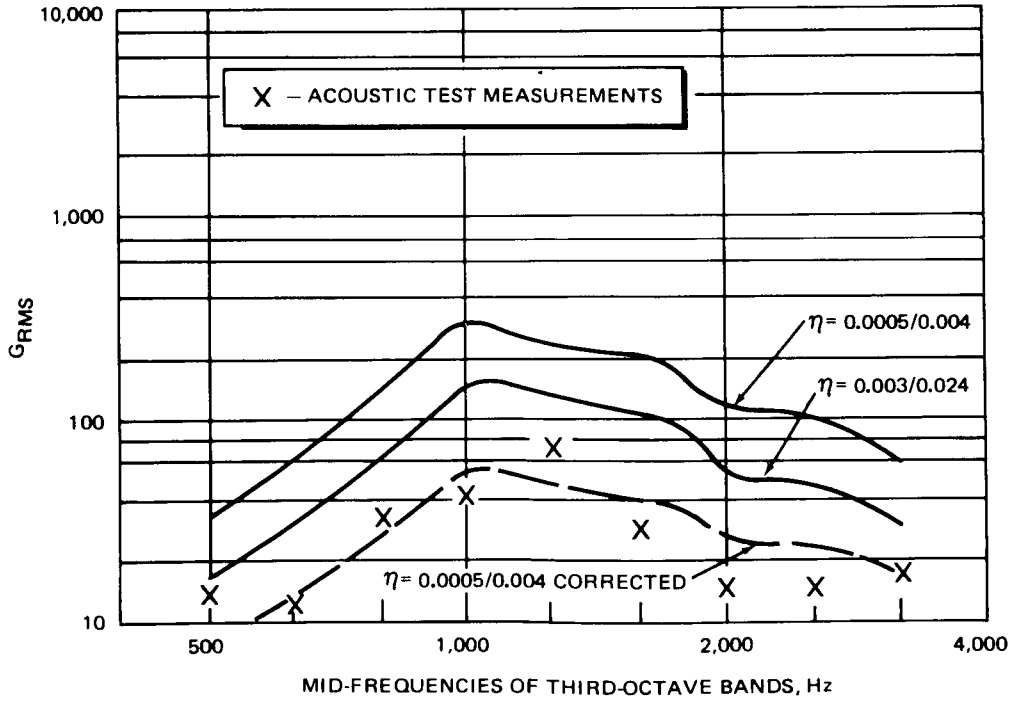

Figure 58. Direct Impingement – Section I – Top – $\phi_c = 50\ \phi_o$ – Damping Tape Applied to Sections I and II

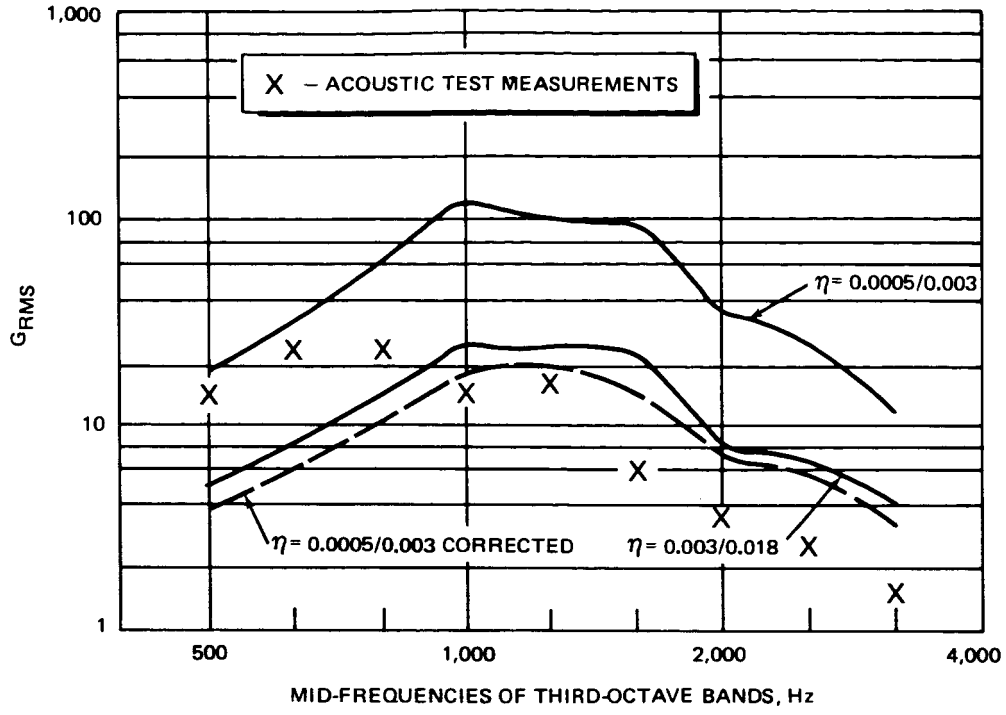

Figure 59. Direct Impingement – Section II Top – $\phi_c = 50\,\phi_o$ – Damping Tape Applied to Sections I and II

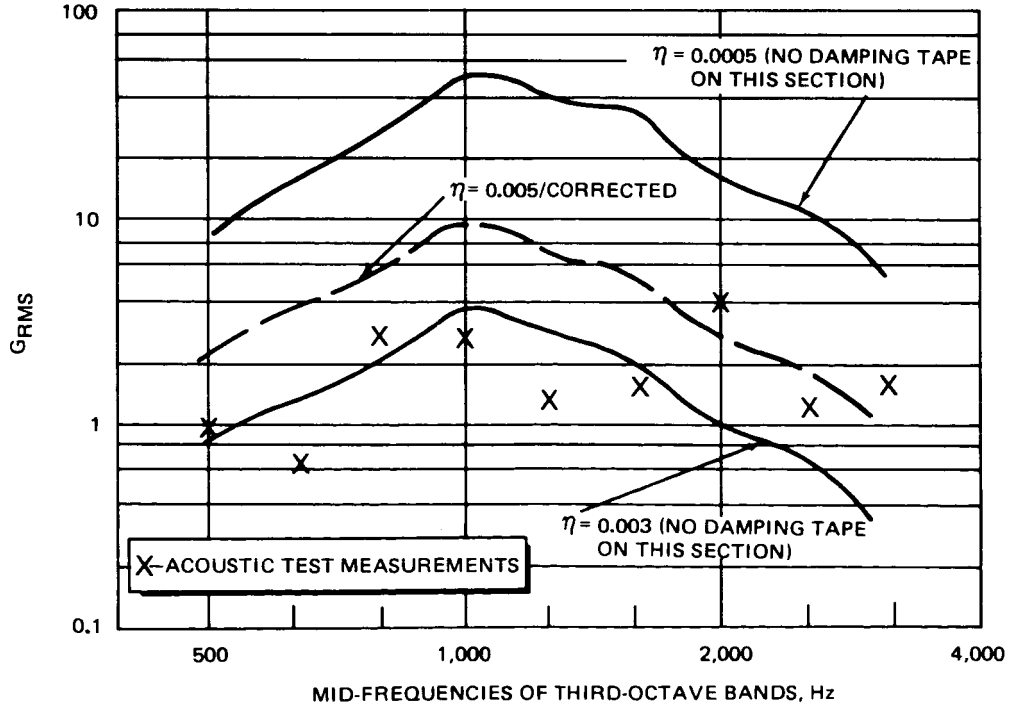

Figure 60. Comparison of Test and Computed Results – Direct Impingement – Section IV – Top – $\phi_c = 50\,\phi_o$ – Damping Tape Applied to Sections I and II

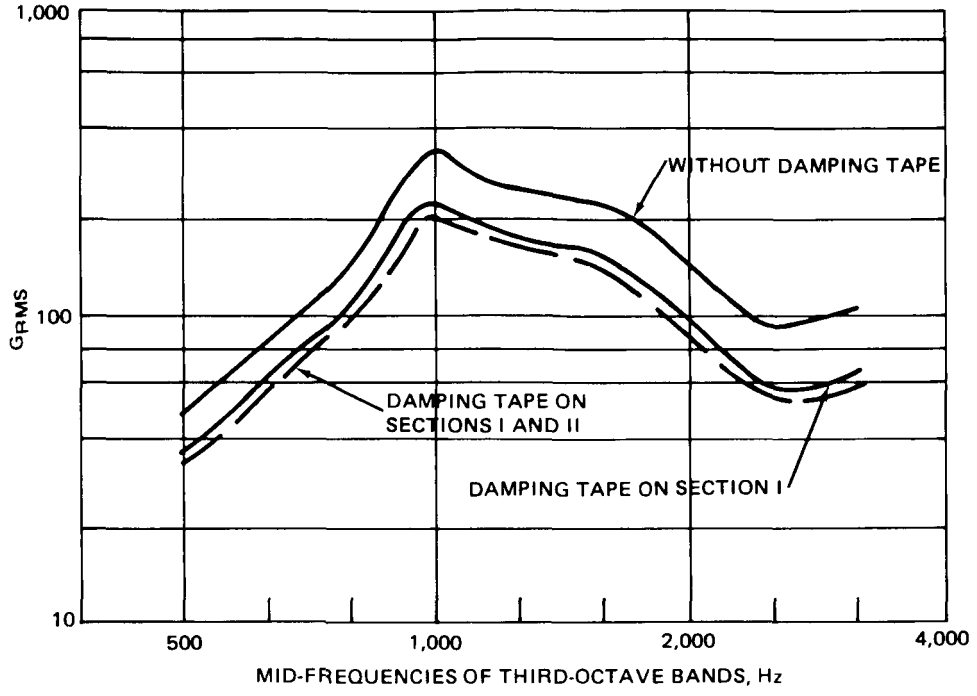

Figure 61. Direct Excitation - Computed Response of Section I (Top) with Various Configurations of Damping Tape Applied to Specimen (η = 0.0005 for Bare Structure, See Text for η of Sections with Damping Tape)

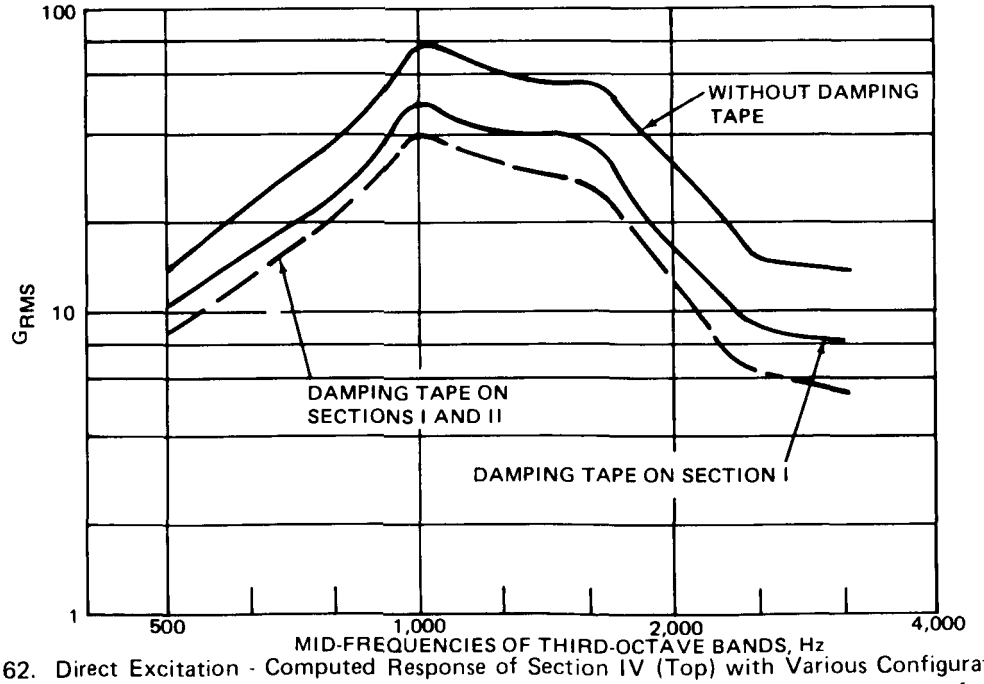

Figure 62. Direct Excitation - Computed Response of Section IV (Top) with Various Configurations of Damping Tape Applied to Specimen (η = 0.0005 for Bare Structure, See Text for η of Sections with Damping Tape)

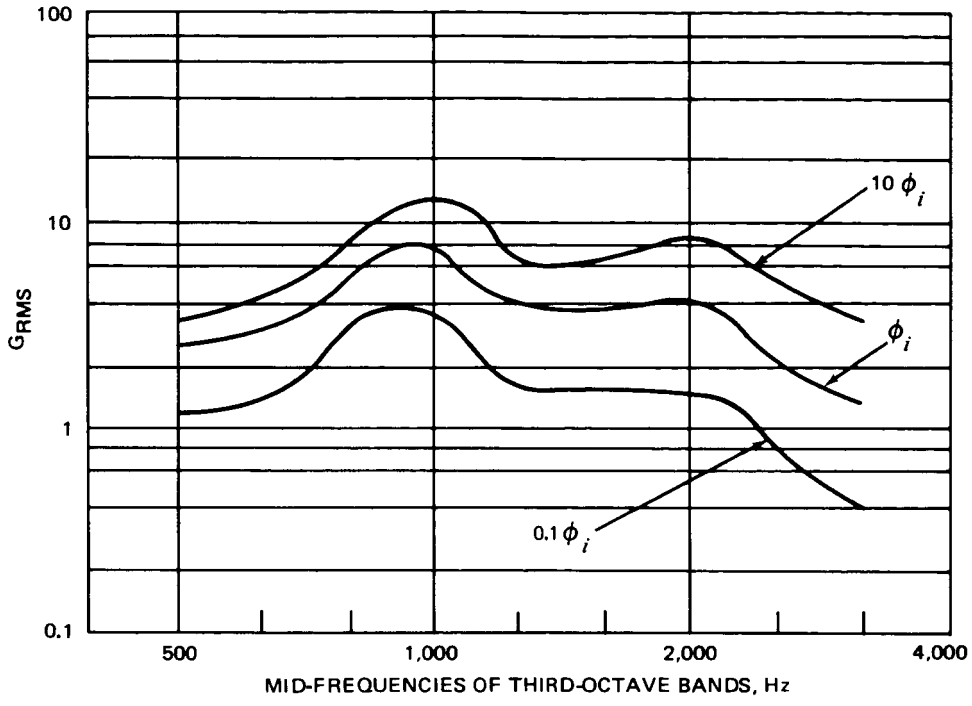

Figure 63. Effect of Variation in ϕ with η = 0.003 - Reverberant (Aft Plate Only) - Section I

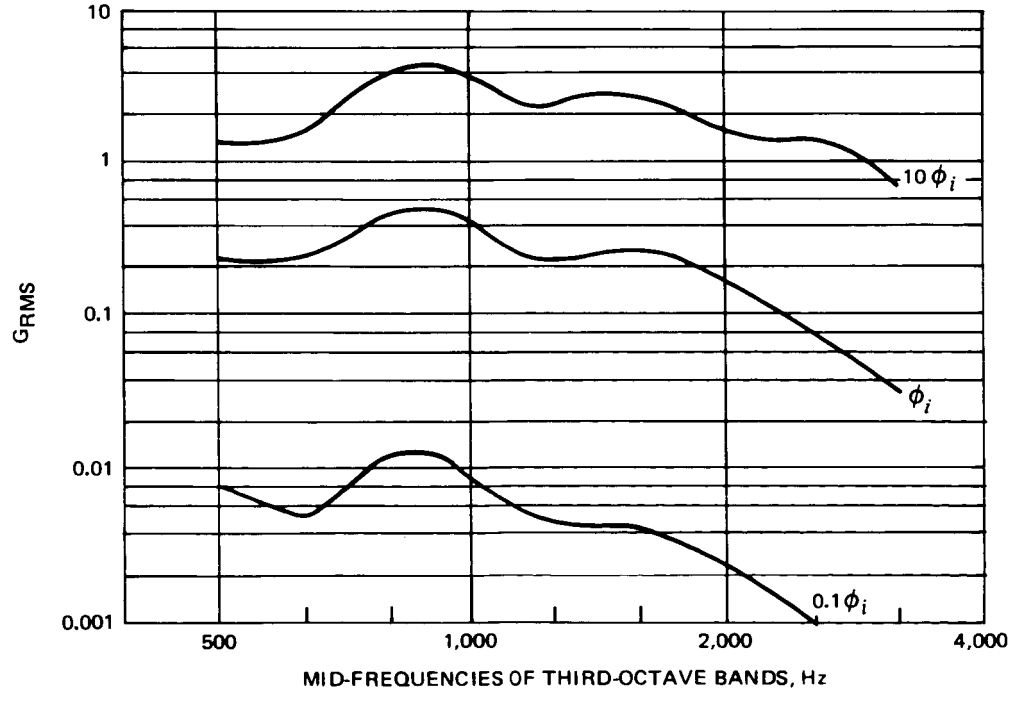

Figure 64. Effect of Variation in ϕ with η = 0.003 - Reverberant (Aft Plate Only) - Section IV

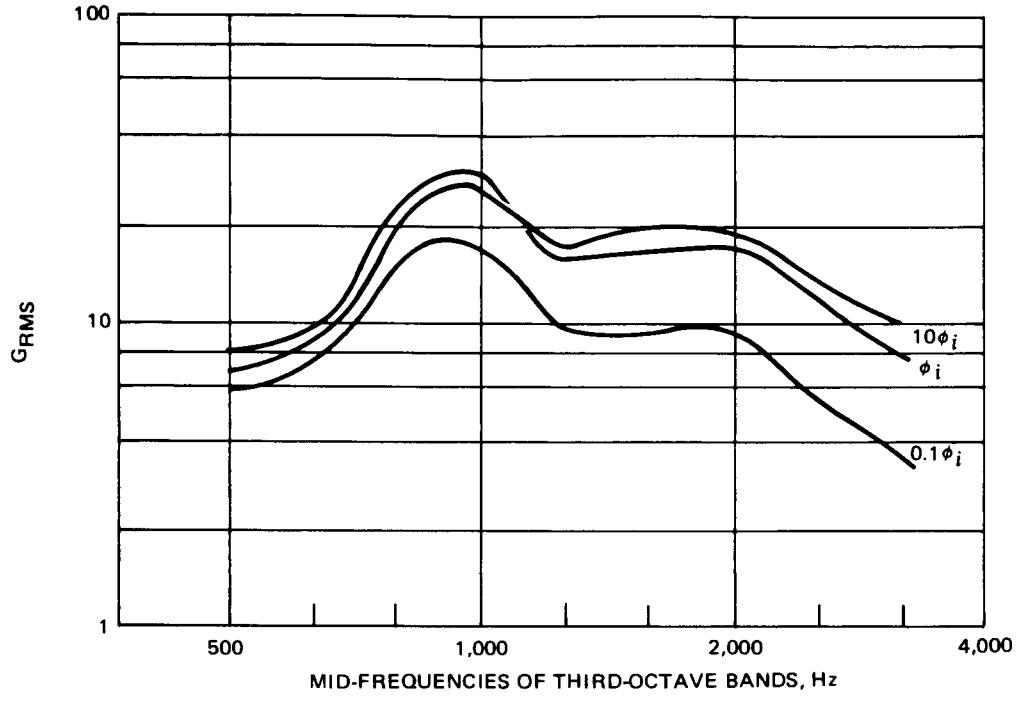

Figure 65. Effect of Variation in ϕ with η = 0.0005 - Reverberant (Aft Plate Only) - Section I

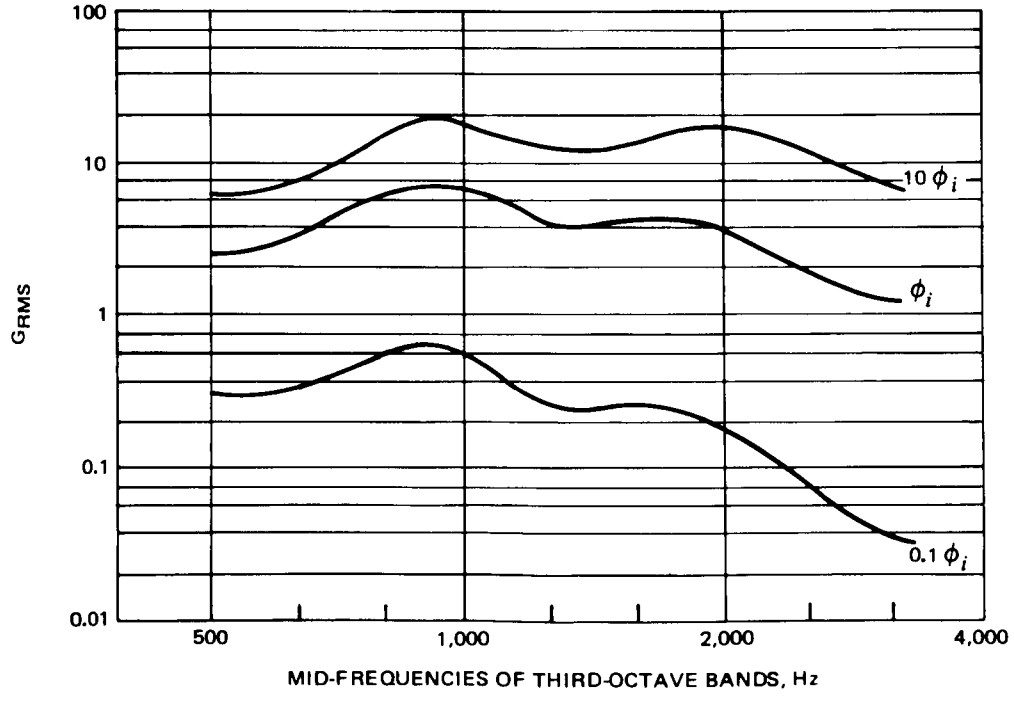

Figure 66. Effect of Variation in ϕ with η = 0.0005 - Reverberant (Aft Plate Only) - Section IV

coupling, an element with high energy will begin to give up a larger proportion of the energy to other elements (in this case Section II). The system then begins to approach a reverberant condition in which the energy is distributed equally among the system modes.

The change in slope of the three response curves which is most notable in Figure 66 is also of interest. The changing slope indicates that, as coupling is decreased, the high-frequency response falls off more rapidly than the lower frequencies. This may be the result of relative changes in modal density.

One additional means of parameterization was accomplished during the course of the study. That parameterization consisted of evaluating the use of an approximate cylindrical correction factor for the modal density. Figures 67 to 70 show the effects on the computed response for the Reverberant (aft plate only) configuration of using either of the two methods presented in the section of this report on specimen modeling.

It should be noted that the acoustic input configurations which have been examined cover the entire realm of response problems:

A. Fully Reverberant – vehicle completely surrounded by a significant acoustic field.
B. Reverberant (aft plate only) – identical to internal structure or substructure excited by a portion of the external skin.
C. Direct Impingement – vehicle has localized "hot spots" on the skin.

Because SEA consists of linear techniques, the contribution to a system of each type of excitation may be determined and the squares of the responses summed, therefore providing the total response.

A scaling method must be developed in order to evaluate the significance of this study to general structural systems. A classical means of scaling frequency dependent data on cylindrical shells is to replace frequency with frequency times radius of curvature ($f \cdot r$). This scaling minimizes the effects of curvature on the values being evaluated.

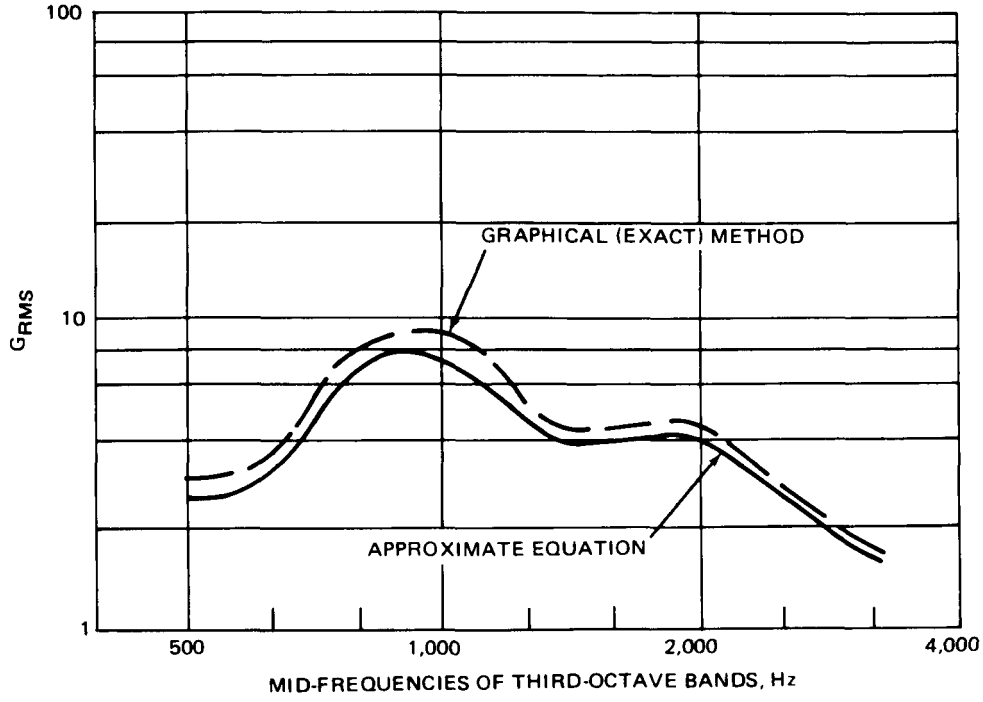

Figure 67. Comparison of Methods for Evaluating Modal Density Cylindrical Correction Factors - Reverberant (Aft Plate Only) η = 0.003, Section I

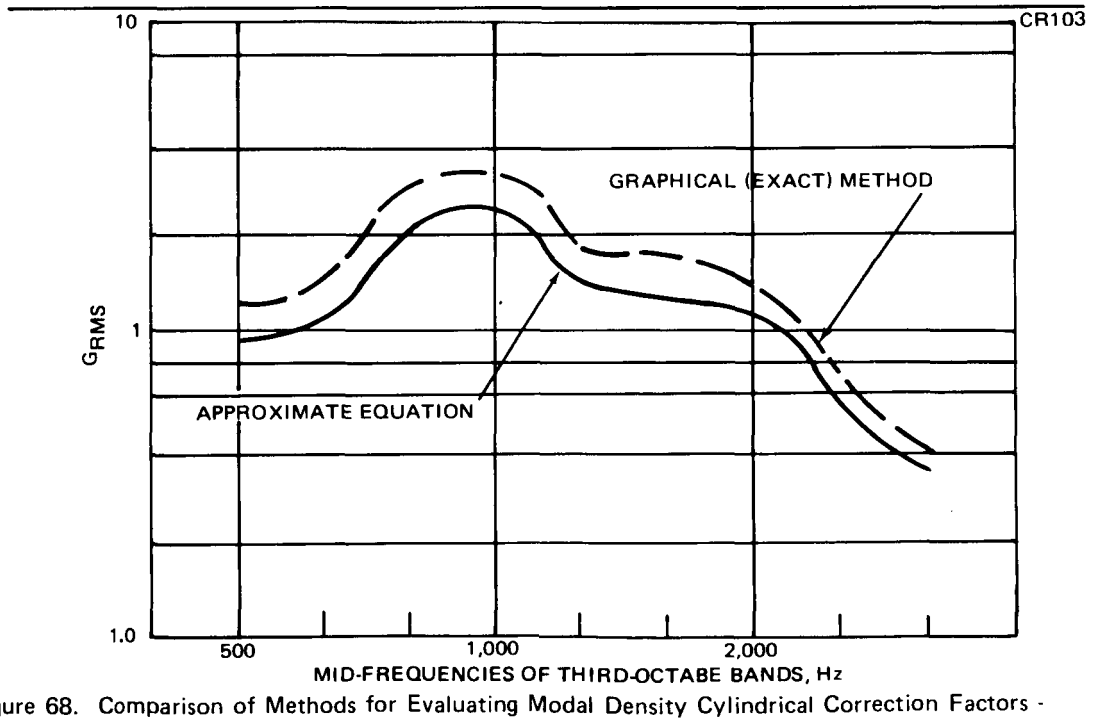

Figure 68. Comparison of Methods for Evaluating Modal Density Cylindrical Correction Factors - η = 0.003 - Reverberant (Aft Plate Only), Section II

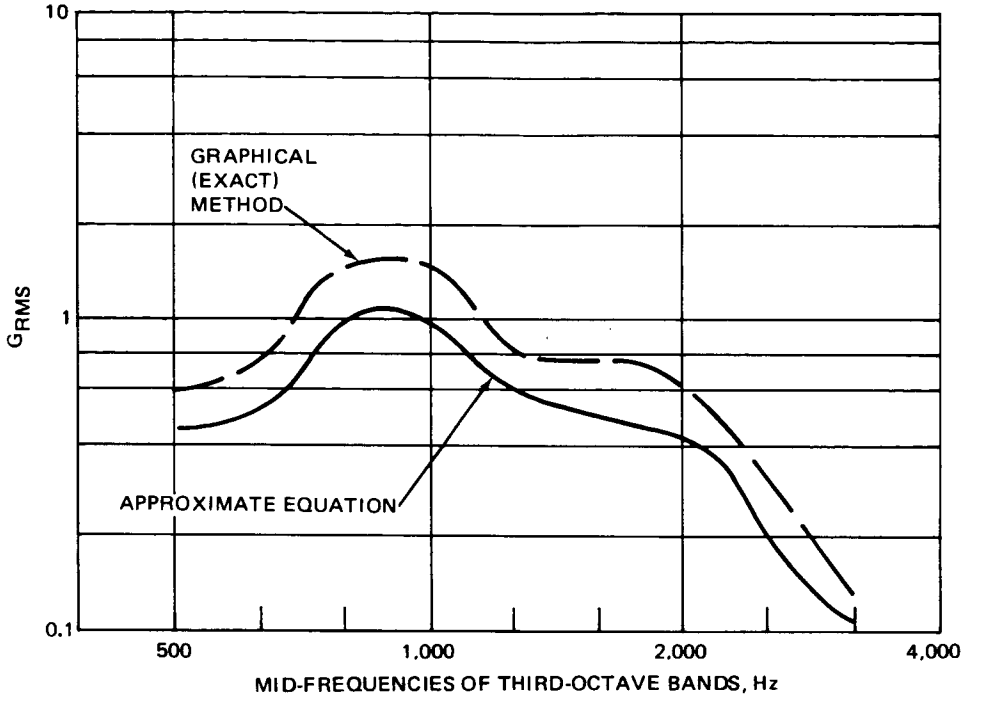

Figure 69. Comparison of Methods for Evaluating Modal Density Cylindrical Correction Factors - $\eta = 0.003$ - Reverberant (Aft Plate Only), Section III

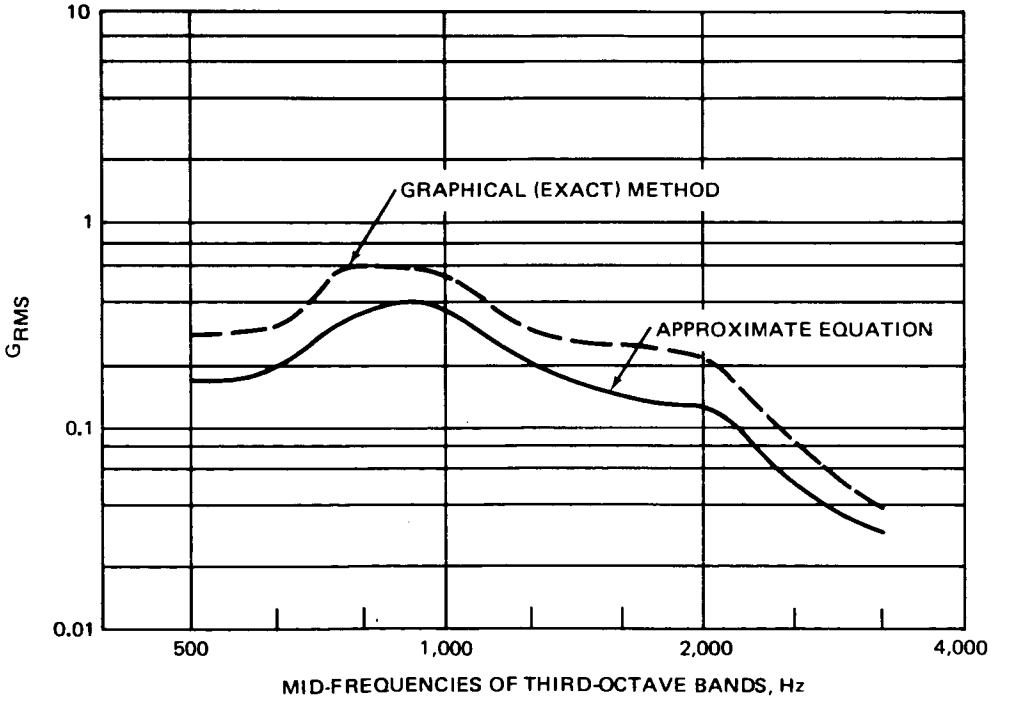

Figure 70. Comparison of Methods for Evaluating Modal Density Cylindrical Correction Factors - Reverberant (Aft Plate Only) $\eta = 0.003$, Section IV

Figure 71 compares the accuracy of the predictions, using predicted response for $\eta = 0.0005$ divided by measured response as the indicator of accuracy, as a function of such a scaled frequency for the fully-reverberant case.

The first observation is that a damping value of $\eta = 0.001$ would yield better agreement (since η is inversely proportional to g^2) and that error in the prediction does not exceed ±3 dB above fr ≃ 2, 500 Hz ft (except for one point). If the error band is increased to ±6 dB, the value for the applicable range of fr can be reduced to approximately 1, 500 Hz ft. These frequencies multiplied by radii correspond to a little less than the ring frequency to one-half of the ring frequency. It should be noted that although it appears that damping was underestimated, the same results would be obtained by overestimating the acoustic input.

The same presentation for the aft plate excitation is presented in Figure 72. The predicted value is based on $\eta = 0.0005$. The error in the predicted value

CR103

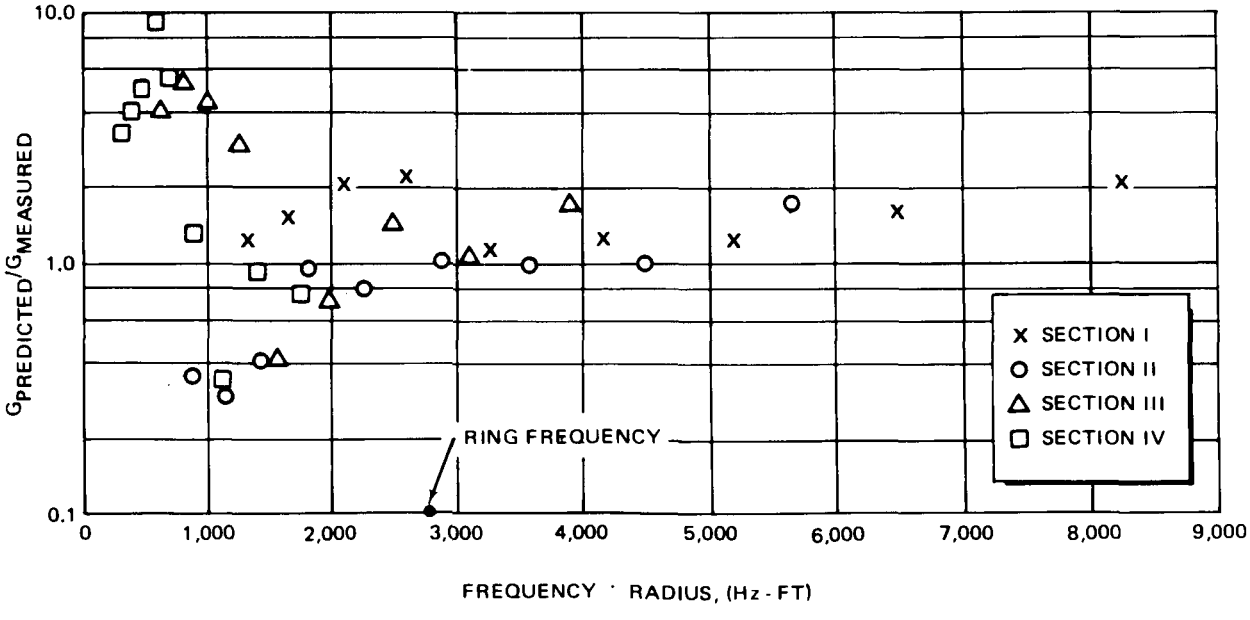

Figure 71. Prediction Accuracy of SEA as a Function of Adjusted Frequency - Reverberant

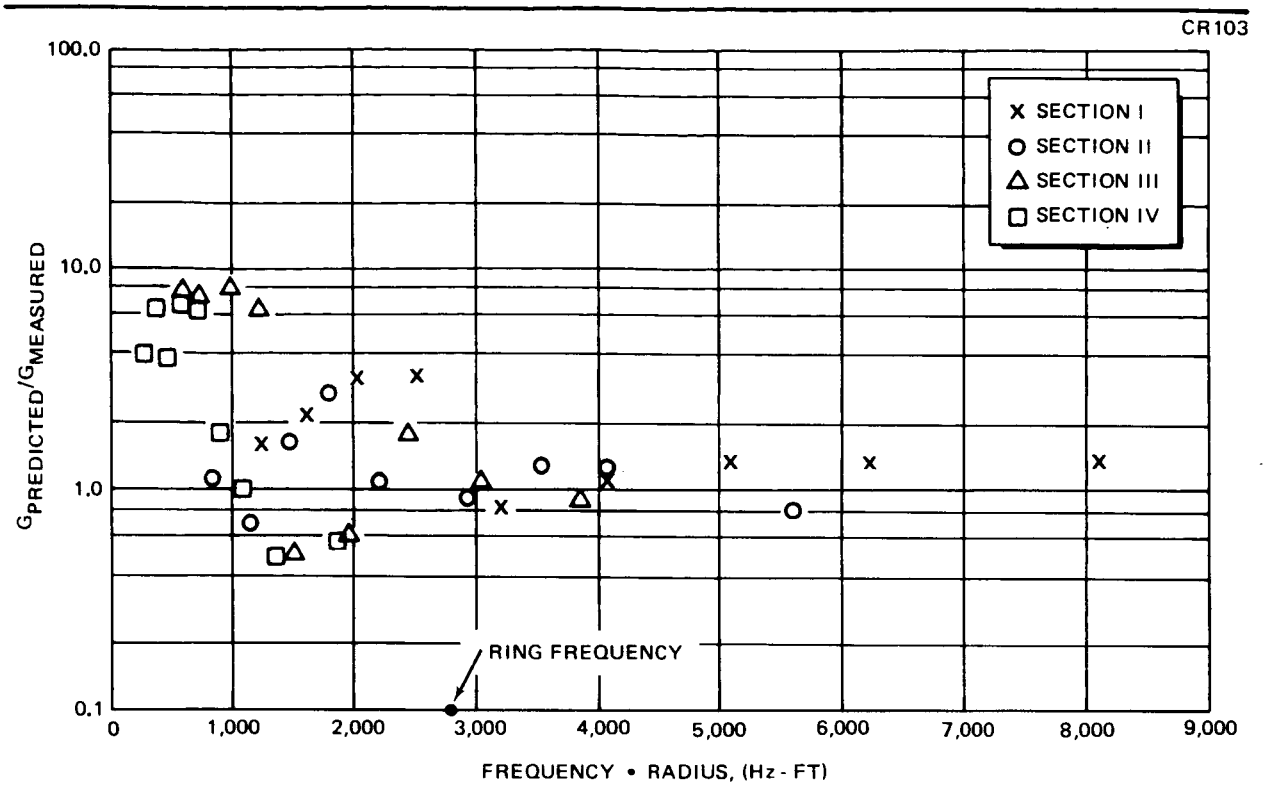

Figure 72. Prediction Accuracy of SEA as a Function of Adjusted Frequency - Reverberant (Aft Plate Only)

is less than 3 dB for values of fr greater than 2, 500 Hz ft. This agreement does indicate that the discrepancy in Figure 72 is the result of underestimating the acoustic input or, at least, the damping value of 0. 0005 is compatible with the coupling factor used.

Figure 73 which presents the direct impingement data shows that the proper correction to apply to the predicted values of $\eta = 0.0005$ would be 4 and that the scatter band does not exceed 3 dB above fr = 3500.

The main conclusions to be drawn from Figures 71 to 73 are that if the input energies were properly defined, the UpSTAGE analysis, using damping and coupling factors measured on simple systems, would yield results with ±3 dB accuracy above the ring frequency of local structure and acceptable estimates of the levels to one-half of the ring frequency. These conclusions are based on curved panels that have about 20 percent of the area and modes of cylinders with corresponding curvature. Therefore, the conclusions drawn above may be conservative. Because of this conservatism, it is possible that the ±3-dB accuracy would extend to even lower corrected frequencies.

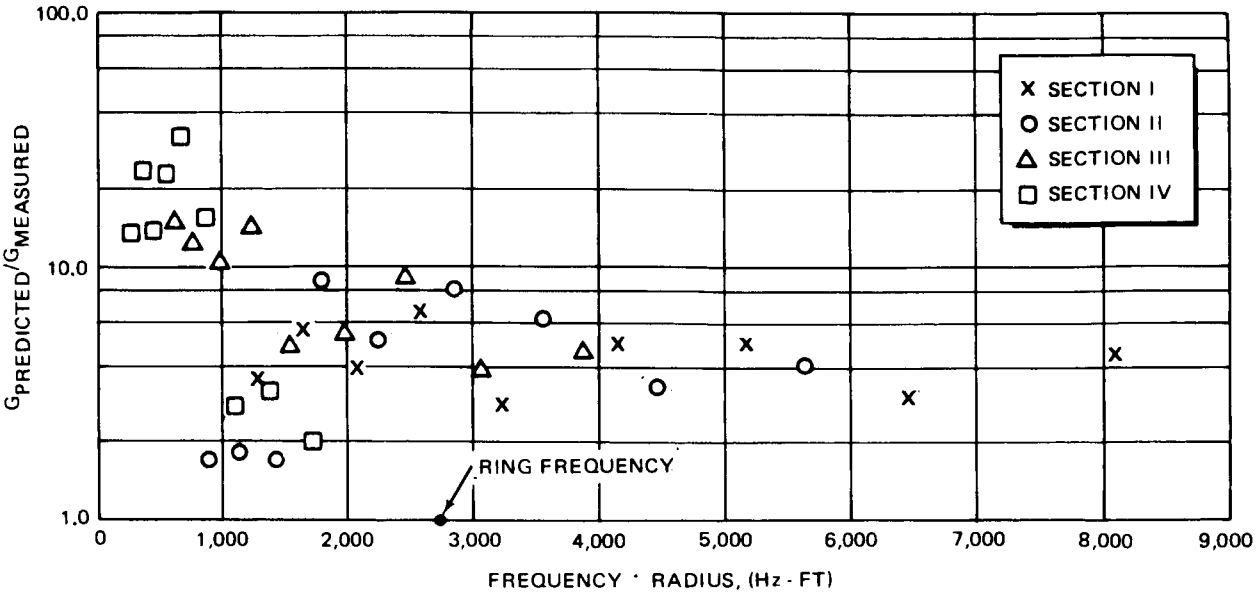

Figure 73. Prediction Accuracy of SEA as a Function of Adjusted Frequency - Direct Impingement

The classical scaling of frequency with radius which has been accomplished is very useful when cylindrical or curved structures are being considered. However, a scaling method which is valid for flat or curved structures would have even more general use. Since the lower limit of validity for SEA is considered to be a function of the number of element modes participating in the frequency bands, scaling by number of modes would seem to be indicated.

Figures 74 to 76 evaluate system accuracy based on the number of element modes present in each frequency band. The main change from the scaling on radius is that Section II replaces Section I as having the most significant (largest scaled frequencies) values. The fully reverberant and direct impingement cases exhibit slightly less accuracy than with radius scaling, while the aft plate excitation shows extremely good accuracy. Convergence to the limits of accuracy appears to occur at about 20 element modes per band.

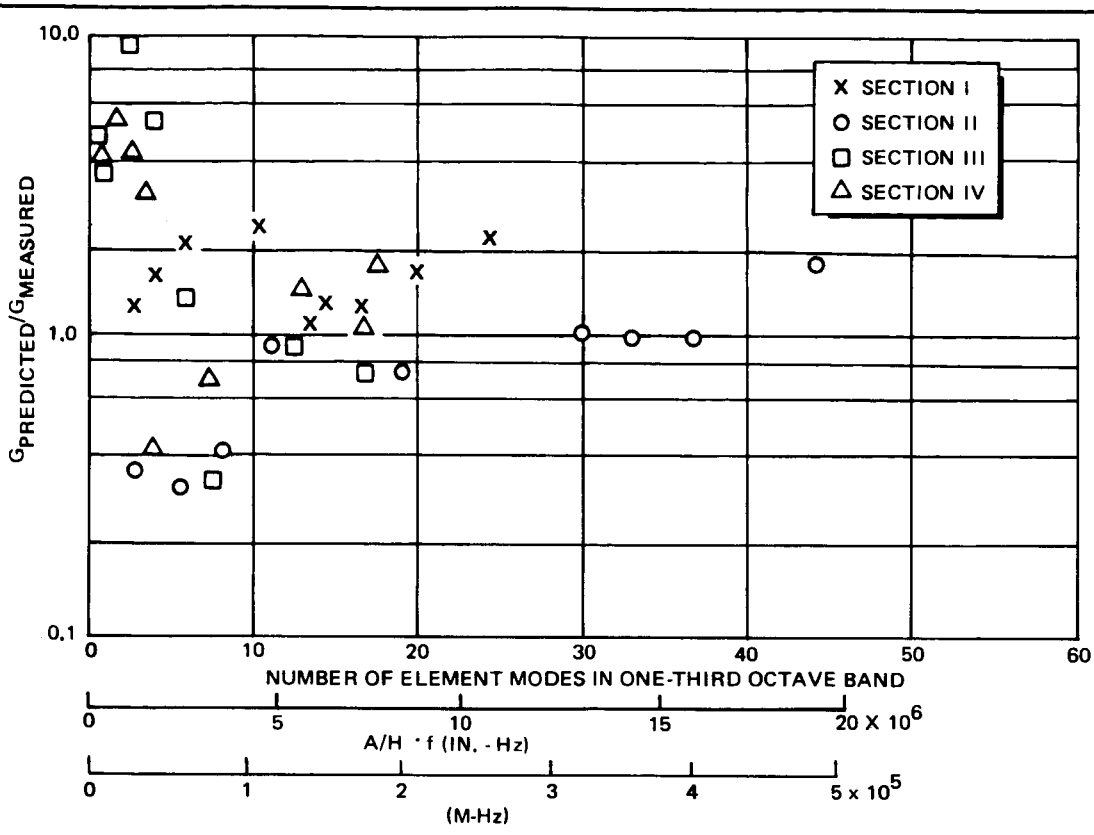

Figure 74. Prediction Accuracy of SEA as a Function of Number of Element Modes Participating — Reverberant

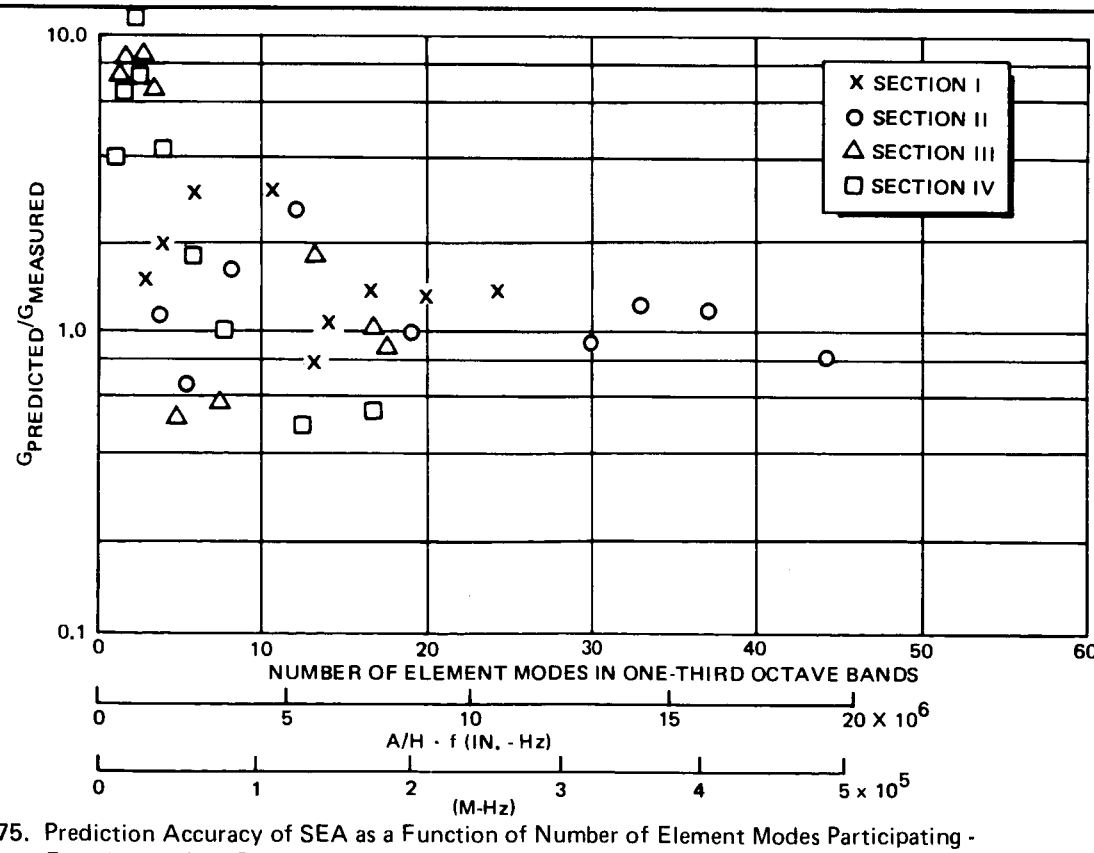

Figure 75. Prediction Accuracy of SEA as a Function of Number of Element Modes Participating - Reverberant (Aft Plate Only)

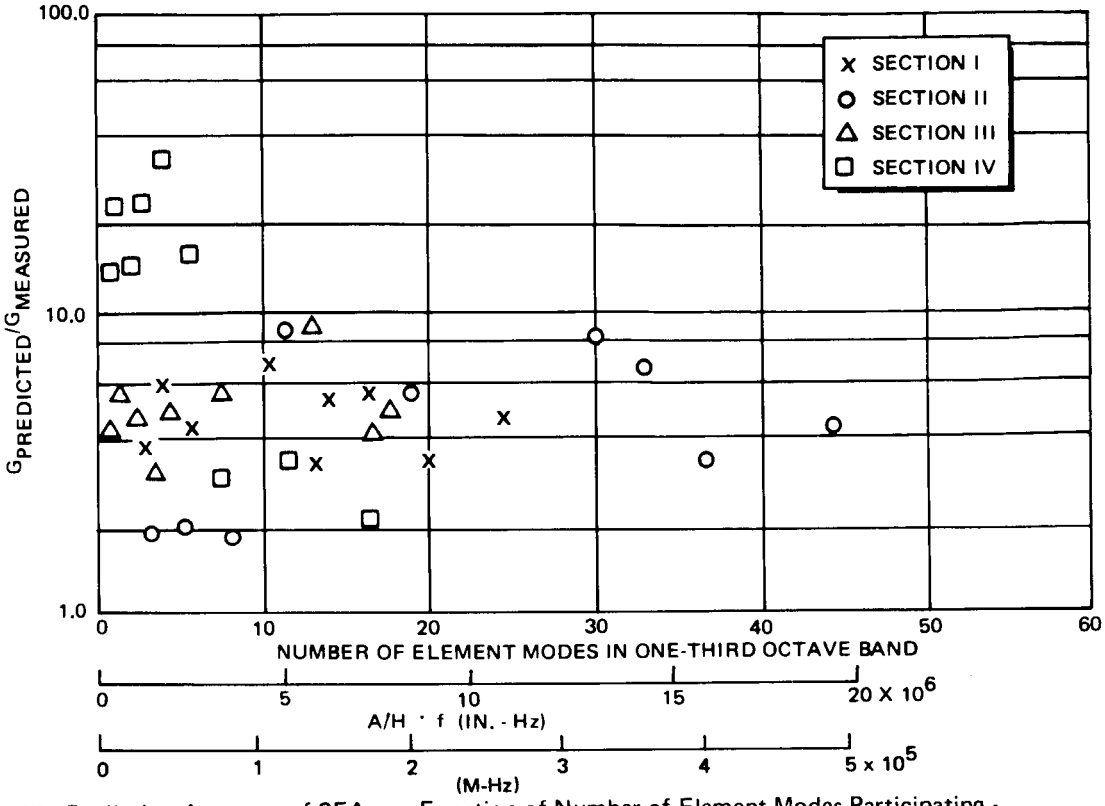

Figure 76. Prediction Accuracy of SEA as a Function of Number of Element Modes Participating - Direct Impingement

The number of modes per element when using constant percentage bandwidths for flat plates is strictly a function of (A/h)·f. Figures 74 and 76 have their abscissas marked to show the corresponding value of this scaling parameter valid for aluminum or steel) to aid in application of the graphs. The spacing of the points plotted on the graphs indicates the effects of curvature on distribution of modal density with frequency.

Due to the positioning of the acoustic input for the specimen, the frequency scaling on radius or size (number of modes) may be misleading with regard to the accuracy of SEA in this study. The scaling places major emphasis on predictions in Sections I and II. Because these sections are adjacent to the input, response is most directly affected by the input and by the damping, but not necessarily coupling. Consequently, Figures 77 to 79 are included to demonstrate accuracy without scaling of the frequency.

These figures still indicate a convergence of the predicted levels. Much of the spread in the high frequencies is due to Section IV, which has the lowest scaled frequencies.

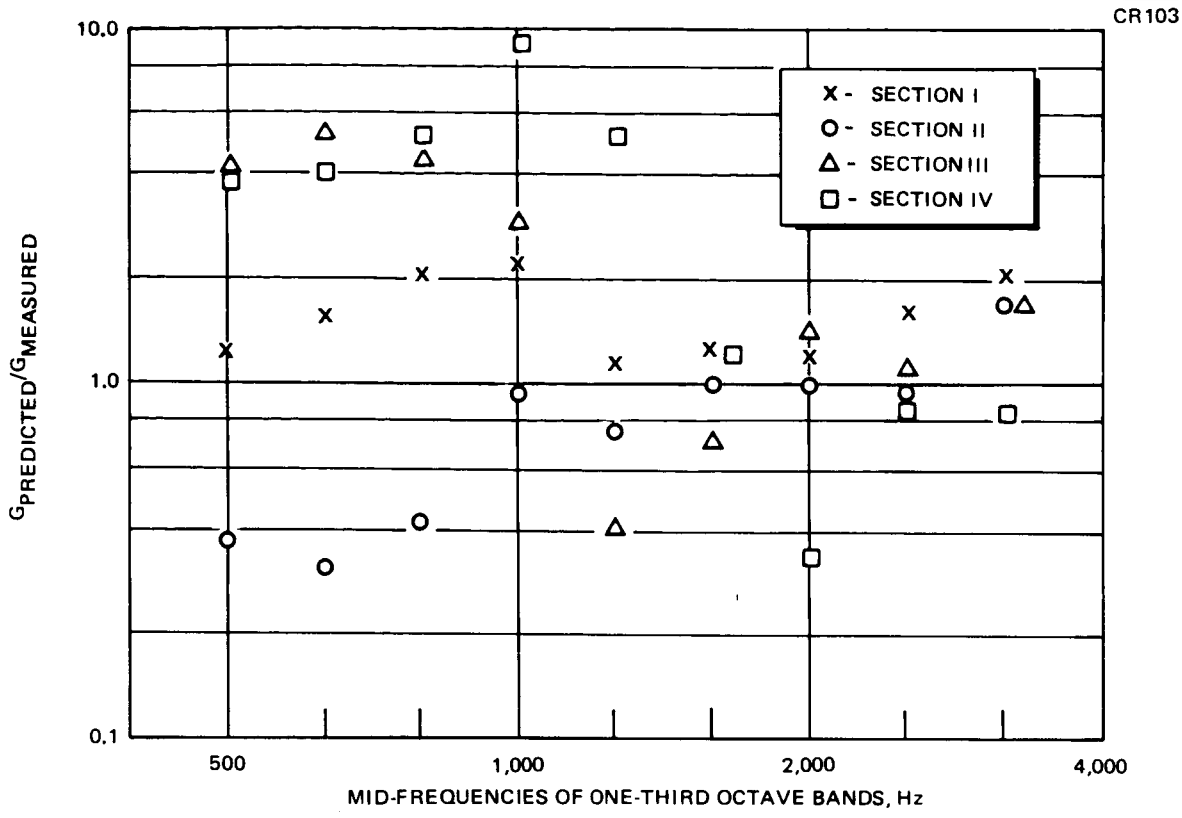

Figure 77. Prediction Accuracy of SEA as a Function of Frequency - Reverberant

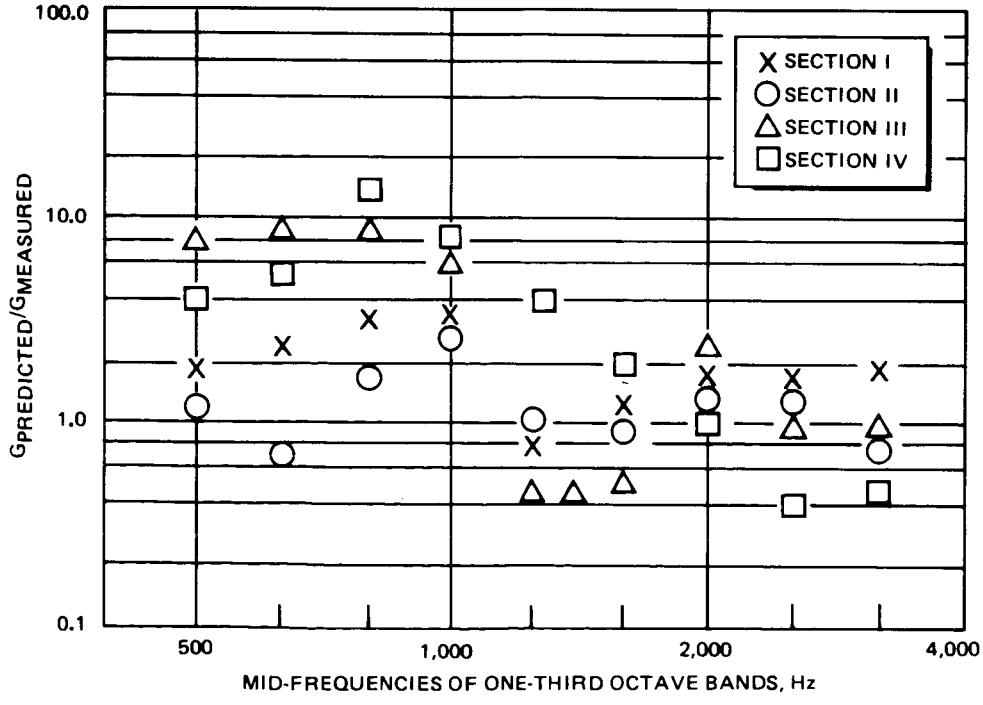

Figure 78. Prediction Accuracy of SEA as a Function of Frequency - Reverberant (Aft Plate Only)

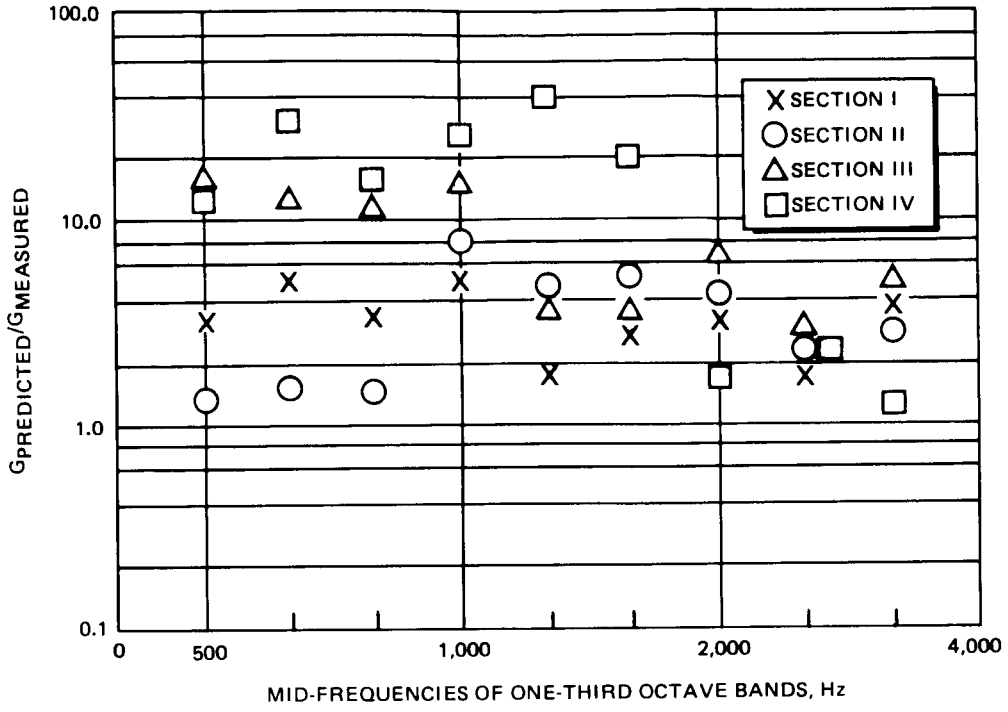

Figure 79. Prediction Accuracy of SEA as a Function of Frequency - Direct Impingement

These figures show that the accuracy in Sections I, II, and III converges very closely to the same value in the high frequencies for all three input configurations. This indicates the same parameter or parameters is causing the inaccuracy in all sections. This would indicate the coupling values are correct, since the coupling would affect Section III predictions relative to Section I. Consequently, the overemphasis on Sections I and II when using the scaling techniques should not be misleading as to the indicated accuracy of the SEA approach.

Combining the information provided by the three accuracy evaluation techniques, this study indicates that SEA is capable of prediction accuracies of ±3 dB above the ring frequencies of curved structure or when the structural model has 20 or more modes per element participating in a one-third-octave frequency band. This accuracy was attained in conjunction with simple test methods used to evaluate the damping and coupling parameters for the structure. Consequently, the results verify the validity of the simple test methods as a means of evaluating these SEA parameters for complex structures.

CONCLUSIONS

The primary conclusions reached during this study are:

A. SEA has a demonstrated capability of structural response prediction accuracies of ±3 dB above the ring frequency of cylindrical structure or when 20 or more modes per model element are participating in a one-third octave frequency band.

B. The simple test methods and panel specimens presented in the section of this report on the test program are capable of defining the SEA damping and coupling parameters for complex structures. Of special interest is that the very low damping obtained during test did yield the proper results.

C. Overmodeling of continuous structural elements can be an important obstacle to a successful SEA application.

Additional accomplishments are:

A. The SEA approach was put into a computer-compatible matrix form.

B. General information concerning SEA and high-frequency response was gained from a study of simple systems.

AREAS FOR ADDITIONAL WORK

This report establishes SEA as a useful tool for random vibration analysis of complex structures. For this application, additional effort is required to (1) measure or gather coupling values for typical structural joints and catalog these results; (2) define coupling, damping and modal density properties of components or vehicle equipment.

SEA can be extended to other areas of interest. Such applications have received little attention even though the extension of SEA should be straightforward. These include:

A. Application of SEA to high frequency shock predictions. The authors see no basic distinction between the high frequency transient and steady-state problems.

B. Application of SEA to component testing by exciting lightly damped, high modal density structures that have attached components. The control methods would be based on component response as calculated from the high modal density response. This would eliminate the question of over- or undertesting due to impedance difficulties encountered with dynamic shakers.

C. Application of SEA to define multiple inputs, either acoustic or mechanical, to simulate acoustic-type environments for large structures. Acoustic testing is most desirable if a system can be tested in existing facilities. This method could possibly eliminate the need for the construction of special facilities to perform acoustic-type tests on new systems.

The ultimate extension of SEA would be to combine it with the classical approach, i.e., modeling high modal density structure using SEA, low modal density structure using classical techniques and combining the results. This would require relaxation of the SEA equal modal coupling assumption.

OUTLINE FOR AN SEA APPLICATION

This section of the report outlines a sequence to be followed for the application of statistical energy methods to a general structural problem. The information gained during this study is used to indicate significant aspects of the various topics.

The following sequence is recommended for applying SEA to a flight vehicle.

A. Will a statistical analysis be useful and valid for the system?
   1. Response predictions are statistical – keep in mind the basic assumptions of SEA:
      a. The modes of the elements of a system contain all the vibratory energy of the system.
      b. Only modes occurring within the same frequency band are coupled.
      c. The energy in one frequency band of a system element is equally distributed among the modes of that element occurring in the frequency band.
      d. For two coupled elements, all of the modes occurring in one of the elements in one frequency band are equally coupled to each mode occurring in the same frequency band in the other element.
   2. Valid only for "resonant" systems – see Reference 3.
   3. Consider frequency range of interest – SEA complements, does not replace, classical modal analyses.

B. Select a model for the structural system.
   1. Model elements should represent generally gross, continuous portions of the structure. Two attempts were made during the present study to model continuous portions of structure as

more than one element. This type of modeling was successful for one case (circumferential modeling) and caused drastic problems in the other case (aft subsections), so caution is advised in the use of this technique.

2. Give special consideration to elements with external excitation and the main path of coupling to elements where the response is critical. More attention should be directed to defining the main transmission paths to critical elements than on secondary aspects of the structure (Note: a parameter study can be run after a response solution is obtained to insure that effects of certain portions of the structure are indeed secondary).

C. Establish the system of equations for the model.

1. Establish a solution format as in this report. For very simple systems an explicit form of the equations may be used for solutions. For complex systems, the matrix format established in this study is simple, straightforward, and applicable to most, if not all, systems.

2. Select an input method for acoustic or mechanical inputs. The input is a very critical aspect of any analysis. This study presented a method for coupling a reverberant acoustic field to a structural system which yielded excellent results. This method may be extendable to nonreverberant acoustic fields if a suitable radiation efficiency (which actually determines the magnitude of the coupling) can be determined for the structural interaction with the field. Alternate forms may also be developed to introduce acoustic energy. Mechanical input of power should be easily accomplished for the SEA equations.

3. Establish the coupling matrix – it must agree with the system model. The coupling matrix is the only matrix having nondiagonal terms which appears in the matrix format developed for solution in this study. Consequently, errors in this matrix are the most likely to go unnoticed. Care must be taken to insure that the matrix agrees with the model being used (unconnected elements should have zero coupling).

4. Incorporate the physical characteristics of the elements (mass, area, etc.) into the equations.

D. Determine values for the SEA parameters of the system.

1. Modal density – may be computed analytically and corrected for curvature, if necessary. The expressions presented in this report (from Reference 7) are valid approximations for the frequency range of interest in statistical analyses. The only foreseeable difficulty in application of these expressions is in determining, for example, whether a structural element is responding as a plate or as a beam.
2. Radiation efficiency (if used). Test data on this parameter for both flat panels and cylinders are presented in Reference 4 for a reverberant field. These data yielded values for the radiation efficiency which gave excellent results in this study. Values for this parameter in nonreverberant acoustic fields have not been noted.
3. Damping – must generally be measured or estimated for each system. The "bop" tests performed in this study to measure damping are simple, quick, and inexpensive. The damping parameter measured in this manner resulted in excellent response predictions. The measured damping also agreed with published data for the structural material in Reference 9, an indicated aid for estimating damping. Selection of low (conservative) values for the damping will not necessarily result in conservative predictions if the damping varies among model elements.
4. Coupling – at least a base value must be evaluated with a test since information is almost nonexistent for this parameter. One additional method using response data from previous tests with very simple structural configurations having applicable joint construction is possible: use the response data to perform a reversed analysis solving for the coupling parameter. Without valid information on the system coupling, only parametric studies can be accomplished.

E. Test Program (if included)

1. Test specimen should be of the most significant features of the structure. The specimen should represent the most important structural features between the input and the critical response elements along the major transmission path. This approach insures the most valid response predictions with the minimum amount of testing.
2. Keep test specimen simple to permit straightforward evaluation of results. Test specimens having complex configurations may appear to give a more valid representation than very simple specimens. However, when specimens are used which must be modeled as SEA systems with more than two elements which are not symmetric or which have unusual shapes, it may be very difficult to isolate the effects of the individual parameters. The results achieved in this study were accomplished with extremely simple test specimens.

F. Solve for response of the system. This may be accomplished explicitly for very simple systems. For complex systems, the matrix format presented in this report is easily adapted to solution with any matrix abstraction program.

G. Evaluation of Results

1. If results are based on damping and coupling values measured using methods presented in this study, the study results indicate predicted response should agree well with actual response.
2. If all parameters were not well defined, the results should be treated as a parametric study to determine the effects on system response of parameter variation throughout the expected range of values.
3. Reread Item A to ensure that results are interpreted in light of the SEA assumptions.

REFERENCES

1. Manning, Jerome E.; and Remington, Paul J.: Statistical Energy Methods. Report 2064, Bolt Beranek and Newman, March 26, 1971.

2. Hines, D. E.; Parker, G. R.; and Hellweg, R. D.: Prediction of UpSTAGE Random Environments Using a Statistical Energy Approach. 41st Shock and Vibration Bulletin, 1970.

3. Pope, Larry Debbs: On the Transmission of Sound through Finite, Closed Shells: Statistical Energy Analysis, Modal Coupling, and Nonresonant Transmission. Report 21, University of Houston, August 1970.

4. Lyon, Richard H.; and Maidanik, Gideon: Statistical Methods in Vibration Analysis. AIAA Journal, Vol. 2, No. 6, June 1964, pp. 1015-1024.

5. Morse, P. M.: Vibration and Sound, Second ed., McGraw-Hill Book Co., Inc., 1948.

6. Burrow, Laurie R., Jr.: Some Analog Methods of Power Spectral Density Analysis. Technical Publication PS-1, Spectral Dynamics Corporation of San Diego, October 1965, revised January 1968.

7. Ungar, Eric E.: Fundamentals of Statistical Energy Analysis of Vibrating Systems. Technical Report No. AFFDL-TR-66-52, Air Force Flight Dynamics Laboratory, May 1966.

8. Lazan, B. J.: Damping of Materials and Members in Structural Mechanics. Pergamon Press Inc., 1968.

9. Lee, L. T.: A Graphical Compilation of Damping Properties of Both Metallic and Non-Metallic Materials. Technical Report No. AFML-TR-66-169, Air Force Materials Laboratory, May 1966.

10. Lyon, Richard H.; Random Noise and Vibration in Space Vehicles. SM-1, The Shock and Vibration Information Center, United States Department of Defense, 1967.

11. Bolotin, V. V.: On the Density of the Distribution of Natural Frequencies of Thin Elastic Shells. J. Appl. Math. and Mech., Vol 27, No. 2, 1963, pp. 538-543.